LIÈGE université
Gembloux
Agro-Bio Tech

Effects of high hydrostatic pressure on structure and gelation properties of sweet potato protein

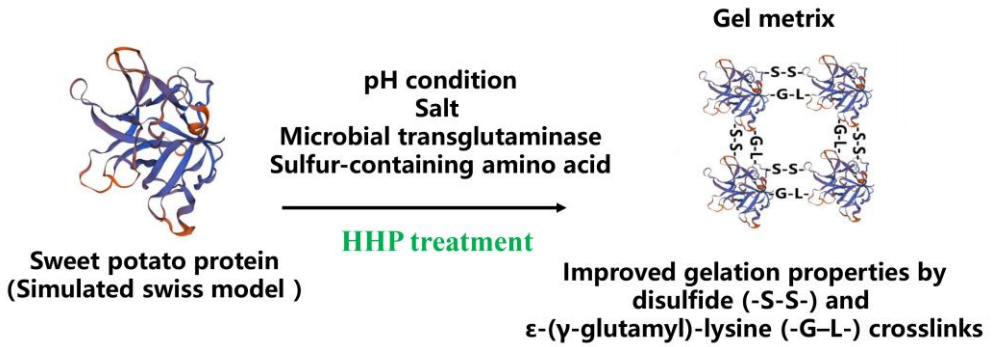

Author: Zhongkai ZHAO

Promotors: Prof. Aurore RICHEL & Prof. Taihua MU

2019

COMMUNAUTÉ FRANÇAISE DE BELGIQUE

UNIVERSITÉ DE LIÈGE – GEMBLOUX AGRO-BIO TECH

Effects of high hydrostatic pressure on structure and gelation properties of sweet potato protein

Zhongkai ZHAO

Dissertation originale présentée en vue de l'obtention du grade de docteur en sciences agronomiques et ingénierie biologique

Promotor: Prof. Aurore RICHEL & Prof. Taihua MU

Année civile: 2019

Résumé

Zhongkai ZHAO (2019). Effets de la pression hydrostatique élevée sur la structure et les propriétés de gélification de la protéine de patate douce (PhD thesis).

Gembloux Agro-Bio Tech, Université de Liège.

171 pages, 25 figures, 18 tableaux.

La présente étude a examiné les effets d'une haute pression hydrostatique (HPH) combinés avec quatre facteurs principaux sur la structure et les propriétés de gélification de la protéine de patate douce (SPP), notamment une modulation des conditions de pH et l'addition d'ions de sel, d'une transglutaminase microbienne ou d'un soufre enzymatique. contenant des acides aminés, respectivement.

Tout d'abord, les effets d'une HPH (250, 400 et 550 MPa) associés à un traitement de pH différent (3,0, 6,0 et 9,0) sur les forces chimiques, la structure et les propriétés de gélification de la SPP ont été étudiés. L'hydrophobicité de surface (Ho) et le potentiel zêta de la SPP ont considérablement augmenté, passant de 250 à 550 MPa ($p < 0.05$) dans les trois conditions de pH. La quantité totale de groupes sulfhydryle (-SH-) dans la SPP a diminué après un traitement par HPH à pH 9,0, tandis que la quantité de -SH- libre a augmenté. Des agrégats de masse moléculaire élevée (> 180 kDa) ont été observés dans la SPP après traitement par HPH à pH 6,0 et 9,0 par SDS-PAGE. Le module de stockage (G′) de la SPP était significativement augmenté après le traitement par HPH. En raison de la réticulation covalente au sein de la SPP par la formation de liaisons disulfure, les propriétés texturales et la capacité de rétention d'eau des gels fabriqués à partir de la SPP après un traitement à 250 et 400 MPa à pH 9,0 ont été considérablement améliorées et les gels ont présenté un gel compact et uniforme réseau avec l'apport de fractions d'eau immobilisée.

Ensuite, les effets du traitement à 400 MPa associé à des sels monovalents (NaCl) ou divalents ($CaCl_2$ et $MgCl_2$) à différentes concentrations sur la structure et les propriétés de gélification de la SPP ont été évalués. L'hydrophobicité de surface et le potentiel zêta de la SPP diminuent de manière significative à mesure que la concentration en sels augmente. La quantité totale de groupes sulfhydryle (-SH-) dans la SPP a diminué avec l'ajout de NaCl, $CaCl_2$ et $MgCl_2$ sous HPH, alors que les liaisons disulfure ont augmenté de 0,59 à 0,80 et 0,74 μmol/g avec l'ajout de 0,1 et 0,2 mol/L de $CaCl_2$ combinés avec le traitement à haute pression hydrostatique, respectivement. Le contenu en α-hélice au sein de la SPP a été augmenté pour les trois sels mais diminué en tant que sels combinés au HPH, tandis que la teneur en feuilles β a augmenté avec une force ionique élevée avec le HPH, en particulier en présence de $CaCl_2$ et de $MgCl_2$, passant de 30,40 à 33,45. et 33,55 %, respectivement. Le module de stockage (G′) du SPP était amélioré par les sels et le HPH, même s'il diminuait avec une force ionique élevée. Les propriétés texturales et la capacité de rétention d'eau des gels de la SPP ont été améliorées avec les ions de sel lors du traitement par HPH, en raison de la quantité accrue d'eau liée.

Après cela, les effets d'un HPH (250, 400 et 550 MPa) associé à la transglutaminase microbienne (MTGase) sur la structure et les propriétés de gélification de la SPP ont été étudiés à pH 7,0. La MTGase a induit la formation d'agrégats de SPP de masse moléculaire élevée par réticulation intermoléculaire. La taille moyenne des particules de la SPP a augmenté pour un traitement HPH à 250-550 MPa, passant de 249,5 nm (0,1 MPa) à 270,2 nm (550 MPa). Bien qu'elle ait été réduite par la catalyse ultérieure de MTGase, celle-ci a montré la valeur la plus basse de 200,3 nm à 550 MPa, ce qui indique la formation de liaisons intramoléculaires. La quantité de groupes sulfhydryle et la température de dénaturation thermique ont été augmentées lors du HPH et de l'ajout de MTGase, la valeur maximale étant de 3,5 μmol/g de protéine et de 80,4 °C dans de la SPP catalysé par MTGase avec un prétraitement de 400 MPa. Les propriétés texturales des gels fabriqués à partir de la SPP traitée par HPH ou de ceux ayant une catalyse supplémentaire par MTGase ont été améliorées en raison de la liaison covalente des liaisons disulfure (-S-S-) et des liaisons isopeptides ε- (γ-glutaminyl) lysine. De plus, les résultats par RMN à faible champ ont montré une augmentation des fractions de surface correspondantes de A_{2b} et A_{21}, attribuable au fait que davantage de fractions d'eau liée ou immobilisée étaient piégées dans la matrice de gel SPP.

De plus, les effets du traitement à 400 MPa associé à des acides aminés soufrés (L-cystéine ou L-cystine) à différentes concentrations sur la structure et les propriétés de gélification de la SPP ont été étudiés. Les additifs ont modifié la température de dénaturation et réduit l'enthalpie de dénaturation de la SPP. Des teneurs plus élevées en hélice α ont été observées dans de la SPP non traitée ou traitée par HPH avec de la L-cystéine ou de la L-cystine, tandis que les unités de structure de feuillet β et de boucles aléatoires étaient diminuées. Les spectres FTIR ont montré une faible absorbance de la SPP traitée par HPH avec de la L-cystéine et de la L-cystine. Le module de stockage (G') de la SPP non traitée ou traitée par HPH a été amélioré par la L-cystéine et la L-cystine. Les propriétés texturales des gels de SPP ont été améliorées par l'addition d'acides aminés soufrés sous HPH, correspondant aux liaisons disulfure, en particulier pour la L-cystéine. La RMN à faible champ a indiqué que l'eau se liait plus étroitement aux molécules de SPP en présence de L-cystéine et de L-cystine, et qu'une fraction d'eau plus immobilisée était piégée dans une matrice de gel de SPP, suggérant une amélioration de la capacité de rétention d'eau.

Mots clés: Protéine de patate douce; haute pression hydrostatique; gélification; condition de pH; ions de sel; transglutaminase microbienne; acides aminés soufrés

Abstract

Zhongkai ZHAO (2019). Effects of high hydrostatic pressure on structure and gelation properties of sweet potato protein (PhD thesis).

Gembloux Agro-Bio Tech, University of Liège, Belgium.

171 pages, 25 figures, 18 tables.

The present study investigated effects of high hydrostatic pressure (HHP) combined with four main factors on structure and gelation properties of sweet potato protein (SPP), including a modulation of pH conditions, addition of salt ions, enzyme microbial transglutaminase and sulfur-containing amino acids respectively.

First of all, effects of HHP (250, 400 and 550 MPa) combined with different pH (3.0, 6.0 and 9.0) on chemical forces, structure and gelation properties of SPP were investigated. Surface hydrophobicity (Ho) and zeta potential of SPP significantly increased from 250 to 550 MPa at all three pH conditions ($p < 0.05$). The total amount of sulfhydryl (-SH-) groups in SPP decreased after HHP treatment at pH 9.0, whereas the amount of free -SH- increased. High molecular mass aggregates (>180 kDa) were observed in SPP after HHP treatment at pH 6.0 and 9.0 by SDS-PAGE. Storage modulus (G′) of SPP were significantly increased after HHP treatment. Due to the covalent cross-linking of SPP by the formation of disulfide bonds, textural properties and water-holding capacity of gels made from SPP after 250 and 400 MPa treatment at pH 9.0 were significantly improved, and the gels showed a compact and uniform gel network with the contribution of immobilized water fractions.

Next, effects of 400 MPa treatment combined with monovalent (NaCl) or divalent ($CaCl_2$ and $MgCl_2$) salts in different concentrations on structure and gelation properties of SPP were evaluated. Surface hydrophobicity and zeta potential of SPP significantly decreased as salts concentration increased. The total amount of sulfhydryl (-SH-) groups in SPP decreased with addition of NaCl, $CaCl_2$ and $MgCl_2$ under HHP, whereas the disulfide bonds increased from 0.59 to 0.80 and 0.74 μmol/g with addition of 0.1 and 0.2 mol/L of $CaCl_2$ combined with HHP, respectively. The α-helical content of SPP was increased by all three salts, but decreased as salts combined with HHP, while β-sheet content was increased at high ionic strength with HHP, especially in the presence of $CaCl_2$ and $MgCl_2$, being increased from 30.40 to 33.45 and 33.55 %, respectively. Storage modulus (G′) of SPP was enhanced by salts and HHP, even though it decreased at high ionic strength. Textural properties and water holding capacity of SPP gels were improved with salt ions by HHP, being attributed to more bound water.

After that, effects of HHP (250, 400 and 550 MPa) combined with microbial transglutaminase (MTGase) on structure and gelation properties of SPP were investigated at pH 7.0. MTGase induced the formation of high molecular mass aggregates of SPP by the inter-molecular cross-linking. The average particle size of SPP was increased by HHP at 250-550 MPa, being increased from 249.5 nm (0.1 MPa) to 270.2 nm (550 MPa). While it was decreased by the subsequent MTGase catalysis and showed the lowest value of 200.3 nm at 550 MPa, indicating the

formation of intra-molecular linkages. The amount of sulfhydryl groups and thermal denaturation temperature were increased by HHP and MTGase, which showed the highest value of 3.5 μmol/g protein and 80.4 °C in MTGase catalyzed SPP with 400 MPa pretreatment. Textural properties of the gels made from HHP treated SPP or those with further MTGase catalysis were both enhanced due to the covalent linkage of disulfide bonds (-S-S-) and ε-(γ-glutaminyl) lysine isopeptide bonds. In addition, low-field NMR results showed an increase in corresponding area fractions of A_{2b} and A_{21}, being attributed to more bound or immobilized water trapped in SPP gel matrix.

Furthermore, effects of 400 MPa treatment combined with sulfur-containing amino acids (L-cysteine or L-cystine) in different concentrations on structure and gelation properties of SPP were studied. Additives altered the denaturation temperature and reduced the denaturation enthalpy of SPP. Higher α-helical contents were observed in untreated or HHP treated SPP with L-cysteine or L-cystine, while β-sheet and random coil structure unit were decreased. FTIR spectra showed a weak absorbance in HHP treated SPP with L-cysteine and L-cystine. Storage modulus (G′) of untreated or HHP treated SPP was enhanced by L-cysteine and L-cystine. Textural properties of SPP gels were improved by the addition of sulfur-containing amino acids under HHP corresponding to the disulfide linkages, especially for L-cysteine. Low-field NMR indicated that water bound more closely to SPP molecules in the presence of L-cysteine and L-cystine, and more immobilized water fraction was trapped in SPP gel matrix, suggesting an improvement in water holding capacity.

Keywords: Sweet potato protein; high hydrostatic pressure; gelation; pH condition; salt ions; microbial transglutaminase; sulfur-containing amino acids

Acknowledgments

I would like to extend my sincere thanks to all of the members who contributed to the achievement of my PhD dissertation.

It's my fortune under the kind supervision of Prof. Aurore Richel and Prof. Taihua Mu, as well as Dr. Miao Zhang in the past 4 years, who provided me the great opportunity to realize the fascinating and challenging work on protein chemistry.

I am grateful to all the staff of Department of Biomass and Green Technologies, Gembloux Agro-Bio Tech, University of Liege. Thanks for their facilitation, warm guidance and help assisted to better orient various aspects of my work and life in Europe.

I am also thankful to all the members of the Laboratory of Food Chemistry and Nutrition Science, Institute of Food Science and Technology, Chinese Academy of Agricultural Sciences. Thanks for providing me with a convenient and friendly research environment.

Unspeakable gratitude to my dear friends, thanks for not abandoning me at hard moment whenever I suffer from much pressure, confusion and disappointment, and support me with endless courage and confidence.

Special thanks to my family members, who enabled me to accomplish this task through their moral support, love and prayers.

Zhongkai ZHAO

June, 2019 in Gembloux, Belgium

Table of contents

List of Figures

List of Tables

Table sequence

Chapter VII /

List of Abbreviations

Abbreviation sequence	
Vocabulary abbreviations	**SPP,** sweet potato protein **HHP,** high hydrostatic pressure **Ho,** surface hydrophobicity **FI,** fluorescence intensity **-SH-,** sulfhydryl group **-SS-,** disulfide bond **LVER,** linear viscoelasticity range **G′,** storage modulus; **G″,** loss modulus; **To,** onset denaturation temperature **Tp,** peak denaturation temperature **Td,** final denaturation temperature **ΔH,** denaturation enthalpy (J/g) **MTGase,** microbial transglutaminase **T_{gel},** gelation point **T_2,** transverse relaxation time **CPMG,** Carr-Purcell-Meiboom-Gill **RF,** resonance frequency **RG,** receiver gain **GDL,** glucono-δ-lactone
Chemical abbreviations	**ANS,** 1-anilinonaphthalene-8-sulfonic acid **DTNB,** 5, 5′-dinitrobis (2-nitrobenzoic acid) **EDTA,** ethylene diamine tetraacetic acid **SDS,** sodium dodecyl sulfonate
Technology abbreviations	**CD,** circular dichroism **SEM,** scanning electron microscopy **DSC,** differential scanning calorimetry **FTIR,** fourier transform infrared spectroscope **WHC,** water-holding capacity **SDS-PAGE,** sodium dodecyl sulfate polyacrylamide gel electrophoresis **NMR,** nuclear magnetic resonance

Chapter I

General introduction

Chapter I General introduction

Abstract

This chapter provides an overview of frame structure of the thesis with a brief description on sweet potato utilization in China and the consideration of experimental design by recycling SPP element. The objective of the present study correlated to the combination treatment of HHP with pH conditions, salt ions, microbial transglutaminase (MTGase) and sulfur-containing amino acids were introduced. In addition, the research technology roadmap and preparation of SPP were also highlighted.

Keywords

Utilization; Protein recycling; Objective; Technology roadmap

1. Background

Sweet potato (*Ipomoea batatas* [L]. Lam) is a dicotyledonous plant belongs to the morning glory family (*Convolvulaceae*), and has long been utilized for vegetable consuming, starch processing and manufacture of alcohol in China (Mohanraj, & Sivasankar, 2014). As the leading country of sweet potato production in the world, China accounts for 63.84 % and 90.49 % of total output worldwide and in Asia, respectively (FAOSTAT, 2017). About 55 % of the production is normally applied for starch processing (Zhang, Wang, & Liu, 2009). A great deal of effluent thus produced along with starch processing, which contains approximately 1.5 % crude protein fractions but is normally discarded, resulting in environmental pollution and resource waste (Mu, Tan, & Xue, 2009). Recycling the protein element from starch processing waste water, both have environmental and economic concerns.

According to our previous studies, SPP has high nutritive values, good physicochemical properties, emulsifying property, antioxidant activity (*in vitro*), anticancer activity (*in vitro and in vivo*) and certain gelation properties, therefore can be developed as an interesting protein resource (Sun, Mu, Zhang, & Arogundade, 2012; Guo & Mu, 2011; Zhang, Mu & Sun, 2014; Li, Mu & Deng, 2013; Arogundade, Mu, & Añón, 2012).

Indeed, food products are complicated. The ability of protein to form a viscoelastic gel makes it suitable to adjust the textural behavior of food products, and also could make the improvement in their functional properties, such as water absorption, thickening, binding, emulsifying and foam-stabilizing activities (Baier, & McClements, 2005). However, as an undeveloped protein resource, no information about gelation properties of SPP is currently available. Moreover, gelation behavior of SPP element affected by different factors is still unclear.

Nowadays, the increasingly health-conscious consumers are demanding high quality food with fresh-like sensory and additive free attributes, which led to the development of non-thermal food processing technologies. As the most praiseworthy commercialized non-thermal processing technology, high hydrostatic pressure (HHP) has been successfully applied in preservation and sterilization of milk, meat, fruit and vegetable products at an industrial scale, due to its microbial inhibition, low price, as well as the less requirement for food shape (Huang, Wu, Lu, Shyu, & Wang, 2017). In addition, literature has been widely reported that HHP showed a positive effect on unfolding, aggregation and gelation for different vegetable proteins, such as soy bean and walnut protein, which provide a new consideration for us by using HHP technique for SPP gelling analysis (Tang, & Ma, 2009; Qin, et al., 2013).

Thus, in present study, the influence of four main factors combined with HHP treatment on structure and gelation properties of SPP were investigated, corresponding to the environmental factors (pH conditions), functional additives (salt ions), specific enzymatic cross-linking (Microbial transglutaminase) and functional nutrient supplements (sulfur-containing amino acids) concerns, respectively. Our findings would be of great help for understanding the gelling behaviors of SPP with different factors, and also might be useful for providing basic

information about HHP, and handling of SPP as a potential functional ingredient in gel-like food.

2. Objective

The objectives of this study are as follows:

(1) To investigate effects of HHP on chemical forces (surface hydrophobicity, zeta potential, sulfhydryl group), structure, rheological properties and gelation properties of SPP as affected by HHP (250, 400 and 550 MPa) at below (pH 3.0), near (pH 6.0) or far away from (9.0) the isoelectric point of SPP (4.0), respectively.

(2) To investigate effects of HHP (400 MPa) on chemical forces, structure and rheological properties of SPP in the presence of monovalent (NaCl) or divalent salts ($CaCl_2$, $MgCl_2$) at different concentrations, as well as textural properties, water holding capacity, mobility and water distribution of SPP gels after HHP treatment.

(3) To investigate effects of HHP (250, 400 and 550 MPa) combined with MTGase treatment on secondary structure, molecular weight characteristics, particle size distribution and thermal properties of SPP, as well as textural properties, water mobility and distribution of SPP gels.

(4) To identify changes in structural modification and gelation behavior of SPP affected by L-cysteine or L-cystine under HHP (400 MPa), for a better understand of the essential and functional role of additive sulfur-containing amino acids on SPP gelation behaviors.

3. Outline

Chapter I General introduction (current chapter).

In this chapter, the basic information about the research context, objective of present studies, structure of the thesis, research technology roadmap, and the preparation of SPP were introduced.

Chapter II Factors affecting gelation properties of sweet potato protein: A Review.

In this chapter, the details about SPP and research background were introduced. Meanwhile, the factors affecting gelation properties of SPP were also reviewed, mainly focused on HHP treatment, pH, salt, microbial transglutaminase and sulfur-containing amino acids, respectively.

Chapter III Effects of pH and high hydrostatic pressure on structure and gelation properties of sweet potato protein.

In this chapter, effects of HHP (250, 400 and 550 MPa) combined with three different pH values on structure and gelation properties of SPP were investigated, corresponding to the pH condition at below (pH 3.0), near (pH 6.0) or far away from (pH 9.0) the isoelectric point of SPP (pH 4.0), respectively.

Chapter IV Effects of salt and high hydrostatic pressure on structure and gelation properties of sweet potato protein.

In this chapter, the commonly used monovalent salt of NaCl, and divalent salt of $CaCl_2$ in the food industry was selected. As well as magnesium salt was also taken into consideration, due to its protective function in human heart blood vessels and the ability to partially substitute for sodium salt to improve the gel textural properties of proteins. Consequently, effects of HHP (400 MPa) treatment combined with monovalent (NaCl) or divalent ($CaCl_2$ and $MgCl_2$) salts in different concentrations on structure and gelation properties of SPP were investigated.

Chapter V Effects of microbial transglutaminase and high hydrostatic pressure on structure and gelation properties of sweet potato protein.

As an efficient and low-cost gelation improver, MTGase has been successfully applied in reconstruction of meat products and dairy products manufacturing in China, by catalyzing the covalent cross-linking of proteins between γ-carboxamide groups of glutamine residues and ε-amino groups of lysine residues. SPP is rich in glutamic and lysine acid residues, which might be an interesting substrate for MTGase catalysis. On the other hand, considering that the enzyme activity of MTGase could be affected by HHP treatment. Moreover, the enzymatic catalysis strongly depend on the applied pressure conditions, thus effects of HHP (250, 400 and 550 MPa) combined with subsequent MTGase catalysis on structure and gelation properties of SPP were designed.

Chapter VI Effects of sulfur-containing amino acids and high hydrostatic pressure on structure and gelation properties of sweet potato protein

In this chapter, effects of 400 MPa treatment combined with sulfur-containing amino acids (L-cysteine or L-cystine) in different concentrations (0.1, 0.5 and 1.0 %) on structure and gelation properties of SPP were studied.

Chapter VII General discussion, conclusion and future perspective

4. Research technology roadmap

The present studies are mainly focused on two parts: protein dispersion system (chemical forces, secondary structure, thermal properties and rheological properties) and protein gels (gel rheological properties, textural properties, gel microstructure and water distribution). The research technology roadmap is shown in Fig. 1-1.

5. SPP preparation

Sweet potato cultivar Shangshu No. 19 (starch type, white species) was used as the raw material for protein extraction in present study. SPP was prepared as described according to our previous reports by Arogundade & Mu, (2012) with slight modification (Fig. 1-2). Simply, freshly peeled sweet potato tuberous roots were grounded with 0.1 % sodium bisulfite solution (for color protection) at a solid-to-solvent ratio of 1:2. After that, the slurry was sieved with cheese cloth (0.15 mm pore diameter) to remove the residues, and centrifuged at 10,000 *g* for 45 min to collect clear supernatant. The pH condition of supernatant was then adjusted to 4.0 (using 2.0 mol/L HCl), and centrifuged at 6,000 *g* for 30 min to collect the precipitate, followed by re-solubilizing precipitate in distilled water at pH 7.0 by

using 2.0 mol/L NaOH at a sample-to-solvent ratio of 1:3, and centrifuged at 10,000 *g* for 45 min again. The final collected clear supernatant was used for ultrafiltration, and lyophilized it to obtain SPP power, which with a high purity of 92.95 % in a dry weight basis.

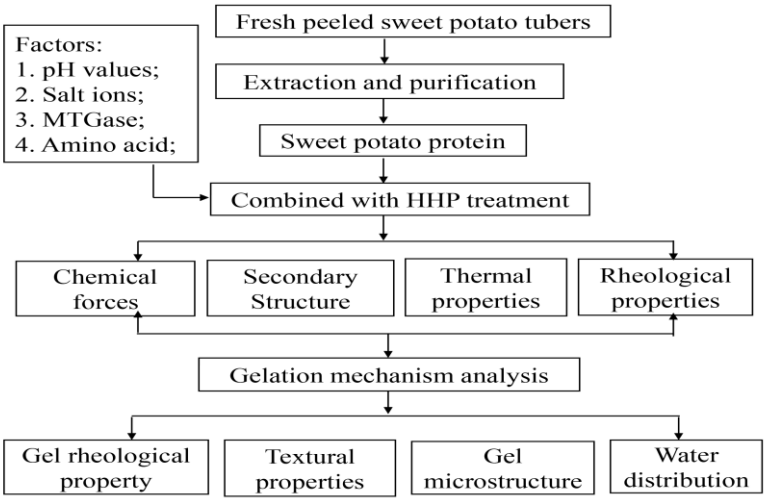

Fig. 1-1 Technology roadmap of present thesis

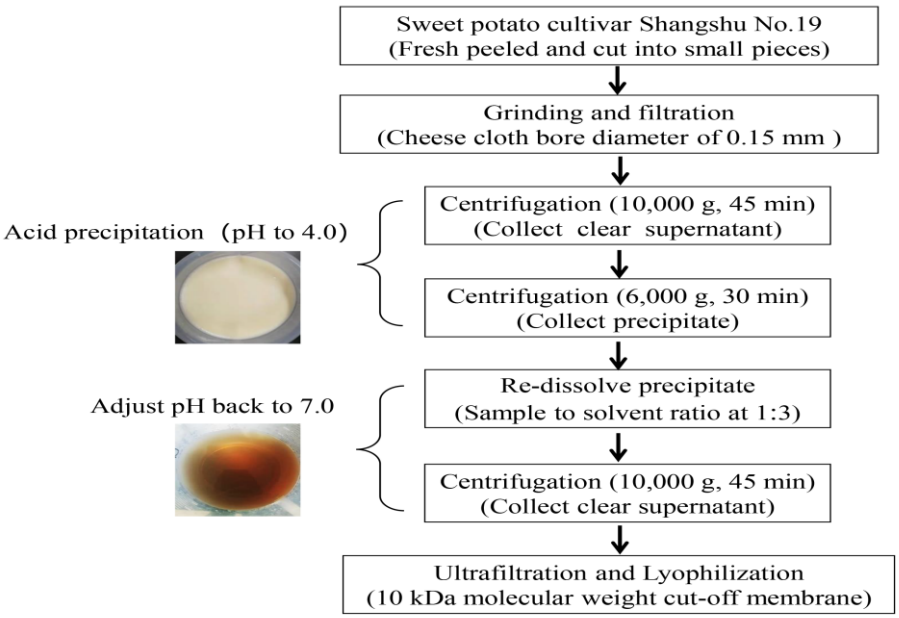

Fig. 1-2 Preparation of SPP

Reference

Arogundade, L. A., & Mu, T. H. (2012). Influence of oxidative browning inhibitors and isolation techniques on sweet potato protein recovery and composition. *Food Chemistry*, 134 (3), 1374-1384.

Arogundade, L. A., Mu, T. H., Añón, M. C. (2012). Heat-induced gelation properties of isoelectric and ultrafiltered sweet potato protein isolate and their gel microstructure. *Food Research International*, 49, 216-225.

Baier, S. K., & McClements, D. J. (2005). Influence of cosolvent systems on the gelation mechanism of globular protein: thermodynamic, kinetic, and structural aspects of globular protein gelation. *Comprehensive Reviews in Food Science and Food Safety*, 4 (3), 43-54.

FAOSTAT. (2017). Production quantity [Internet]. Food and Agricultural Organization. http://www.fao.org/faostat/en/#data/QC. Accessed 01/06/19.

Guo, Q., & Mu, T. H. (2011). Emulsifying properties of sweet potato protein: effect of protein concentration and oil volume fraction. *Food Hydrocolloids*, 25 (1), 98-106.

Huang, H. W., Wu, S. J., Lu, J. K., Shyu, Y. T., & Wang, C. Y. (2017). Current status and future trends of high-pressure processing in food industry. *Food Control*, 72, 1-8.

Li, P. G., Mu, T. H., & Deng, L. (2013). Anticancer effects of sweet potato protein on human colorectal cancer cells. *World Journal of Gastroenterology*: WJG, 19 (21), 3300.

Mohanraj, R., & Sivasankar, S. (2014). Sweet Potato (*Ipomoea batatas* [L.] Lam)-A valuable medicinal food: A review. *Journal of Medicinal Food*, 17 (7), 733-741.

Mu, T. H., Tan, S. S., & Xue, Y. L. (2009). The amino acid composition, solubility and emulsifying properties of SPP. *Food Chemistry*, 112 (4), 1002-1005.

Qin, Z., Guo, X., Lin, Y., Chen, J., Liao, X., Hu, X., & Wu, J. (2013). Effects of high hydrostatic pressure on physicochemical and functional properties of walnut (Juglans regia L.) protein isolate. *Journal of the Science of Food and Agriculture*, 93 (5), 1105-1111.

Sun, M., Mu, T., Zhang, M., & Arogundade, L. A. (2012). Nutritional assessment and effects of heat processing on digestibility of Chinese sweet potato protein. *Journal of Food Composition and Analysis*, 26 (1-2), 104-110.

Tang, C. H., & Ma, C. Y. (2009). Effect of high pressure treatment on aggregation and structural properties of soy protein isolate. *LWT-Food Science and Technology*, 42 (2), 606-611.

Zhang, M., Mu, T. H., Sun, M. J. (2014). Purification and identification of antioxidant peptides from sweet potato protein hydrolysates by Alcalase. *Journal of Functional Foods*, 7, 191-200.

Zhang, L., Wang, Q., & Liu, Q. (2009). Sweet potato in China. In The sweet potato (pp. 325-358). Springer, Dordrecht.

Chapter II

Factors affecting gelation properties of sweet potato protein: A review

Chapter II Factors affecting gelation properties of sweet potato protein: A review

Abstract

Protein gelation is essential to make desirable sensory and textural structure in food by adjusting water-holding capacity, thickening and connection. Gelation can be achieved by a driving force to unfold the native protein structure, followed by an aggregation retaining a certain degree of order in the protein matrix, and further cross-linked between protein molecules. Gelation involves in the protein-protein and protein-solvent interactions. China is rich in sweet potato resource. Gelation behavior of SPP is varied by processing conditions, and sensitive to the environmental factors. In this study, the main external factors effect on gelation properties of SPP have been reviewed, including HHP, pH values, salt ions, MTGase and sulfur-containing amino acids, to have a better understand on potential applications of SPP as a functional supplement in food.

Keywords

Sweet potato protein; High hydrostatic pressure; Gelation properties; Environmental factors; Chemical forces; Interactions

1. Introduction

1.1. Sweet potato

Sweet potato (*Ipomoea batatas* [L]. Lam) is a dicotyledonous plant belongs to the morning glory family (*Convolvulaceae*), originates from tropical America, and is widely cultivated in the southern part of the United States, tropical America and the Caribbean, the warmer islands of the Pacific, Japan, and parts of Russia (Bovell-Benjamin, 2007). It has long been utilized for vegetable consuming, starch processing and manufacture of alcohol (Oke & Workneh, 2013). As one of the most promising economic crops, China accounts for 63.84 % and 90.49 % of total output worldwide and in Asia, respectively (FAOSTAT, 2017). The production of sweet potato is approximately 0.72 million tons per year, which becomes the fifth major cultivated crops in China, and inferior to rice, corn, wheat and potato (FAOSTAT, 2017).

Fig. 2-1 Sweet potato in different varieties

The utilization of sweet potato can be identified by the color of the tubers range from white to orange and occasionally purple inside (Fig. 2-1), corresponding to the characteristic of high starch content, abundant reducing sugar and edible pigment (Leksrisompong, Whitson, Truong & Drake, 2012). Regarding to the sweet potato consumption (Fig. 2-2), 55 % of total production is normally applied for starch processing, 30 % production is planned for fresh eating, 10 % is used to fodder, seed and primary products (e.g. chips, mash, dry cubes), and another 5 % is available to starch products (e.g. starch noodles and vermicelli), respectively (Cui, et al., 2007; Mohanraj & Sivasankar, 2014).

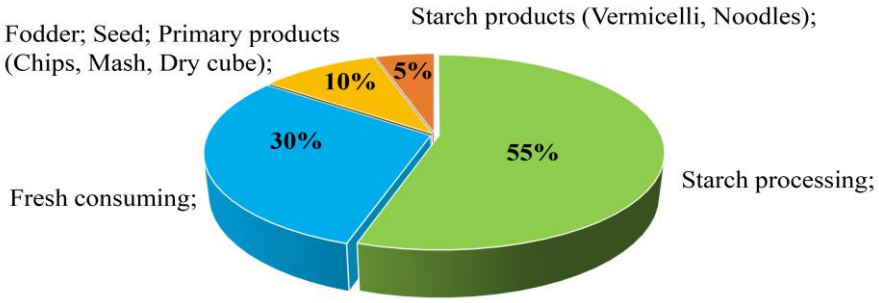

Fig. 2-2 Sweet potato processing proportion in China

Moreover, as a homology resource of food and medicine, the remarkable functionality of sweet potato is attributed to the high level of valuable compounds in white, orange and purple species, e.g. protein, β-carotene and polyphenols (Park, et al., 2016). These bioactive compounds make sweet potato become a star food material with available benefits for human body, such as antioxidant and anticancer activities (Zhang, Mu & Sun, 2014; Li, Mu & Deng, 2013), meanwhile provide a series of functionality in adjusting food qualities, especially for emulsifying (Guo & Mu, 2011), gelation, textual and holding capacity (Arogundade, Mu & Añón, 2012).

1.2. SPP

In recent years, market demand has steadily grown for protein ingredients, especially for elements those have multiple benefits, which can be act as a nutritional supplement and also have functional properties (Betoret, Betoret, Vidal & Fito, 2011). Vegetable protein receives increasing interests due to their various health beneficial functions, e.g., nutritional diet, intervention of obesity-induced metabolic dysfunction, and antioxidant activities, etc. (Sarmadi & Ismail, 2010; Abuajah, Ogbonna & Osuji, 2015; Lin, et al., 2017). Incidentally, high acceptability and desirable workability make vegetable protein commonly used in dairy beverage and baking sweets, even gradually replacing some meat ingredient for reconstituted meat products or sea food (Asgar, et al., 2010).

Sweet potato tuberous roots contain about 1.73-9.14 % (w/w) protein element on a dry weight basis, and 0.49-2.24 % (w/w) on a wet weight basis, respectively (Sun, Mu, Zhang & Arogundade, 2012). As a major resource of starch, white fleshed cultivars are popular in starch manufacturing. A great deal of effluent will be produced along with starch processing, which includes approximately 1.5 % (w/w) crude protein fractions but is normally discarded, resulting in environmental pollution and resource waste (Mu, Tan & Xue, 2009). Considering the potential valuable of SPP, the protein elements recovered from agro-waste should not be ignored, particularly in developing countries where daily dietary protein intake is relatively low (Rudra, Nishad, Jakhar & Kaur, 2015).

SPP, generally known as “Sporamins”, with a molecular weight of 25 kDa under reducing sodium dodecyl sulfate polyacrylamide gel electrophoresis (SDS-PAGE) conditions (in the presence of β-mercaptoethanol as reducing agent) (Fig. 2-3), which can be divided into Sporamin A (31 kDa) and Sporamin B (22 kDa) under non-reducing SDS-PAGE conditions (Mu, Tan, Chen & Xue, 2009).

SPP is mainly a storage protein with ~80% being soluble part (Hattori, et al., 1985). According to the amino acid sequencing analysis, the primary structure of SPP is composed of about 229 amino acids residues, of which there are two groups of intra-molecular disulfide bond (-S-S-) exist in the 45th and 94th cysteine (Cys 45-Cys 94), 153th and 160th cysteine (Cys 153-Cys 160), respectively (Wang, Nie & Zhu, 2016). The structural difference make SPP easily identified from other protein varieties, and may even vesting it remarkable physicochemical and functional properties, such as foaming (Li & Mu, 2012), emulsifying (Khan, et al., 2015) and gelation properties (Arogundade, Mu & Añón, 2012).

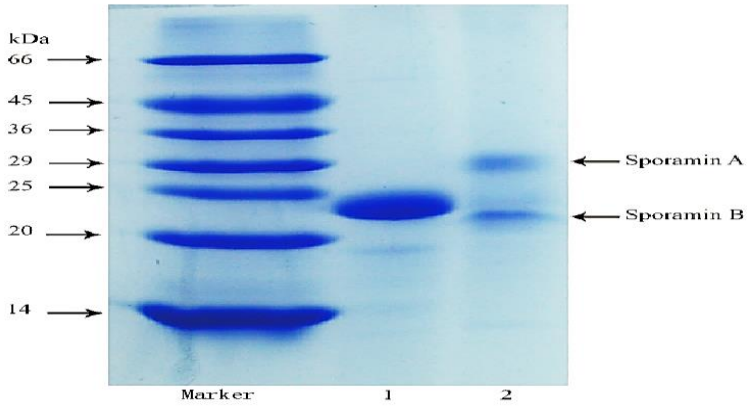

Fig. 2-3 Molecular distribution of SPP under reducing (lane 1) and non-reducing (lane 2) SDS-PAGE conditions

SPP is rich in essential amino acids, and presents high nutritive values compare to other vegetable protein element (Ishida, et al., 2000; Mu, Tan & Xue, 2009). The ratio of essential amino acids (EAA) to total amino acid (TAA) of SPP was 43.27 % (Table 2-1), which is higher than the reference value of 40.00 % recommended by FAO/WHO (1991), thus it can be developed as a good nutritional supplement being potentially applied in functional food.

1.3. Gelation properties of proteins

The ability of protein element to form a viscoelastic gel makes it suitable to adjust textural behavior of food products, and also for improved functional properties of water absorption, thickening, binding, emulsifying and foam-stabilizing actitivies (Gosal & Ross-Murphy, 2000; Van Vliet, Lakemond & Visschers, 2004). Many vegetable proteins have been widely reported as good gelation matrix, e.g. soy protein, pea protein and canola protein, etc. (Maltais, Remondetto, Gonzalez & Subirade, 2005; Sun & Arntfield, 2012; Pinterits & Arntfield, 2008). Gelation is basically including two-step process of denaturation and aggregation of proteins (Totosaus, Montejano, Salazar & Guerrero, 2002), and commonly involved in both non-covalent and covalent reactions (Table 2-2).

Gelation process is identified as the aggregation of denatured molecules with a certain degree of order and a balance between attractive and repulsive forces, resulting in the formation of a continuous network (Brodkorb, Croguennec, Bouhallab & Kehoe, 2016). Gel-induction is obtained by series of physical and chemical ways (Table 2-3). Within different gelation methods, gel has been traditionally achieved by heating process (Durand, Gimel & Nicolai, 2002). Meanwhile, heat-induced gelation is the most commonly studied in food science and technology, due to it is responsible for the structure present in daily food (Han, Wang, Xu & Zhou, 2014).

Table 2-1 Amino acid composition of native SPP

Amino acid composition		Percentage (%)
Essential amino acid (EAA)	Lys	4.00
	Thr	4.90
	Val	6.09
	Met	1.61
	Ile	4.23
	Leu	5.36
	Phe	5.95
	His	1.21
Non-essential amino acid (NEAA)	Glu	7.60
	Asp	13.62
	Ser	5.10
	Gly	3.71
	Ala	3.83
	Cys	1.34
	Tyr	4.06
	Arg	4.47
Total amino acid (TAA)		77.08
EAA		33.35
NEAA		43.73
EAA/TAA		43.27

* Values are means of three determinations, and the variety is Shangshu No. 19.

As temperature increases, globular protein is partly unfolding, and previously hidden reactive groups are exposed, which enhances the inter-molecular interactions, such as protein-protein interactions, surface hydrophobicity, and electrostatic interactions (Clark, Kavanagh & Ross-Murphy, 2001; Alting, De Jongh, Visschers & Simons, 2002). Meanwhile, heat-induced partial or complete denaturation of protein structure is necessary for gelation. During the denaturation, protein unfolding gives extended chains and exposes some of hydrophobic parts to the solvent (Fitzsimons, Mulvihill, & Morris, 2007). When the temperature is increased to the gelation point, covalent bonds are formed between proteins to produce a continuous network (Renkema, & van Vliet, 2002). Chemical forces, such as hydrogen bonds, disulfide linkages, surface hydrophobicity and electrostatic interactions are essential to gel pre-network formation (Sun & Arntfield, 2012). At the end of the cooling stage, a large number of hydrogen bonds are formed, which makes great contribution to the three-dimensional network of final gel matrix (O'Kane, et al., 2004).

1.4. Protein gelation influence factors

Protein network is generally formed via both non-covalent and covalent cross-links, such as electrostatic interactions, hydrophobic interactions or hydrogen bonds, and disulfide bonds (Dondero, Figueroa, Morales & Curotto, 2006). Many physical (high pressure) and chemical processes (e.g. acidification, enzymatic cross-linking, the usage of salts and urea) can be similarly formed protein gels by causing modifications in protein-protein and protein-solvent interactions (Totosaus, Montejano, Salazar & Guerrero, 2002). Notably, the characteristics of each gel are dependent upon different intrinsic and extrinsic factors (Table 2-4).

Compared to extrinsic factors, intrinsic factors are decided by the gene coding and protein resources. Thus, gelation behavior of protein matrix food is mainly controlled by adjusting the extrinsic conditions, and focused on processing technologies, environmental factors, as well as the usage of functional additives, specific enzyme catalysis and functional nutrient supplements, respectively (Sun & Holley, 2011).

1.4.1. HHP

Increasing health concerns demand better food quality, including nutritional value, freshness, flavors and improved food texture. Healthy label food require to be natural and fresh as well as less chemical additives, which has attracted widespread attention among consumers, and also increases the application of emerging non-thermal processing technologies, such as HHP, pulsed electric field, pulsed light, electron beam, plasma, and modified atmosphere packaging, etc. (Pereira & Vicente, 2010). Among, HHP is the most successfully commercialized technologies.

As a novel non-thermal processing technique, HHP has been successfully used to extend the shelf life of fresh and processed food products with minimal impact on its sensory and nutritional values (Huang, et al., 2017). Industrial application of HHP is depending on the desired objective, and mainly performed in a pressure range of 100-800 MPa. Generally, food matrix is hermetically vacuum-sealed in a flexible container and pressurized at room or low temperature by using a liquid (typically use water) as pressure transfer medium, subjecting the interior and surface of the food to achieve pasteurization or structure modification (Chawla, Patil & Singh, 2011).

Compared to the traditional thermal treatment, HHP is not affected by the packaging form and volume of the products, thus it could be applied in food with different statues. In addition, HHP ensures the microbial safety of food without adding preservatives and allows the processed food to maintain natural flavors and nutritional value of the original food material. Therefore, HPP is recognized as a minimal processing technology that ensures both safe and flavor concerns. Meanwhile, HHP could alter molecular interactions (e.g. protein-protein, protein-solvent and solvent-solvent interaction) and some of the epitope structures, leading to the improved functional properties (i.e. emulsifying, gelation, foaming properties, etc.), and to weaken the allergenicity of food proteins (Achouri, & Boye, 2013).

Table 2-2 Interactions involved in stabilizing structure and gelation of protein

Interaction type		**Approach and pathway**	**Reference**
Non-covalent bond	Hydrophobic interaction $-CH_3\cdots CH_3-$	Protein surface hydrophobicity	Singh & Havea, 2003;
	Hydrogen bonds $-H\cdots O\cdots H-$ $-H\cdots N\cdots H-$	Water molecule both as hydrogen bond donor and accepter	Wang, et al., 2017;
	Electrostatic-salt links $-COO^{-}\cdots{}^{+}H_3N-$	Electrostatic interactions	Riebroy, et al., 2008;
	Metal ion bridges $-COO^{-}\cdots Ca^{2+}\cdots {}^{-}OOC-$	With presence of salt ions	
Covalent bond	Disulfide bonds -S-S-	Sulfhydryl oxidation	Liu, Zhao, Xie & Xiong, 2011;
	γ-glutamyl $-CH_2-CH_2-CO\cdots NH-CH_2-CH_2-$	Inter-protein cross-linking	

Table 2-3 Gel formation of protein ingredient

Gel-induction type		**Mechanism**	**Reference**
Physical methods	Thermal process	Globular protein partially unfolded and further aggregated to form a gel network by a certain order.	Han, Wang, Xu & Zhou, 2014;
	High hydrostatic pressure	High hydrostatic pressure (>200 MPa) make contribution to the cross-linkage of protein duo to the exposure of buried hydrophobic and sulfhydryl groups.	Cao, Xia, Zhou & Xu, 2012;
Chemical methods	Salt ions	Salt ions significantly effect on the electrostatic interactions, and leading the modification of secondary structure of proteins.	Maltais, Remondetto, Gonzalez & Subirade, 2005;
	Urea	Urea promotes inter-molecular oxidation of thiol groups.	Cho, Heuzey, Bégin & Carreau, 2006;
	Acid-induction	Acid condition induces denaturation to form clusters or aggregates.	Riebroy, et al., 2008;
	Enzymatic induction	Enzyme catalyzes covalent intra- or inter-molecular cross-linking of proteins.	Pinterits & Arntfield, 2008;

Table 2-4 Protein gelation influence factors

Factors type			**Approach and pathway**	**Reference**
Intrinsic factors	Electrostatic interaction		Electrostatic repulsion or attractive forces	Wang, et al., 2017;
	Hydrophobicity		Nonpolar amino acid residues	
	Disulfide bonds		Thiol-disulfide interchange	
	Amino acid composition		Coagulum (<31.5 % of hydrophobic residues) or translucent gel (>31.5 % of hydrophobic residues)	Totosaus, Montejano, Salazar & Guerrero, 2002;
Extrinsic factors	Protein concentration		Proportional to cross-linking of macromolecules	Singh & Havea, 2003;
	Heating process		Heating temperature, time, arising speed	
	HHP		Pressure level, holding time, temperature, pressure transfer medium	Cao, Xia, Zhou & Xu, 2012;
	pH condition		Isoelectric point (pH is higher or lower than Ip)	Clark, Kavanagh & Ross-Murphy, 2001;
			Acid or alkaline conditions	
	Additives	Salt ions	Salt type (monovalent or divalent salt) and ionic strength;	
		Enzyme	Microbial transglutaminase, laccase;	Dondero, Figueroa, Morales & Curotto, 2006;
		Amino acid	Lysine, L-cystine, L-cysteine;	Cando, Moreno, Borderías & Skåra, 2016;

HHP can affect the sol-gel transition by modifying the native volume of proteins, which is composed by the volume of constituent atoms (compositional volume), internal cavities, and the contribution of solvation (Totosaus, Montejano, Salazar & Guerrero, 2002). Effects of HHP on proteins are related to the rupture on non-covalent interactions within protein molecules, as well as the subsequent reformation of intra- and inter-molecular bonds in protein (Cao, Xia, Zhou & Xu, 2012). HHP is valuable to modify the structure and alter the denaturation, aggregation and gelation of protein, resulting in an improvement of textural properties and water holding capacities (Tang & Ma, 2009).

The gelation properties of protein affected by HHP treatment mainly based on the pressure-induced structure modification and chemical forces or interactions changes. For the pressurization, the pressure level, time and working temperature (normally at room temperature) are the most important indicators, particularly for applied pressure level. Normally, the quaternary structure of protein is mainly stabled by hydrophobic interactions that are very sensitive to the pressure. The split of quaternary structure occurred in the range of 150-200 MPa. Significant changes in the tertiary structure are observed beyond 200 MPa. Secondary structure is affected by 250-700 MPa, and more than 700 MPa pressure could make the irreversible denaturation. Particularly, the primary structure of protein element is composed of amino acid sequences, and highly resistant to pressure conditions. To destroy primary structure of protein, the pressure level should at least reach up to 1000-1500 MPa. Therefore, the pressure-induced denaturation or modification in protein processing (below 800 MPa) is not involved in primary structure changes (Table 2-5), which is mainly focused on the secondary, tertiary, and quaternary structure changes (Tang & Ma, 2009).

In addition, HHP could significantly alter chemical forces or molecular interactions involved in protein systems, and even effects on the functional bonding activities, like thiol-disulfide interchange reactions (Table 2-6). HHP induced cross-linking was occurred under high level pressure conditions (more than 200 MPa), which can be enhanced by covalent disulfide bonding (Considine, et al., 2007). Notably, disulfide bonds among polypeptide chains involved in protein gelation due to its functionality in increasing the apparent chain length of the polypeptide, rather than acting as an initial network stabilizer. HHP treatment is efficiently in promoting the unfolding of protein structure and inducing the further aggregation by the formation of disulfide linkages (-S-S-), thus produce a good gel construction (Hwang, Lai & Hsu, 2007). Furthermore, the unfolding induced by pressurization along with the exposure of functional groups, like sulfhydryl groups (-SH-), which can strengthened protein surface interactions and lead to improvement on gelation, mechanical/texture and water holding properties.

1.4.2. pH condition

Protein molecules are positive or negative charged in natural (Alting, De Jongh, Visschers & Simons, 2002). The net charge on the surface of protein molecule is influenced by pH values, and sensitive to the isoelectric point (pI), where the net charge of protein molecule is close to zero.

Food processing is usually within a wide pH range of 2-10. Any changes in pH condition could ultimately affect the gelation characteristics of protein by interfering with protein solubility, heat stability and protein-protein interactions during gel formation (Clark, Kavanagh & Ross-Murphy, 2001).

Based on the theory of electrostatic interactions, the acid-induced gelation of protein has been widely applied in dairy products manufacturing (i.e. yogurt and sol). Compare to heat-induced gels, acidic gels achieved by heating process to form aggregates first, then reducing the electrostatic repulsion between biomolecules by decreasing the pH level close to the pI of the protein element (Kim, Varankovich & Nickerson, 2016). Lowering the pH condition toward the pI may have also exposed inner hydrophobic groups, leading to the randomly aggregate by increased hydrophobic interactions (Mu, Tan, Chen & Xue, 2009). Although the protein-protein interaction and rheological properties has been enhanced by low pH values, the protein particle becomes less charged with a weaken stability.

Considering the functionality of gelata in adjusting the texture, quality and appearance of food matrix, highly hydrated protein gels have received increasing attention. As the pH level extended far from the pI of protein in food, an increase in net negative charge causes electrostatic repulsion between protein molecules, which provides more binding sites for water molecules and increases the surface available for hydration (Mäkinen, Zannini & Arendt, 2015). The interactions between proteins and solvent therefore increase, and more water molecules are bound in the capillaries of protein matrix. The electrostatic-repulsive forces hinder the formation of random aggregates, resulting in the formation of linear polymers and a compact gel microstructure.

It is known that the water-holding capacity of protein ingredient normally increases as pH differs from the isoelectric point. The increase in net charge creates more sites of hydrogen bonding with the surrounding water. Typically, gels formed at neutral (pH 7.0) or alkaline condition were stronger than more acidic gels, attributing to electrostatic repulsive forces and swelling that occurs in protein as pH increases.

1.4.3. Salt ions

Recent trends demand that healthy food are interested in products with reduced sodium chloride, especially for meat products, which still manufactured with high salt addition (1.5–2.5 %) for desirable textural and improved sensory properties (Shao, et al., 2016). Although salt ions are essential to stabilize food structure and sensory qualities, excessive intake of salt indeed causes imbalance of metabolic and a series of diseases, and may have influence on protein functionalities.

Protein gelation is the formation of a three-dimensional network through the cross-linking of polypeptide chains. The gelling process involve different molecular forces, including hydrogen bonds, ionic/electrostatic interaction, disulfide bonds, and hydrophobic associations. The electrostatic interaction is essentially affected by different type of salts (monovalent or divalent) and ionic strength, which is mainly correlated to the electrostatic shielding effects, non-specific charge neutralization, and direct ion-macromolecule interactions (Ako, Nicolai & Durand, 2010).

Monovalent and divalent salt ions both screen electrostatic interactions between charged protein molecules. It is believed that ion specific effects arise from changes in the hydrophobic core of the proteins. Salt ions affect electrostatic interactions by interacting with charged groups on protein surface at low ionic strength, while the ion specific effects become prominent as concentration increases. Moreover, the microstructure of the gel matrix are highly depend on the ionic strength, where a fine-stranded/ filamentous type gel network is formed with lower salt addition, while high salt levels have been shown to form mixed network structures (Chen, Zhao, Chassenieux & Nicolai, 2017).

Compare to the monovalent salts (i.e. NaCl, KCl, etc.), the divalent salts (i.e. $CaCl_2$, $MgCl_2$, etc.) show more effective on screening electrostatic interactions, and alter the water absorption, swelling and solubility of proteins at much lower concentrations, which may be partially replace the monovalent salts for a lower salt addition in food matrix (Kuhn, Cavallieri & Da Cunha, 2010).

1.4.4. MTGase

The modification of protein element via different methods is available for improving functional properties, such as chemical, physical or enzymatic ways. Due to the mild condition and specific reaction, enzymatic catalysis by MTGase has received increasing interests, even developed for new applications (Kieliszek & Misiewicz, 2014).

As an extracellular enzyme of the transferases class, MTGase (38 kDa) is first isolated from the *Streptoverticillium* sp. strain, and has been commercially produced by traditional microorganism fermentations (Gaspar & de Góes-Favoni, 2015). MTGase acts in a narrow pH ranges of 5.0-8.0, with activity at 40-70 °C, and optimum temperature of 50 °C. As shown in Fig. 2-4, MTGase could efficiently induce the formation of ε-(γ-glutaminyl) lysine isopeptide bonds by catalyzing the acyl-transfer reactions between γ-carboxamide groups of glutamine residues and ε-amino groups of lysine residues (Gaspar & de Góes-Favoni, 2015).

The enzymatic reaction can modify proteins by incorporating amines, and affect intra- and intermolecular cross-links or deamidation, cause profound changes in protein molecular structure, and lead to improved texture, thermal stability, syneresis and gelation. Meanwhile, the catalysis with minimal changes in pH, color, flavor or nutritional quality of food may render food matrix more nutritious due to the possibility of essential amino acids addition (Romeih, & Walker, 2017).

The main industrial applications of MTGase is still in the restructuring of meat products and seafood, to ensure the stability and improved textural properties, as well as lower the cooking loss of material, for an adequate appearance (Gaspar & de Góes-Favoni, 2015). Moreover, the enzyme has also been used in the production of dairy products to prevent syneresis with better water-holding capacities (Romeih, & Walker, 2017). Despite the enzyme's innovative benefits in food production, its industrial use, particularly in derivatives of vegetal origin, is still little exploited.

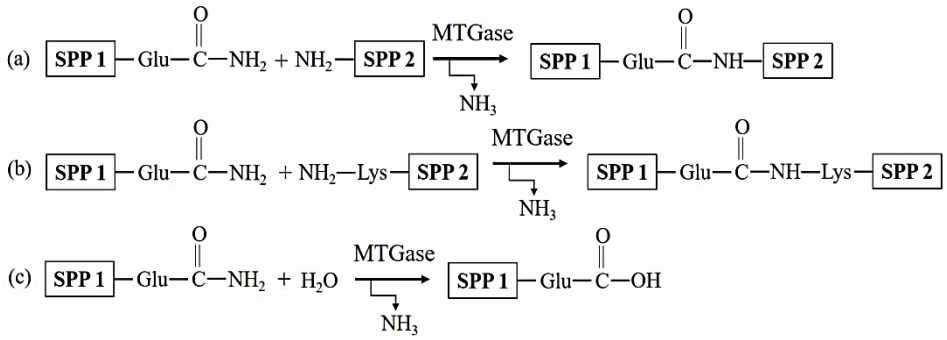

Fig. 2-4 MTGase catalyzed enzymatic reactions: (a) acyl-transfer; (b) cross-linking of lysine and glutamine residues; (c) deamidation

1.4.5. Sulfur-containing amino acids

Amino acids play central roles both as building blocks of proteins and functional supplement. Within the natural amino acids, sulfur-containing amino acids are innovatively considered as availably additives improving functional and nutritional properties of daily food (Brosnan & Brosnan, 2006).

Methionine, cysteine and cysteine are the three main sulfur-containing amino acids (Brosnan & Brosnan, 2006). Although methionine is the initiating amino acid in the synthesis of virtually all eukaryotic proteins, only the cysteine and cysteine are successfully used in food manufacturing (Fig. 2-6), due to their structural particularities in thiol/disulfide groups, which can be act as a mechanical linkage in stabilizing three-dimensional structure of protein molecules (Visschers & de Jongh, 2005).

Considering the great contribution to form disulfide bonds, cysteine plays a crucial role in products processing and protein-folding pathways. As a weak oxidant and thiol group donor, cystine/cysteine maximize the formation of inter protein cross-linking and promote the high molecular weight aggregates, thus could be potentially applied in gel-like food as a nutritional supplement and gel improver.

The addition of low concentrations of sulfur-containing amino acids has been shown to be effective for improving surimi gelation (Cando, Moreno, Borderías & Skåra, 2016). Moreover, additive lysine and cystine significantly improve the water binding capacity and mechanical properties of surimi gels with reduced NaCl concentrations (Cando, Herranz, Borderías & Moreno, 2016). However, no information about the functional role of sulfur-containing amino acids on structure and gelation properties of vegetal proteins is available, even for sweet SPP resources.

Table 2-5 HHP-induced modification on protein structure

Structure type	**Pressure**	**Structural composition**	**Stable forces**	**Reference**
Primary	1000-1500 MPa	Amino acid sequences	Peptide bonds	Wang, Huang, Hsu, & Yang, 2016)
Secondary	250-700 MPa	α-helix, β-sheet, β-turn and random coil	Hydrogen bonds (intra/intro)	Achouri & Boye, 2013;
Super-secondary		α-helix, β-sheet motifs		
Tertiary structure	250 MPa	Monomeric	Hydrophobic/electrostatic interaction	Chawla, Patil & Singh, 2011;
Structural domains		Multimeric protein molecules		
Quaternary	150-200 MPa	Polypeptide chains (subunits)		

Table 2-6 HHP-induced chemical forces or interaction changes in protein systems

Interaction type	**Stable forces**	**Introduction**	**Reference**
Hydrophobic interaction	Protein surface hydrophobicity	HHP could expose interior functional groups and make denaturation of proteins, leading the increase in surface hydrophobicity.	Considine, et al., 2007;
Electrostatic interaction	Zeta potential	Electrostatic interaction correlated to the electrostriction, unfolding and aggregation of biomolecules.	Boye, et al., 1995;
Hydrogen bonds	Intra-/intro-molecular cross-linking	The secondary structure unit of α-helix and β-sheet are respectively stabled by the Intra- and intro-molecular hydrogen bonding.	Huang, et al., 2017;
Covalent bonds	Disulfide linkage	HHP-induced covalent bonding depend on the applied pressure level. Disulfide bond make a great contribution to protein cross-linking.	Cando, Moreno, Borderías, & Skåra, 2016;

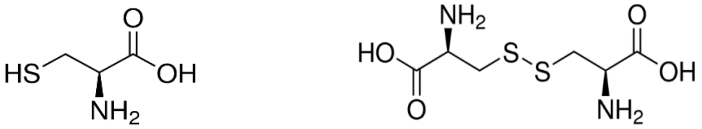

Fig. 2-5 Sulfur-containing amino acids of L-cysteine (life) and L-cystine (right)

2. Conclusion and future trends

Sweet potato is the relatively cheap source of food proteins. Recycling protein element from starch processing waste-water can effectively improve the utilization of by-products. SPP are recognized for their high nutritional values and superior functional properties (i.e. antioxidant activities, emulsifying properties, etc.). Among these functional properties, gel forming ability upon heating is especially important for the application in gel-like food, and can be enhanced by HHP.

Gelation is sensitive to the processing condition, mainly correlated to environmental factors (pH values), functional additives (salt ions), specific covalent cross-linking enzyme (MTGase) and functional nutrient supplement (sulfur-containing amino acids). Although the considerable number of reports about effects of different factors on structure and gelation properties of various vegetal proteins, the mechanisms involved in gelation of SPP still deserve more attention.

Reference

Abuajah, C. I., Ogbonna, A. C., & Osuji, C. M. (2015). Functional components and medicinal properties of food: a review. *Journal of Food Science and Technology*, 52 (5), 2522-2529.

Achouri, A., & Boye, J. I. (2013). Thermal processing, salt and high pressure treatment effects on molecular structure and antigenicity of sesame protein isolate. *Food Research International*, 53 (1), 240-251.

Ako, K., Nicolai, T., & Durand, D. (2010). Salt-induced gelation of globular protein aggregates: structure and kinetics. *Biomacromolecules*, 11 (4), 864-871.

Alting, A. C., de Jongh, H. H., Visschers, R. W., & Simons, J. W. F. (2002). Physical and chemical interactions in cold gelation of food proteins. *Journal of Agricultural and Food Chemistry*, 50 (16), 4682-4689.

Arogundade, L. A., Mu, T. H., & Añón, M. C. (2012). Heat-induced gelation properties of isoelectric and ultrafiltered sweet potato protein isolate and their gel microstructure. *Food Research International*, 49 (1), 216-225.

Asgar, M. A., Fazilah, A., Huda, N., Bhat, R., & Karim, A. A. (2010). Nonmeat protein alternatives as meat extenders and meat analogs. *Comprehensive Reviews in Food Science and Food Safety*, 9 (5), 513-529.

Betoret, E., Betoret, N., Vidal, D., & Fito, P. (2011). Functional foods development:

trends and technologies. *Trends in Food Science & Technology*, 22 (9), 498-508.

Boye, J. I., Alli, I., Ismail, A. A., Gibbs, B. F., & Konishi, Y. (1995). Factors affecting molecular characteristics of whey protein gelation. *International Dairy Journal*, 5 (4), 337-353.

Bovell-Benjamin, A. C. (2007). Sweet potato: a review of its past, present, and future role in human nutrition. *Advances in Food and Nutrition Research*, 52, 1-59.

Brodkorb, A., Croguennec, T., Bouhallab, S., & Kehoe, J. J. (2016). Heat-induced denaturation, aggregation and gelation of whey proteins. *In advanced dairy chemistry* (pp. 155-178). Springer, New York, NY.

Brosnan, J. T., & Brosnan, M. E. (2006). The sulfur-containing amino acids: an overview. *The Journal of Nutrition*, 136 (6), 1636S-1640S.

Cando, D., Herranz, B., Borderías, A. J., & Moreno, H. M. (2016). Different additives to enhance the gelation of surimi gel with reduced sodium content. *Food Chemistry*, 196, 791-799.

Cando, D., Moreno, H. M., Borderías, A. J., & Skåra, T. (2016). Combined effect of high hydrostatic pressure and lysine or cystine addition in low-grade surimi gelation with low salt content. *Food and Bioprocess Technology*, 9 (8), 1391-1398.

Cao, Y., Xia, T., Zhou, G., & Xu, X. (2012). The mechanism of high pressure-induced gels of rabbit myosin. *Innovative Food Science & Emerging Technologies*, 16, 41-46.

Chawla, R., Patil, G. R., & Singh, A. K. (2011). High hydrostatic pressure technology in dairy processing: a review. *Journal of Food Science and Technology*, 48 (3), 260-268.

Chen, N., Zhao, M., Chassenieux, C., & Nicolai, T. (2017). The effect of adding NaCl on thermal aggregation and gelation of soy protein isolate. *Food Hydrocolloids*, 70, 88-95.

Cho, J., Heuzey, M. C., Bégin, A., & Carreau, P. J. (2006). Effect of urea on solution behavior and heat-induced gelationof chitosan-β-glycerophosphate. *Carbohydrate Polymers*, 63 (4), 507-518.

Clark, A. H., Kavanagh, G. M., & Ross-Murphy, S. B. (2001). Globular protein gelation-theory and experiment. *Food Hydrocolloids*, 15 (4-6), 383-400.

Considine, T., Patel, H. A., Anema, S. G., Singh, H., & Creamer, L. K. (2007). Interactions of milk proteins during heat and high hydrostatic pressure treatments-a review. *Innovative Food Science & Emerging Technologies*, 8 (1), 1-23.

Cui, K., Wang, X. M., Song, L. R., Zhou, Q. L., & Liu, Y. L. (2007). Analysis of practical value of sweet potato and prospect in China [J]. *Journal of Jilin Agricultural Sciences*, 3, 10-23.

Dondero, M., Figueroa, V., Morales, X., & Curotto, E. (2006). Transglutaminase effects on gelation capacity of thermally induced beef protein gels. *Food Chemistry*, 99 (3), 546-554.

Durand, D., Gimel, J. C., & Nicolai, T. (2002). Aggregation, gelation and phase

separation of heat denatured globular proteins. *Physica A: Statistical Mechanics and its Applications*, 304 (1-2), 253-265.

FAOSTAT. (2017). Production quantity [Internet]. Food and Agricultural Organization. http://www.fao.org/faostat/en/#data/QC. Accessed 01/06/19.

Feng, G., Gong, Y. F. & Zhang. P. B., (2000). Production and deployment of virus-free sweet potato in China. *Crop Protection*, 19 (2), 105-111.

Fitzsimons, S. M., Mulvihill, D. M., & Morris, E. R. (2007). Denaturation and aggregation processes in thermal gelation of whey proteins resolved by differential scanning calorimetry. *Food Hydrocolloids*, 21 (4), 638-644.

Gaspar, A. L. C., & de Góes-Favoni, S. P. (2015). Action of microbial transglutaminase (MTGase) in the modification of food proteins: A review. *Food Chemistry*, 171, 315-322.

Gosal, W. S., & Ross-Murphy, S. B. (2000). Globular protein gelation. *Current Opinion in Colloid & Interface Science*, 5 (3-4), 188-194.

Guo, Q., & Mu, T. H. (2011). Emulsifying properties of sweet potato protein: effect of protein concentration and oil volume fraction. *Food Hydrocolloids*, 25 (1), 98-106.

Han, M., Wang, P., Xu, X., & Zhou, G. (2014). Low-field NMR study of heat-induced gelation of pork myofibrillar proteins and its relationship with microstructural characteristics. *Food Research International*, 62, 1175-1182.

Hattori, T., Nakagawa, T., Maeshima, M., Nakamura, K., & Asahi, T. (1985). Molecular cloning and nucleotide sequence of cDNA for sporamin, the major soluble protein of sweet potato tuberous roots. *Plant Molecular Biology*, 5 (5), 313-320.

Hou, W. & Lin, Y. (1997). Dehydroascorbate reductase and monodehydroascorbate reductase activities of trypsin inhibitors, the major sweet potato (*Ipomoea batatas* [L.] Lam) root storage protein. *Plant Science*, 128 (2), 151-158.

Huang, H. W., Wu, S. J., Lu, J. K., Shyu, Y. T., & Wang, C. Y. (2017). Current status and future trends of high-pressure processing in food industry. *Food Control*, 72, 1-8.

Hwang, J. S., Lai, K. M., & Hsu, K. C. (2007). Changes in textural and rheological properties of gels from tilapia muscle proteins induced by high pressure and setting. *Food Chemistry*, 104 (2), 746-753.

Ishida, H., Suzuno, H., Sugiyama, N., Innami, S., Tadokoro, T., & Maekawa, A. (2000). Nutritive evaluation on chemical components of leaves, stalks and stems of sweet potatoes (Ipomoea batatas poir). *Food Chemistry*, 68 (3), 359-367.

Khan, N. M., Mu, T. H., Ali, F., Arogundade, L. A., Khan, Z. U., Zhang, M., & Sun, H. N. (2015). Effects of high hydrostatic pressure on emulsifying properties of sweet potato protein in model protein–hydrocolloids system. *Food Chemistry*, 169, 448-454.

Kieliszek, M., & Misiewicz, A. (2014). Microbial transglutaminase and its application in the food industry. A review. *Folia Microbiologica*, 59 (3), 241-250.

Kim, J. H. J., Varankovich, N. V., & Nickerson, M. T. (2016). The effect of pH on the gelling behavior of canola and soy protein isolates. *Food Research International*, 81, 31-38.

Kuhn, K. R., Cavallieri, Â. L. F., & Da Cunha, R. L. (2010). Cold-set whey protein gels induced by calcium or sodium salt addition. *International Journal of Food Science & Technology*, 45 (2), 348-357.

Leksrisompong, P. P., Whitson, M. E., Truong, V. D., & Drake, M. A. (2012). Sensory attributes and consumer acceptance of sweet potato cultivars with varying flesh colors. *Journal of Sensory Studies*, 27 (1), 59-69.

Li, P. G., & Mu, T. H. (2012). Recovery of sporamin from naturally fermented sweet potato starch slurry by foam fractionation. *International Journal of Food Science & technology*, 47 (9), 1889-1895.

Li, P. G., Mu, T. H., & Deng, L. (2013). Anticancer effects of sweet potato protein on human colorectal cancer cells. *World Journal of Gastroenterology: WJG*, 19 (21), 3300.

Lin, D., Lu, W., Kelly, A. L., Zhang, L., Zheng, B., & Miao, S. (2017). Interactions of vegetable proteins with other polymers: Structure-function relationships and applications in the food industry. *Trends in Food Science & Technology*, 68, 130-144.

Liu, R., Zhao, S. M., Xie, B. J., & Xiong, S. B. (2011). Contribution of protein conformation and intermolecular bonds to fish and pork gelation properties. *Food Hydrocolloids*, 25 (5), 898-906.

Mäkinen, O. E., Zannini, E., & Arendt, E. K. (2015). Modifying the cold gelation properties of quinoa protein isolate: influence of heat-denaturation pH in the alkaline range. *Plant Foods for Human Nutrition*, 70 (3), 250-256.

Maltais, A., Remondetto, G. E., Gonzalez, R., & Subirade, M. (2005). Formation of soy protein isolate cold-set gels: Protein and salt effects. *Journal of Food Science*, 70 (1), 67-73.

Mohanraj, R., & Sivasankar, S. (2014). Sweet potato (*Ipomoea batatas* [L.] Lam)-A valuable medicinal food: a review. *Journal of Medicinal Food*, 17 (7), 733-741.

Mu, T. H., Tan, S. S., Chen, J. W., & Xue, Y. L. (2009). Effect of pH and $NaCl/CaCl_2$ on the solubility and emulsifying properties of sweet potato protein. *Journal of the Science of Food and Agriculture*, 89 (2), 337-342.

Mu, T. H., Tan, S. S., & Xue, Y. L. (2009). The amino acid composition, solubility and emulsifying properties of sweet potato protein. *Food Chemistry*, 112 (4), 1002-1005.

O'Kane, F. E., Happe, R. P., Vereijken, J. M., Gruppen, H., & van Boekel, M. A. (2004). Heat-induced gelation of pea legumin: Comparison with soybean glycinin.

Journal of Agricultural and Food Chemistry, 52 (16), 5071-5078.

Oke, M. O., & Workneh, T. S. (2013). A review on sweet potato postharvest processing and preservation technology. *African Journal of Agricultural Research*, 8 (40), 4990-5003.

Park, S. Y., Lee, S. Y., Yang, J. W., Lee, J. S., Oh, S. D., Oh, S., ... & Cho, H. S. (2016). Comparative analysis of phytochemicals and polar metabolites from colored sweet potato (*Ipomoea batatas* L.) tubers. *Food Science and Biotechnology*, 25 (1), 283-291.

Pereira, R. N., & Vicente, A. A. (2010). Environmental impact of novel thermal and non-thermal technologies in food processing. *Food Research International*, 43 (7), 1936-1943.

Pinterits, A., & Arntfield, S. D. (2008). Improvement of canola protein gelation properties through enzymatic modification with transglutaminase. *LWT-food Science and Technology*, 41 (1), 128-138.

Renkema, J. M., & van Vliet, T. (2002). Heat-induced gel formation by soy proteins at neutral pH. *Journal of Agricultural and Food Chemistry*, 50 (6), 1569-1573.

Riebroy, S., Benjakul, S., Visessanguan, W., Erikson, U., & Rustad, T. (2008). Comparative study on acid-induced gelation of myosin from Atlantic cod (Gardus morhua) and burbot (Lota lota). *Food Chemistry*, 109 (1), 42-53.

Romeih, E., & Walker, G. (2017). Recent advances on microbial transglutaminase and dairy application. *Trends in Food Science & Technology*, 62, 133-140.

Rudra, S. G., Nishad, J., Jakhar, N., & Kaur, C. (2015). Food industry waste: mine of nutraceuticals. Int. J. Sci. *Environ. Technol*, 4 (1), 205-229.

Sarmadi, B. H., & Ismail, A. (2010). Antioxidative peptides from food proteins: a review. *Peptides*, 31 (10), 1949-1956.

Shao, J. J., Zou, Y. F., Xu, X. L., Zhou, G. H., & Sun, J. X. (2016). Effects of NaCl on water characteristics of heat-induced gels made from chicken breast proteins treated by isoelectric solubilization/precipitation. *CyTA-Journal of Food*, 14 (1), 145-153.

Singh, H., & Havea, P. (2003). Thermal denaturation, aggregation and gelation of whey proteins. *In Advanced Dairy Chemistry-1 Proteins* (pp. 1261-1287). Springer, Boston, MA.

Sun, M., Mu, T., Zhang, M., & Arogundade, L. A. (2012). Nutritional assessment and effects of heat processing on digestibility of Chinese sweet potato protein. *Journal of Food Composition and Analysis*, 26 (1-2), 104-110.

Sun, X. D., & Arntfield, S. D. (2012). Molecular forces involved in heat-induced pea protein gelation: effects of various reagents on the rheological properties of salt-extracted pea protein gels. *Food Hydrocolloids*, 28 (2), 325-332.

Sun, X. D., & Holley, R. A. (2011). Factors influencing gel formation by myofibrillar proteins in muscle foods. *Comprehensive Reviews in Food Science and*

Food Safety, 10 (1), 33-51.

Tang, C. H., & Ma, C. Y. (2009). Effect of high pressure treatment on aggregation and structural properties of soy protein isolate. *LWT-Food Science and Technology*, 42 (2), 606-611.

Totosaus, A., Montejano, J. G., Salazar, J. A., & Guerrero, I. (2002). A review of physical and chemical protein-gel induction. *International Journal of Food Science & Technology*, 37 (6), 589-601.

Van Vliet, T., Lakemond, C. M., & Visschers, R. W. (2004). Rheology and structure of milk protein gels. *Current Opinion in Colloid & Interface Science*, 9 (5), 298-304.

Visschers, R. W., & de Jongh, H. H. (2005). Disulphide bond formation in food protein aggregation and gelation. *Biotechnology Advances*, 23 (1), 75-80.

Wang, C. Y., Huang, H. W., Hsu, C. P., & Yang, B. B. (2016). Recent advances in food processing using high hydrostatic pressure technology. *Critical Reviews in Food Science and Nutrition*, 56 (4), 527-540.

Wang, K. Q., Luo, S. Z., Zhong, X. Y., Cai, J., Jiang, S. T., & Zheng, Z. (2017). Changes in chemical interactions and protein conformation during heat-induced wheat gluten gel formation. *Food Chemistry*, 214, 393-399.

Wang, S., Nie, S., & Zhu, F. (2016). Chemical constituents and health effects of sweet potato. *Food Research International*, 89, 90-116.

Zhang, M., Mu, T. H., & Sun, M. J. (2014). Purification and identification of antioxidant peptides from sweet potato protein hydrolysates by Alcalase. *Journal of Functional Foods*, 7, 191-200

Chapter III

Effects of pH and high hydrostatic pressure on the structure and gelation properties of sweet potato protein

Chapter III Effects of pH and high hydrostatic pressure on structure and gelation properties of sweet potato protein

This chapter is adapted from the published article:

Chemical forces, structure, and gelation properties of sweet potato protein as affected by pH and high hydrostatic pressure

*Zhong-Kai Zhao[1,2]· Tai-Hua Mu[*1]· Miao Zhang[1]· Aurore Richel[2]*

1 Laboratory of Food Chemistry and Nutrition Science, Institute of Food Science and Technology, Chinese Academy of Agricultural Sciences; Key Laboratory of Agro-Products Processing, Ministry of Agriculture and Rural Affairs, No. 2 Yuan Ming Yuan West Road, Haidian District, P.O. Box 5109, Beijing 100193, P. R. China.

2 University of Liège, Gembloux Agro-Bio Tech, Biological and Industrial Chemistry Unit, Passage des Déportés, 2, 5030 Gembloux, Belgium

Reference

Zhao, Z. K., Mu, T. H., Zhang, M., & Richel, A. (2018). Chemical forces, structure, and gelation properties of sweet potato protein as affected by pH and high hydrostatic pressure. *Food and Bioprocess Technology*, 11 (9), 1719-1732.

DOI

https://doi.org/10.1007/s11947-018-2137-y

Abstract

Sweet potato is one of cheap sources for starch industries in the worldwide, exploiting starch wastewater as an alternative protein source is mainly environmental and economic concerns. In this study, the effects of HHP (250, 400 and 550 MPa) on chemical forces, structure and gelation properties of SPP at pH 3.0, 6.0, and 9.0 were investigated. The values of surface hydrophobicity and absolute value of zeta potential of SPP significantly increased from 250 to 550 MPa ($p < 0.05$) at all three pH conditions. The total amount of -SH- groups in SPP decreased after HHP at pH 9.0, whereas the amount of free -SH- increased. High molecular mass aggregates (>180 kDa) were observed in SPP after HHP at pH 6.0 and 9.0 by SDS-PAGE. Regarding elastic rheological behaviors, storage modulus (G′) values of SPP were significantly strengthened after HHP treatment. In addition, textural properties and water-holding capacity of gels made from SPP after 250 and 400 MPa at pH 9.0 were significantly improved, and the gels showed a compact and uniform gel network with the contribution of immobilized water fractions. The gel properties exhibited by SPP after HHP treatment at different pHs, in particular after 400 MPa at pH 9.0, suggested that it could be potential protein resources as new gelling reagent in the food system.

Keywords

Sweet potato protein; High hydrostatic pressure; Rheology; Low field NMR; Microstructure; Gelation properties

1. Introduction

In recent years, market demand has steadily grown for protein ingredients, especially those that have multiple functions, such as ingredients that act as a supplement and also have functional properties. The ability of protein to form a gel makes it suited to improve the textural and functional properties of food products (Han et al. 2014). Many plant proteins have been reported to have gelation properties, including soy protein (Wu et al. 2017), pea protein (Sun & Arntfield 2012), gluten (Wang et al. 2017a), and canola protein (Chang et al. 2015). Meanwhile, many modification methods have been developed to improve the functional properties of proteins, including physical (Wihodo & Moraru 2013), chemical (Boutureira & Bernardes 2015), and enzymatic treatments (Gaspar & De Góes-Favoni, 2015).

HHP has made significant development over the last twenty years, which is utilized realistically in food system and offers the applications in the innovation of novel textures and tastes of foods (Norton & Sun, 2008). As a non-thermal, safe and promising technology, HHP treatment can be used to produce healthy and fresh-like foods due its minimal effects on nutritional and aroma compounds (De Maria, Ferrari, & Maresca 2016). HHP also presents encouraging potential to manipulate the functionality, extractability, allergenicity and bioavailability of micronutrients and components in foods (Barba et al., 2015). HHP has interesting functional effects based on how it changes protein structure, as well as how it affects the chemical forces between protein molecules, including surface hydrophobic activity, electrostatic interactions, disulfide linkages, and hydrogen bonding (Sun & Arntfield 2012; Wang et al. 2017b). HHP treatment could induce protein molecule aggregation, promote surface hydrophobicity of protein isolates, change the secondary structure of the protein, and result in good gel textural properties (He et al. 2014). Zhang et al. (2017) reported that as pressure increased, the -SH- group content of myofibrillar protein decreased and the absolute zeta potential increased. Puppo et al. (2004) indicated that HHP modified secondary structure of soybean protein isolates by leading to a more disordered structure and resulting in insoluble aggregates. Peyrano et al. (2016) found that HHP was more efficient than thermal treatment to enhance gelation properties and water holding capacities of cowpea protein isolates. Moreover, Yang et al. (2014) also showed better mechanical strength of canola protein gels formed at high pH level compared to that of low pH conditions over a broad range of pHs (5–11).

Sweet potato (*Ipomoea batatas* [L.] Lam) is one of the main food crops and a source of starch in China, and accounts for 67.3 % and 90.1 % of sweet potato production worldwide and in Asia, respectively (FAOSTAT, 2016). It is considered to be one of the most promising economic crops with remarkable spectrum of antioxidant activities, based on the high level of valuable compounds in extracts, such as protein and polyphenols (e.g. anthocyanins) (Zhu et al., 2017). Sweet potato contains about 1.7 %–9.1 % crude protein on a dry weight basis (Zhang, Mu, & Sun,

2014). SPP has a high content of essential amino acids, and therefore, has higher nutritive value than most other plant proteins (Mu et al. 2009b), but is normally discarded as industrial waste in the process of sweet potato starch manufacturing. In our recent study, we investigated the structure, physicochemical properties, emulsifying properties and in vitro digestibility of SPP after HHP treatment, and found that HHP (200–600 MPa) could improve emulsifying properties, alter in vitro digestibility and reduce thermodynamic stability of SPP (Khan et al. 2013; Khan et al. 2014; Khan et al. 2015; Sun et al. 2014). Additionally, we studied the gelation properties and gel microstructure of isoelectric and ultrafiltered SPP at atmospheric pressure and pH 7.0 (Arogundade, Mu & Añón 2012b). The gelation behavior and chemical forces of protein were varied by the protein types and significantly modulated by pH (Wang et al. 2014; Kim et al. 2016). However, no study on the effects of pH on the chemical forces, structure and gelation properties of SPP after HHP treatment is currently available, even the basic information both including dispersion, thermal gelation process and SPP gel products are still limited.

Normally, the most popular pressure levels used in commercial applications are ranged from 200 to 600 MPa (San Martin, Barbosa-Cánovas & Swanson 2002). Moreover, the applied pH of almost gel-like food or soft gel-like food (e.g. beverages and yogurt) is slightly below pH 7.0, being closer to pH 6.0. And the pH of some fruit juice and baked products is usually close to 3.0 and 9.0, respectively. The -SH- groups could easily form disulfide bonds by intermolecular interactions at alkaline condition of pH 9.0, which might further contribute to the gel texture (Chang et al. 2015). Hence, the real aims of this study are to investigate the effects of HHP treatment on chemical forces (surface hydrophobicity, zeta potential, sulfhydryl group), structure, rheological properties and gelation properties of SPP as affected by HHP (250, 400 and 550 MPa) at below (pH 3.0), near (pH 6.0) or far away from (9.0) the isoelectric point of SPP (4.0), respectively, to provide basic information about the gelation properties of SPP and its potential applications as a functional agent in food industry.

2. Materials and methods

2.1. Materials

Sweet potatoes of the cultivar Shang Shu No. 19 were provided by Shangqiu Academy of Agriculture and Forestry Sciences, Henan province, China. All chemicals used were of analytical grade and purchased from Sigma-Aldrich (St. Louis, MO., USA).

2.2. SPP preparation

SPP was prepared as described previously by Arogundade & Mu (2012a), with slight modifications. Briefly, fresh peeled tubers were grounded with 0.1 % sodium bisulfite solution at a solid-to-solvent ratio of 1:2, sieved with cheese cloth (0.15–mm pore diameter) and centrifuged at 10,000 g for 45 min to collect supernatant.

The pH value of the supernatant was adjusted to 4.0 (using 2 M HCl), and then centrifuged at 6,000 g for 30 min to collect the precipitate, which was resolubilized in distilled water at pH 7.0 using 2 M NaOH, centrifuged at 10,000 g for 45 min, ultrafiltered and then lyophilized to obtain SPP with purity of 92.95 % by the Kjeldahl method (N × 6.25).

2.3. HHP treatment

HHP treatment was performed using a laboratory-scale HHP unit (model HHP–L3–600/0.6; HuaTaiSenMiao Engineering & Technique Ltd. Co., Tianjin, China) with a 0.6–L cylindrical pressure vessel (60 × 210 mm) and a water jacket for temperature control at 25 ℃. For HHP processing, each dispersion of SPP (4 %, w/v) at pH 3.0 (50 mM glycine–HCl buffer), 6.0 (50 mM phosphate buffer), and 9.0 (50 mM glycine–NaOH buffer) was vacuum-packed in food-grade polyethylene bags, pressurized at a speed of 3.5 MPa/s, and then held at 250, 400, and 550 MPa for 30 min before the pressure was released within 5 s, respectively. SPP dispersion without pressurization (0.1 MPa) at pH 3.0, 6.0 and 9.0 were used as reference. Each SPP dispersion was then freeze dried, and stored at -18 ℃ for subsequent analysis.

2.4. Chemical forces of SPP

2.4.1. Surface hydrophobicity (Ho)

Ho of SPP was determined using 1-anilinonaphthalene-8-sulfonic acid (ANS) as a hydrophobic fluorescence probe according to Chang et al., (2015) with some modification. The stock solution (0.1 %, w/v) was prepared by dissolving SPP in 10 mM phosphate buffer (pH 7.0), then serially diluted to a final concentration of 0.004–0.02 % (w/v) with the same buffer. An aliquot of 20 μL ANS (8.0 mM in 10 mM phosphate buffer, pH 7.0) was added to 4.0 mL of each diluted solution. The fluorescence intensity (FI) was measured using a fluorescence spectrometer (F2500; Hitachi, Tokyo, Japan) at wavelengths of 390 nm (excitation) and 470 nm (emission). The initial slope of FI versus the protein concentration plot (calculated by linear regression analysis) was used as an index of Ho.

2.4.2. Zeta potential

The zeta potential was measured using a zetasizer (Nano-ZS90; Malvern Instruments Ltd. Malvern, UK) equipped with an avalanche photodiode detector based on the previous literature (Yang et al., 2014). SPP solution (1.0 mg/mL) was prepared by dissolving SPP powder into Milli-Q water. A 1.0-mL aliquot of SPP solution (1.0 mg/mL) was injected into a disposable clear test cell (DTS1060C; Malvern Instruments Ltd.) and equilibrated at 25 ℃ for 3.0 min before starting the test. The absolute value of the zeta potential is positively related to the electrostatic interactions of the charged amino acids (Zhang et al., 2015; Chang et al., 2015).

2.4.3. -SH- groups

Total and free -SH- group contents were measured according to the method of He et al. (2014). The total -SH- group was determined by dissolving SPP in Tris–glycine buffer (containing 0.086 mol/L Tris, 0.09 mol/L glycine, and 0.004 mol/L

EDTA; pH 8.0) with 8.0 mol/L urea to break the disulfide bonds and make the molecular internal -SH- group exposed. An aliquot (1.0-mL) of SPP solution (1.0 mg/mL) was mixed with 50 μL DTNB (5, 5′-dinitrobis [2-nitrobenzoic acid], 4.0 mg/mL) and incubated for 20 min at 25 ℃, then centrifuged at 10,000 g for 20 min. The absorbance of the supernatant was read at 412 nm by a UV–Vis spectrophotometer (TU-1810; Puxi Instrument Ltd. Co. Beijing, China) using a molar extinction coefficient value of 13,600 mol/cm^{-1}. The content of free -SH- groups was measured by using the same procedure with Tris–glycine buffer in the absence of 8.0 mol/L urea.

2.5. CD

The secondary structure of SPP was performed using the circular dichroism (CD) spectrophotometry with the modified method described by Han et al. (2015). Far-ultraviolet spectra (190 to 250 nm) of SPP solutions (1.0 mg/mL) were recorded on a MOS-450/AF-CD chromatograph (Bio-Logic Co., Seyssinet-Pariset, France) under constant nitrogen flush with a 0.1 cm optical path–length quartz cell. The spectra obtained represent a mean of three consecutive scans at a speed of 1,000 nm/min, bandwidth of 1.0 nm, response time of 0.5 s, and a step resolution of 0.5 nm. The secondary structures were predicted using the online tool "DichroWeb" website according to the method by Whitmore & Wallace (2004). Data were expressed according to mean residue ellipticity (θ) in deg·cm^2/dmol.

2.6. SDS–PAGE

Molecular weight distribution of SPP treated by HHP was investigated using SDS-PAGE according to the method described by Laemmli (1970). Mixtures of 40 μL of SPP solution (5.0 mg/mL) and 10 μL of sample solubilizing solution (containing 1 % SDS, 50 mM Tris-HCl buffer [pH 6.8], 60 mM EDTA-2Na, and 12 % sucrose) were prepared with or without 1 % β-mercaptoethanol. A 10-μL aliquot of each mixture was loaded on each gel lane, and 12.5 % acrylamide separating gel and 5 % acrylamide stacking gel were used. Gel electrophoresis was conducted at 30 mA for 1.5 h. And the molecular weight of the protein bands was compared with a low standard molecular weight marker (10-180 kDa, Sigma-Aldrich).

2.7. Gelation properties

2.7.1. Dynamic shear rheology-temperature relationship

The dynamic shear rheological properties were measured with an Anton Paar rheometer (Physica MCR 301; Graz, Austria) equipped with a temperature-controlled Peltier system. The test was conducted using our previous method (Arogundade, Mu & Añón, 2012b) by making a 10 % (w/v) SPP dispersion (10 mM phosphate buffer, pH 7.0) at a constant angular frequency of 10 s-1 and strain of 0.5 % (within the linear viscoelasticity range). Invariable 2.3-mL of protein dispersion was loaded onto the lower platen, and the upper parallel platen (PP–50 probe; 50 mm diameter) was lowered to contact the sample with 1.0 mm gap. The temperature was increased from 25 to 95 °C at a heating rate of 2 °C/min, held at

95 °C for 30 min, and then cooled to 25 °C at a cooling rate of 2 °C/min. Silicon oil was applied to the exposed part to prevent the sample from drying out during heating. The storage modulus (G′), loss modulus (G″), and complex viscosity (η*) were followed during a heating–cooling cycle for each sample, and the phase angle tangent (tan δ) was computed from the raw oscillatory data using the accompanying software (32V3.21).

2.7.2. Preparation of SPP Gels

For gelation experiments, SPP gels were prepared with 10 % (w/v) SPP dispersion in 10 mM phosphate buffer (pH 7.0). The SPP dispersion were injected into glass mold with 2.3 cm internal diameters, covered with aluminum foil, placed in water bath, heated from 25 to 95 °C, and. maintained at 95 °C for 30 min. Then, SPP gels in glass molds were immediately cooled under running water, and stored at 4 °C for 12 h. The cylindrical gels were used for the measurements of scanning electron microscopy (SEM), mechanical properties, water-holding capacity (WHC) and low field NMR relaxation test.

2.7.3. SEM

The microstructure of SPP gels was observed using a scanning electron microscope (Hitachi S-3400n, Japan). SPP gels were cut into small piece, fixed, dehydrated, pasted on a copper stub with double-sided tabs, and rendered conductive by coating with platinum, of which the microstructure was viewed with a scanning electron microscope (S-3400n; Hitachi) at an accelerating voltage of 15.0 kV and ×2000 magnification.

2.7.4. Mechanical properties

The mechanical properties of the prepared gels were assessed by uniaxial compression test using a TA-XT2i texture analyzer (Stable Micro System Ltd., Godalming, UK) equipped with a 35 mm-diameter cylindrical plate and a 12.0 mm-diameter probe (P 0.5R). The cylindrical protein gels (1.0 cm in height and 2.3 cm in diameter) were compressed to 30 % of their original height at a crosshead speed of 0.3 mm/s for 5 s. The resulting data were interpreted using Texture Expert analysis software (Stable Micro Systems Ltd.), and following parameters could be obtained: Hardness (maximum peak force of the first compression cycle), springiness (height during the second compression divided by the original compression distance), and cohesiveness (ratio of the positive force area during the second compression to that of the first compression). Chewiness was then calculated as hardness × cohesiveness × springiness.

2.7.5. Low field NMR

NMR relaxation measurement was performed using low field NMR according to the method of Han et al. (2014) and Zhang et al. (2015) with some modification. Freshly prepared gel was placed in a cylindrical glass tube (2.3 cm internal diameters) of a Niumag pulsed NMR analyzer (MesoMR23-060H-I, Niumag Electric Corporation, Shanghai, China). The analyzer was operated at 32 °C and using the Carr-Purcell-Meiboom-Gill (CPMG) sequence with spectral width (SW) of

250 kHz, resonance frequency (RF) of 23 MHz, and receiver gain (RG) of 10 db. A total of 10,000 echoes were recorded and conducted by the MultiExp Inv Analysis software (Niumag Electric Corporation, Shanghai, China). The parameters of T2b and T21 were presented as the relaxation components, and A2b and A21 were the corresponding area fractions, respectively.

2.7.6. Water-holding capacity (WHC)

The WHC was determined according to the method of Wang et al. (2017b). After gelation by thermal treatment, fresh SPP gels were stored at 4 °C for 12 h to enhance and stabilize the net structure during cooling. Each SPP gel (2.0 g) was centrifuged at 10,000 g at 4 °C for 15 min. Subsequently, the supernatant, which is related to the free water component or un-bound water released by loose structural units, was carefully removed. The centrifuge tube containing SPP gel was weighed both before and immediately after centrifugation. Thus, allowing the WHC to be expressed as the ratio of the gel weight after centrifugation to the initial weight:

$$WHC\ (\%) = (W_2 – W_0) / (W_1 – W_0) \times 100 \qquad (1)$$

Where W_2 and W_1 are the weight (g) of the centrifuge tube containing the SPP gel after and before centrifugation, respectively; W_0 is the weight (g) of the empty centrifuge tube.

2.8. Statistical analysis

All experiments were carried out in triplicate, and the data were expressed as means ± SD. The statistical analysis was performed by means of one-way ANOVA followed by a Duncan's multiple range test using SAS 8.1 software (SAS Institute Inc., Cary, NC, USA). And the differences were considered significantly at $p < 0.05$.

3. Results and discussion

3.1. Chemical forces of SPP

3.1.1. Surface hydrophobicity (Ho)

Fluorescence scanning was performed to determine the optimal excitation wavelength of SPP, and a wavelength of 390 nm was employed (data not shown). As shown in Fig. 3-1, Ho of SPP at pH 3.0 was higher than that at pH 6.0 and 9.0, both for non-HHP (0.1 MPa) and HHP treated ones (250, 400 and 550 MPa). The dissociation of protein subunits at pH 3.0 might explain the higher hydrophobicity relative to the other pHs (Chang et al. 2015). Furthermore, with increasing of pressure level, Ho of SPP steadily increased at different pH values, which indicated that HHP remarkably improved the Ho, reflecting conformation changes of SPP structure during HHP (Chen et al. 2014). Khan et al. (2015) indicated that HHP treatment for 15 min showed a significant increase in Ho with pressure increased from 200 to 600 MPa at pH 3.0, but a decrease at pH 6.0 and 9.0. While in the present work, Ho of HHP treated SPP showed an increase tendency at pH 3.0, 6.0 and 9.0 for a longer holding time of 30 min. This suggested that HHP induced

changes in SPP structure were sensitive to the applied pH and pressure, as well as the pressurization time, which caused more hydrophobic groups exposed to the external environment. The application of pressure resulted in extension of SPP peptide chains, which exposed a large number of hydrophobic residues or non-polar active binding sites from SPP interior (He et al. 2014), and might have contributed to the molecular interactions, including intra-protein molecules, protein–protein interactions and protein-solution interactions (Wang et al. 2017b). Moreover, unfolding was also a necessary prior step of the molecular interactions in the SPP dispersion system.

Fig. 3-1. Surface hydrophobicity (Ho) of SPP treated by HHP at different pH values.

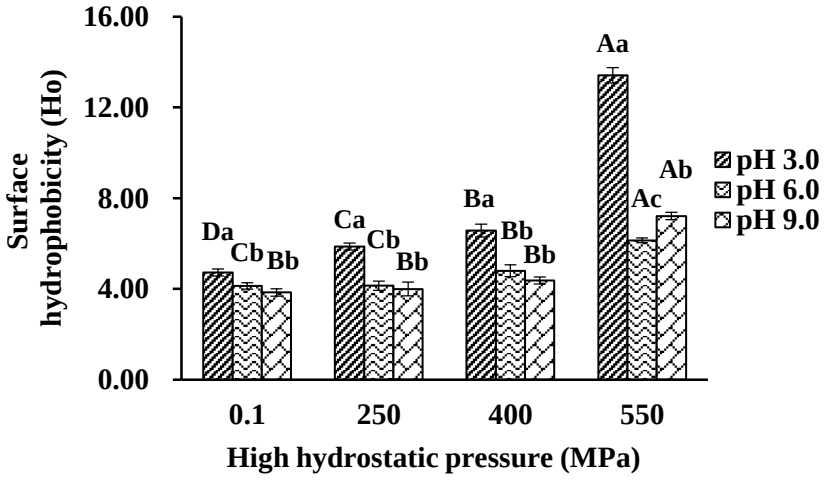

* Bars with different uppercase letters (A-D) indicate significant differences of SPP treated by same pH values but under different pressure; and bars with different lowercase letters (a-c) mean significant differences of SPP treated by same pressure but combined with different pH values ($p < 0.05$).

3.1.2. Electrostatic interactions

The changes of zeta potential of SPP after HHP at different pH values are shown in Fig. 3-2. The absolute value of zeta potential of SPP at pH 9.0 was higher than that at pH 3.0 and 6.0. This might be due to the intensive electrostatic interactions between SPP molecules when the pH value was much higher than its isoelectric point (about pH 4.0). The lowest zeta potential was found for SPP at pH 3.0 (0.1 MPa), which attributed to the fewer charged amino acids exposed at the protein surface at low pH (Kim et al. 2016), as well as the isoelectric counteraction between positive and negative charges. In addition, the absolute value of zeta potential slightly increased with pressure increasing from 0.1 to 400 MPa, and significantly

enhanced by 550 MPa at pH 3.0, 6.0, and 9.0 ($p < 0.05$). The above results suggested that HHP could induce partial unfolding of SPP structure and expose more interior functional residues and charged amino acids to the protein surface (Tang & Ma 2009), which contributed to the increase in absolute value of zeta potential, thus enhanced the electrostatic interactions between SPP molecules. In addition, as varied by pH conditions, the charged amino acids increased with pH increasing, resulting in strong electrostatic repulsion between SPP molecules, which would also promoted the unfolding of protein structure (De Maria, Ferrari, & Maresca 2016).

Fig. 3-2. Zeta potential of SPP treated by HHP at different pH values.

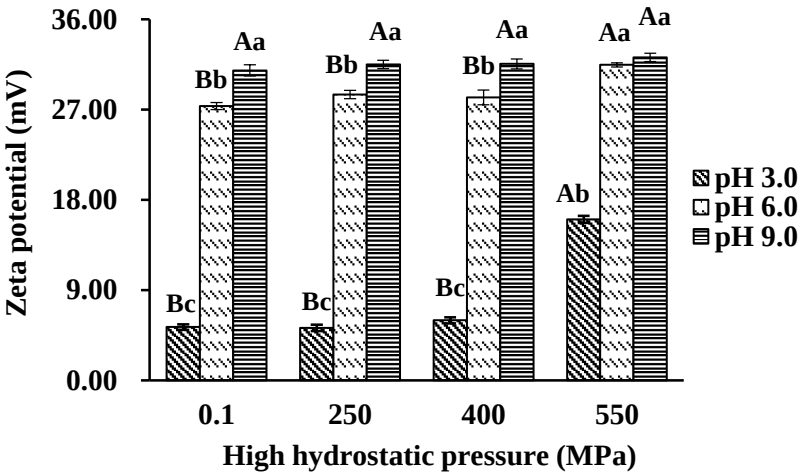

* Bars with different uppercase letters (A-D) indicate significant differences of SPP treated by same pH values but under different pressure treatment; and bars with different lowercase letters (a-c) mean significant differences of SPP treated by same pressure but combined with different pH values ($p < 0.05$).

3.1.3. -SH- groups

Disulfide bonds (-S-S-) are formed by the oxidation of -SH- groups and can be found in cysteine residues, which play an important role in the formation of the three-dimensional gel network structure (Wang et al. 2017). Changes in total -SH- and free -SH- contents are shown in Table 3-1. The total -SH- content of SPP treated at pH 6.0 was greater than that at pH 3.0 and 9.0 for both non-HHP (0.1 MPa) and HHP treated SPP. In the case of pH 3.0, the total -SH- content decreased from 13.1 % (0.1 MPa) to 11.9 % (400 MPa), then increased to 12.6 % (550 MPa). It continuously increased from 13.5 % (0.1 MPa) to 14.2 % (550 MPa) at pH 6.0. And, it first increased then reduced from 10.6 % (250 MPa) to 10.0 % (550 MPa) at pH 9.0. The total -SH- content of actomyosin of tilapia decreased sharply with the increase of pressure were also reported by Zhou et al., (2014). The decrease in total

-SH- content could possibly be explained by the formation of disulfide bonds as intensified by the protein–protein interactions (De Maria, Ferrari, & Maresca, 2016), which greatly contributed to the final gel network and enhanced textural properties and WHC of SPP gels (Zhang et al., 2015).

On the other hand, the free -SH- content decreased with increasing pH at 0.1 and 250 MPa, whereas it first increased then decreased at pH 6.0 and 9.0 at 400 and 550 MPa. In addition, free -SH- content decreased with HHP treatment from 250-550 MPa at pH 3.0. However, it steadily increased from 9.7 % (0.1 MPa) to 12.7 % (550 MPa) and from 6.7 % (0.1 MPa) to 9.9 % (550 MPa) at pH 6.0 and 9.0, respectively. The increase in free -SH- content could be resulted from the exposure of the internal -SH- groups during unfolding and extension induced by pressurization (De Maria, Ferrari, & Maresca, 2016). The above results mainly suggested that with pH increase up to pH 6.0, especially at alkaline condition of pH 9.0, HHP induced partial or complete unfolding of SPP, expose of internal -SH- groups and the formation of disulfide bonds, which further contributed to the subsequent covalent aggregation by formation of disulfide bonds and final gel quality.

3.2. CD

The changes in secondary structure of SPP after HHP at different pH values over the far-UV range of 190-250 nm are shown in Table 3-1. For non-HHP treated SPP (0.1 MPa), α-helix and random coil contents increased with pH value increasing from 3.0 to 9.0, while β-sheet decreased and β-turn slightly changed. Moreover, it exhibited a negative band over the range of 200-208 nm in the spectrogram (data not shown), and the peak wavelength shifted from 205 nm (pH 3.0) to 207 nm (pH 9.0), which indicated the reduction of hydrophobicity of SPP. Meanwhile, the ellipticity of SPP at pH 9.0 was greater than that at pH 3.0 and 6.0 (data not shown), reflecting the increase of α-helix content and unfolding of structure (He et al. 2014). These findings were consistent with hydrophobicity (Fig. 3-1) and zeta potential (Fig. 3-2) results, suggesting that high pH value (pH 9.0) might cause low hydrophobicity and strong electrostatic interactions between SPP and water molecules, thus promoting the unfolding of protein structure and extension of protein chains.

As shown in Table 3-1, α-helix content of SPP increased from 18.3 % (0.1 MPa) to 20.5 % (250 MPa), β-sheet content decreased from 32.0 % (0.1 MPa) to 30.0 % (550 MPa), and β-turn content slightly decreased at pH 3.0. The exchange of secondary structure component indicated the destruction of natural structure of SPP. On the contrary, α-helix content gradually decreased from 20.3 % (0.1 MPa) to 17.8 % (550 MPa), β-sheet increased from 30.2 % (0.1 MPa) to 32.0 % (550 MPa) at pH 6.0. Khan et al. (2015) reported that the α-helix content of SPP decreased at 200-400 MPa but increased significantly at 600 MPa at pH 6.0 and 9.0, while the β-sheet content conversely increased at 200-400 MPa then decreased at a high level of 600 MPa. Differently, the present work showed a gradually decrease tendency of α-helix and an increase trend in β-sheet content at pH 6.0 with pressure increased from 250 to 550 MPa, while no significant changes in α-helix was observed and β-sheet content decreased first then increased slightly at pH 9.0. The above differences

might be due to the longer holding time and the different applied pressure levels in the present work compare to the previous study.

In addition, functional properties of protein attributed to both structural modification and functional group interactions. Typically, unfolding degree of a protein chain gradually increased with increasing pressure and holding time, accompanied by an increase in the disordered structure and exposed functional groups, which may result in protein rearrangements and/or aggregation, and would induce the improvement in functional properties (Queirós, Saraiva & Da Silva, 2018). The pressure commonly used in food processing mainly focused on changing the secondary (300-600 MPa), tertiary (above 200 MPa) and quaternary (150-200 MPa) structures of proteins (San Martin, Barbosa-Cánovas & Swanson, 2002). Thus, the differences in structural changes of protein chains as affected by different applied pressure levels and holding time might lead to multiple functional characteristics, which provided more possibilities for the utilization of SPP in food systems.

Sun et al. (2014) found that HHP (200-600 MPa) increased the content of β-sheets, but decreased the content of random coils. This suggested that β-sheets and β-turns had better stability than α-helices during HHP treatment, being more vulnerable to pH at the same pressure levels. Moreover, random coil units of SPP steadily increased with increasing pressure at pH 3.0, slightly changed at pH 6.0, and firstly increased from 250-400 MPa then decreased up to 550 MPa at pH 9.0. Previous report believed that α-helix was stabilized by intra-hydrogen bonding, and β-sheets relied on inter-hydrogen bonds (Zhang et al. 2017). With increasing pressure at higher pH levels (pH 6.0 and 9.0), proteins unfolded, α-helix content decreased, and β-sheet and β-turn contents increased, suggesting weaker intra-hydrogen bonding and stronger inter-hydrogen bonding induced by HHP treatment (Grossi et al. 2016). The unfolding resulted in the disruption of ordered secondary structure (α-helix, β-sheet) and the increase of disordered units (β-turn, random coil) respectively, which might lead to the formation of inter-hydrogen bonding thus promote the interactions between proteins (Zhang et al. 2017).

Table 3-1 Sulfhydryl group content (μmol/g protein) and secondary structure composition (%) of SPP treated by HHP at different pH values.

HHP (MPa)	pH	Total -SH-	Free -SH-	α-helix	β-sheet	β-turn	Random coil
0.1	3.0	13.13 ± 0.00^{Ab}	10.94 ± 0.03^{Aa}	18.25 ± 0.35^{Bb}	31.95 ± 0.49^{Aa}	21.50 ± 0.28^{Aa}	28.35 ± 0.21^{Bb}
	6.0	13.51 ± 0.03^{Ca}	9.65 ± 0.03^{Cb}	20.25 ± 0.07^{Aa}	30.20 ± 0.00^{Bb}	20.85 ± 0.35^{ABa}	28.70 ± 0.42^{Ab}
	9.0	10.17 ± 0.03^{Bc}	6.71 ± 0.03^{Dc}	20.25 ± 0.21^{Aa}	28.35 ± 0.07^{Bc}	20.70 ± 0.14^{Aa}	30.70 ± 0.14^{ABa}
250	3.0	12.52 ± 0.03^{Bb}	10.33 ± 0.05^{Ca}	20.50 ± 0.28^{Aa}	30.25 ± 0.07^{BCa}	20.60 ± 0.14^{Ba}	28.70 ± 0.00^{ABb}
	6.0	13.82 ± 0.10^{Bc}	9.69 ± 0.03^{Cb}	19.95 ± 0.35^{ABa}	30.40 ± 0.42^{Ba}	20.70 ± 0.14^{Ba}	28.95 ± 0.21^{Ab}
	9.0	10.61 ± 0.08^{Aa}	7.22 ± 0.03^{Cc}	19.80 ± 0.28^{Aa}	28.15 ± 0.21^{BCb}	20.85 ± 0.07^{Aa}	31.30 ± 0.14^{Aa}
400	3.0	11.88 ± 0.05^{Cb}	10.72 ± 0.03^{Bb}	18.90 ± 0.14^{Bb}	31.15 ± 0.07^{ABa}	21.15 ± 0.07^{Aa}	28.80 ± 0.28^{ABb}
	6.0	13.81 ± 0.08^{Bc}	12.30 ± 0.08^{Ba}	19.65 ± 0.07^{Ba}	30.55 ± 0.07^{Bb}	20.90 ± 0.14^{ABa}	28.95 ± 0.07^{Ab}
	9.0	10.09 ± 0.03^{BCa}	8.81 ± 0.03^{Bc}	20.05 ± 0.21^{Aa}	27.75 ± 0.07^{Cc}	20.80 ± 0.28^{Aa}	31.40 ± 0.57^{Aa}
550	3.0	12.61 ± 0.10^{Bb}	10.26 ± 0.05^{Cb}	20.10 ± 0.00^{Aa}	29.95 ± 0.64^{Cb}	20.60 ± 0.14^{Bb}	29.30 ± 0.42^{Aab}
	6.0	14.21 ± 0.03^{Aa}	12.74 ± 0.03^{Aa}	17.80 ± 0.14^{Cb}	31.95 ± 0.21^{Aa}	21.35 ± 0.07^{Aa}	28.90 ± 0.14^{Ab}
	9.0	10.04 ± 0.00^{Cc}	9.85 ± 0.00^{Ac}	20.30 ± 0.00^{Aa}	29.00 ± 0.28^{Ab}	20.75 ± 0.07^{Ab}	29.95 ± 0.35^{Ba}

* Results are presented as mean ± standard deviation (n=3). Different uppercase (A-D) in the same column means significant differences of SPP treated by same pH values but under different pressure; and different lowercase (a-c) in the same column means significant differences of SPP treated by same pressure but combined with different pH values ($p < 0.05$)

3.3. SDS-PAGE

The molecular weight distribution of non-HHP and HHP treated SPP at different pH values are shown in Fig. 3-3. Both of non-HHP and HHP treated SPP at pH 3.0, 6.0 and 9.0 showed similar characteristics under reducing conditions (Fig. 3-3a, b and c), with the main band located at 25 kDa and a minor band at about 55 kDa indicating the endogenous β-amylase subunit (Jia, Liang, & Zhu 2010).

Under non-reducing conditions, there were no high molecular weight aggregates larger than 180 kDa produced at pH 3.0 under each pressure level when compared with those at pH 6.0 and 9.0 (Fig. 3-3a, b, c), which indicated that SPP still maintained a spherical structure and has a low degree of stretch. These results might be caused by higher Ho and lower zeta potential in acidic environments than in alkaline and neutral environments (Mu et al. 2009a). Notably, compared with non-HHP treated SPP, the bands between new aggregates became more intense with increasing pressure from 250 to 550 MPa at pH 6.0 (Fig. 3b), and even more at pH 9.0 (Fig. 3-3c). This suggested a higher degree of aggregation induced by HHP. Moreover, this aggregation could be ascribed to the formation of disulfide bonds between the molecules at high pressure levels (Cheung, Wanasundara, & Nickerson 2014). A previous report also suggested that pressure above 200 MPa could induce the formation of urea-insoluble complexes, disulfide bonds, and/or other strong protein aggregates (Angioloni & Collar 2013).

In addition, with HHP increased from 0.1 to 550 MPa, surface hydrophobicity, zeta potential, free sulfhydryl group content and band intensity of new aggregates of SPP significant increased at different pH, especially at pH 9.0 (Fig. 3-1, 3-2, 3-3 and Table 3-1). This might be explained by the exposing of hydrophobic site, free sulfhydryl group and charged amino acids of SPP with pressure increasing, and could be contributed to viscoelasticity of SPP gels. The unfolding and aggregation was happened separately during the pressurization. The unfolding of SPP might be responsible for subsequent aggregation and as a precondition of polymerization between protein molecules, leading to the formation of higher molecular weight polymers (Tang & Ma 2009; Qin et al. 2013; De Maria, Ferrari, & Maresca 2016).

3.4. Gelation properties

3.4.1. Dynamic rheology-temperature relationship

Rheological behavior is useful for describing gelation properties of SPP during thermal treatment. G′ value represents the elastic component and strength of the gel structure, and contributes to the three-dimensional gel network, whereas G″ reflects the protein-protein interactions, but does not contribute to the gel network (Arogundade, Mu, & Añón 2012b; Angioloni & Collar 2013; Wu et al. 2017; Renkema, Gruppen, & Van Vliet 2002). As shown in Fig. 3-4a, b and c, the thermomechanical characteristics showed three different models corresponding to the three different pH values (3.0, 6.0 and 9.0). G′ consistently showed higher values at pH 3.0 than that of observed at pH 6.0 and 9.0 for both non-HHP (0.1 MPa) and HHP treated SPP during thermal treatment, which indicated that SPP gels behave in a more elastic manner at the pH close to the isoelectric point.

Fig. 3-3. SDS-PAGE of SPP treated by HHP under non-reducing and reducing conditions.

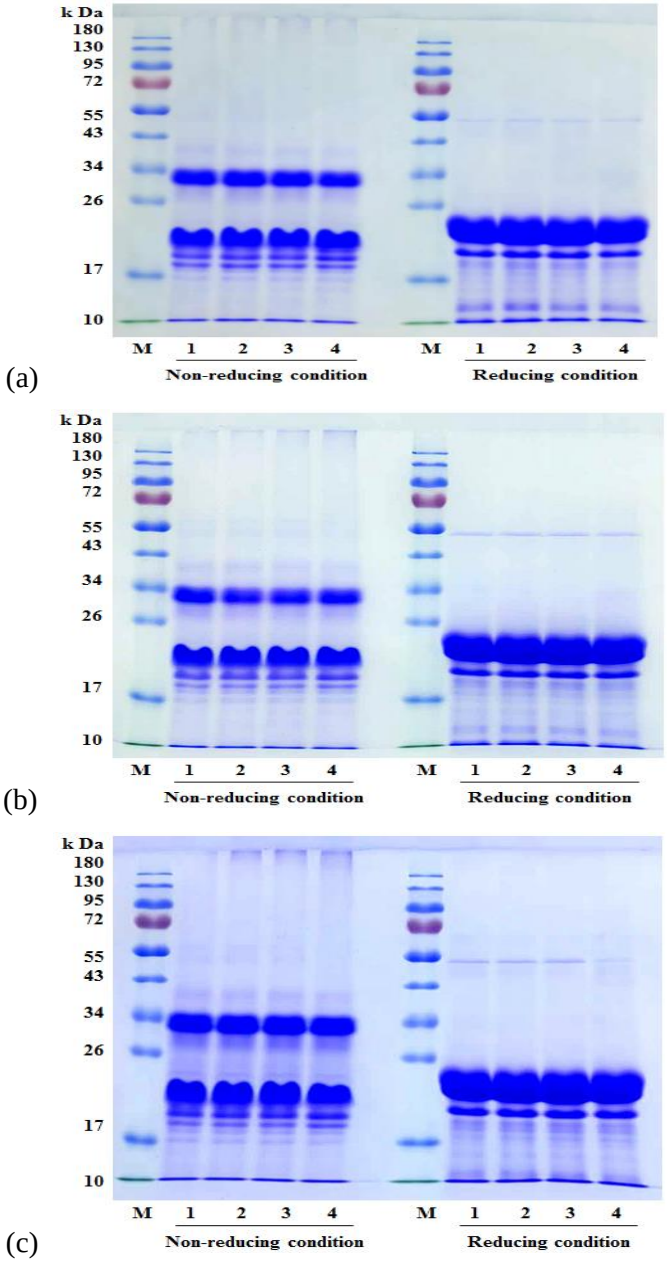

* (a) pH 3.0; (b) pH 6.0; (c) pH 9.0. Lane M is the standard marker, and Lanes 1-4 represent 0.1, 250, 400 and 550 MPa treated SPP, respectively.

For HHP treatment at pH 3.0, the initial G′ rapidly increased at 70.8 °C, which represented the gelation point (Tgel). Arogundade et al. (2012b) and Renkema et al. (2002) also reported that heat denaturation was a prerequisite for gel formation. After Tgel, G′ rapidly peaked, and both Tgel (70.8 °C) and peak denatured temperature Tpeak (82.2 °C) of SPP at 550 MPa were lower than those treated at 0.1, 250 and 400 MPa. Furthermore, HHP treated SPP had a higher G′ value than non-HHP treated one (0.1 MPa), especially at 400 and 550 MPa, which suggested that HHP could significantly improve elastic properties of SPP gel as a result of peptide chains unfolding.

In addition, Cando et al. (2015) reported that the improvement in rheological property induced by HHP treatment could be attributed to the denaturation of SPP followed by further protein aggregation. With pressure increasing at pH 6.0, both non-HHP and HHP treated SPP gels presented the same Tgel (86.5 °C) and Tpeak (90.8 °C), and the highest G′ value was observed at 400 MPa. A continuously increasing trend was seen after Tgel. Moreover, further cooling enhanced gel network structure with a steady increase in G′, which could be attributed to the consolidation of attractive forces, such as van der Waals forces and hydrogen bonding (Arogundade et al., 2012b; Wu et al., 2017). It was also indicated that with increasing of pressure, the irreversible unfolding and the consequent aggregation were promoted by the enhanced chemical forces, thus inducing the formation of stretch-conformation and an increase in viscoelasticity.

3.4.2. Microstructure analysis

Protein gel can be considered as a high moisture three-dimensional polymeric network that traps or immobilizes water molecules within it (Wang et al. 2014). Gelation involves the association and crosslinking of the protein chains to form a rigid network, which can contribute to the microstructure and physical property of protein gels (Zhang et al. 2017; Wang et al. 2017a). The microstructure of heat-induced SPP gels after HHP at different pH values was observed by SEM as shown in Fig. 3-5. For non-HHP treated SPP, a coarse and disordered gel network was observed at pH 3.0 (Fig. 3-5a); a better improved gel network was observed at pH 6.0 (Fig. 3-5e); and a compact gel network was obtained at pH 9.0 (Fig. 3-5i). The lack of charge at pH 3.0 might cause the SPP molecules to be randomly aggregated during the thermal processing (Ni et al. 2014). Moreover, it could be noticed that a much more denser and uniform network after 400 and 550 MPa treatment at pH 9.0 was observed (Fig. 3-5k and l), owing to more functional site being exposed by HHP and intense electrostatic repulsion between proteins. The properties of gel networks were strongly related to the speed of unfolding and aggregation of protein (Zhang et al. 2017). Compared with SPP treated at low pH values (3.0 and 6.0), SPP was more negatively charged at pH 9.0 (Fig. 3-2). The strong electrostatic repulsion between SPP molecules might lead to a slower rate of aggregation than that of unfolding (Kim et al. 2016; Wang et al. 2017a), which could finally form a homogeneous gel network with smaller cavities and contribute to increased hardness and improved WHC (Wang et al. 2014).

Fig. 3-4. Thermomechanical spectra of SPP treated by HHP at different pH values. (a) pH 3.0; (b) pH 6.0; (c) pH 9.0.

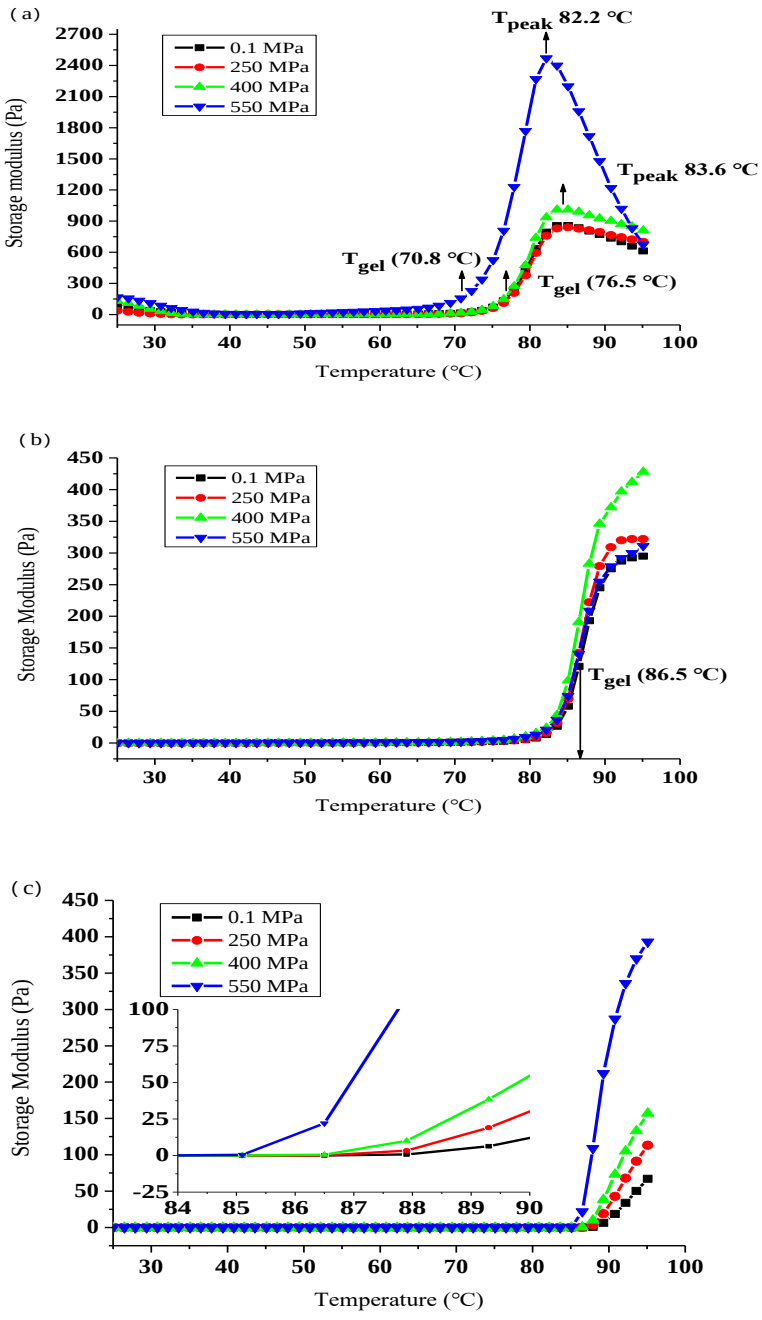

3.4.3. Textural analysis

The textural properties of SPP treated by HHP at different pH values are shown in Fig. 3-6a, b and c. Generally, hardness and springiness are used to describe the quality of protein gels, whereas chewiness is the mouth feel sensation of labored chewing due to sustained, elastic resistance from the food. At pH 3.0, hardness of SPP gels increased from 0.1 to 250 MPa then slightly decreased at 400 and 550 MPa; whereas springiness (Fig. 3-6b) and chewiness (Fig. 3-6c) clearly improved with increasing pressure. At pH 6.0, hardness reduced at 400-550 MPa, while springiness and chewiness increased initially at 250 MPa, then decreased at 400-550 MPa. At pH 9.0, the highest value of hardness of SPP gels was found by HHP at 250 MPa, and both chewiness and springiness were enhanced by HHP at 250, 400 and 550 MPa compared with non-HHP treated SPP. In addition, SPP gels made from non-HHP (0.1 MPa) and HHP treated SPP at pH 9.0 exhibited higher hardness, springiness and chewiness than those at pH 3.0 and 6.0 (Fig. 3-6a, b and c), being consistent with the observation by SEM (Fig. 3-5). The poor performance of texture behaviors observed at low pH value could be due to the intense surface hydrophobicity, the loss of net charge and weak hydration of proteins (Wang et al. 2014). Besides, high pH value presented stronger effect on textural behaviors, which might be significantly depended on the relative speed of unfolding and aggregation and thus led to a rigid mish (Ni et al. 2014; Cando et al. 2015).

3.4.4. Low field NMR

Low-field NMR technique was useful in measuring the mobility and proportion of different water molecules in protein gels without destroying its structures. It had been suggested that T_{2b} component reflected water closely associated with macromolecules, and T_{21} component indicated water trapped within gel networks, viz corresponded to bound and immobilized water fractions, respectively (Han et al. 2014; Zhang et al. 2015).

The changes of T2 relaxation times of SPP gels treated by HHP at different pH values are presented in Table 3-2. T_{2b} decreased with pH increasing from 3.0 to 9.0, while T_{21} increased from pH 3.0 to 6.0, then decreased at pH 9.0, both for non-HHP (0.1 MPa) and HHP treated SPP. With pressure increasing, T_{2b} and T_{21} increased from 0.1-400 MPa then decreased up to 550 MPa at pH 3.0, slightly increased at pH 6.0, and no significant changes were observed at pH 9.0. A short relaxation time (T2) at pH 9.0 indicated water bound more closely to SPP than that with longer T2. The reduction of T_{2b} mainly suggested the bound water (T_{2b}) had lower water mobility than that of T_{21}, and was more closely associated with SPP, which might related to the increase in negative electric (Fig. 3-2). Moreover, the increase in T_{21} upon HHP was probably due to the more unfolding extent of SPP structure, which caused a greater variation of water proton population in final gels (Zhang et al. 2015).

For non-HHP treated SPP, the proportion of A_{2b} of SPP gels decreased at pH 6.0 and 9.0 compared with that at pH 3.0, while A_{21} inversely increased. The opposite trend in A_{2b} and A_{21} was possibly due to the transformation between different water fractions. And the increase in A_{21} suggested that more immobilized water presented in SPP at pH 6.0 and 9.0. For HHP treated SPP, A_{2b} of SPP gels first increased

(0.1-400 MPa) then decreased at pH 3.0; steadily increased from 0.1-550 MPa at pH 6.0; and decreased from 0.1-550 MPa at pH 9.0. In the case of A_{21}, no significant changes were observed from 0.1-400 MPa at different pH values, while it was slightly decreased up to 550 MPa both at pH 3.0 and 6.0. The decrease of A_{21} at low pH values probably related to the loss of immobilized water fractions, which transferred to free water or more loosely immobilized water fractions. The results above were consistent with the microstructure by SEM (Fig. 3-5) and mechanical properties (Fig. 3-6). It was suggested that water mobility in gel system was restricted by high pH values (Han et al. 2014), and the gels formed by HHP treated SPP (250 and 400 MPa) at pH 9.0 hold more immobilized water fractions with a less mobilized state.

3.4.5. WHC

WHC of SPP treated by HHP at different pH values is shown in Fig. 3-6d. WHC is considered to be an important tool for evaluating the ability of adsorbing or binding with active components. As shown in Fig. 3-6d, WHC of SPP firstly increased with pressure increasing from 0.1-400 MPa, then slightly decreased up to 550 MPa at pH 3.0 and 9.0. At pH 6.0, no significant changes were observed in WHC of SPP from 0.1-400 MPa, but presented a slight decrease at 550 MPa. Remarkably, SPP gels treated at pH 9.0 presented higher WHC than those treated at pH 3.0 and 6.0 (Fig. 3-6d), which were consistent with the results from SEM (Fig. 3-5), texture (Fig. 3-6) and NMR (Table 3-2). This might be explained by that high absolute value of zeta potential could lead to fast extension of protein chains, and followed by a reduction in the diameter of gel cavities (Wang et al. 2014). The high pH condition could result in a larger specific surface of SPP, which produced a relatively larger contact area between proteins and water molecules (Zhang et al. 2015; Liang et al. 2016). Wang et al. (2014) also found that WHC of duck blood plasma protein gels significantly increased with pH increasing from 5.5 to 7.5. Furthermore, Wang et al. (2017b) reported that WHC of rabbit myosin gel was enhanced at 100 MPa, suggesting the potential ability of HHP in improvement on the water-holding behavior and gel properties of proteins ingredients.

According to above results, it could be supposed that the gel characteristic of SPP was possibly associated with its chemical forces and protein molecules arrangement. In addition, although the isoelectric point and inherent structure characters varied by SPP and proteins from other sources (e.g. other plant proteins, animal proteins), high quality of gel behavior was constantly obtained at the pH far away from the isoelectric point (Wang et al. 2014; Kim et al. 2016). At pH 3.0, the weak charge density and high hydrophobicity enhanced by HHP might cause fast aggregation of SPP, which tended to form a coarse and disordered gel network and was associated with the lower hardness and WHC of the gels (Ni et al. 2014). With pH values increased to 6.0, particularly up to 9.0, the interactions between SPP molecules were enhanced by HHP, which was attributed to the more exposed functional group and charged amino acid residues due to protein unfolding (Puppo et al. 2004). And a compact gel matrix with small mesh diameter was therefore formed, contributing to better texture, holding capacity and reduced mobility of water molecules (Peyrano et al. 2016).

Fig. 3-5. Scanning electron microscopy (SEM) images (×2000) of gels from SPP treated by HHP at different pH values.

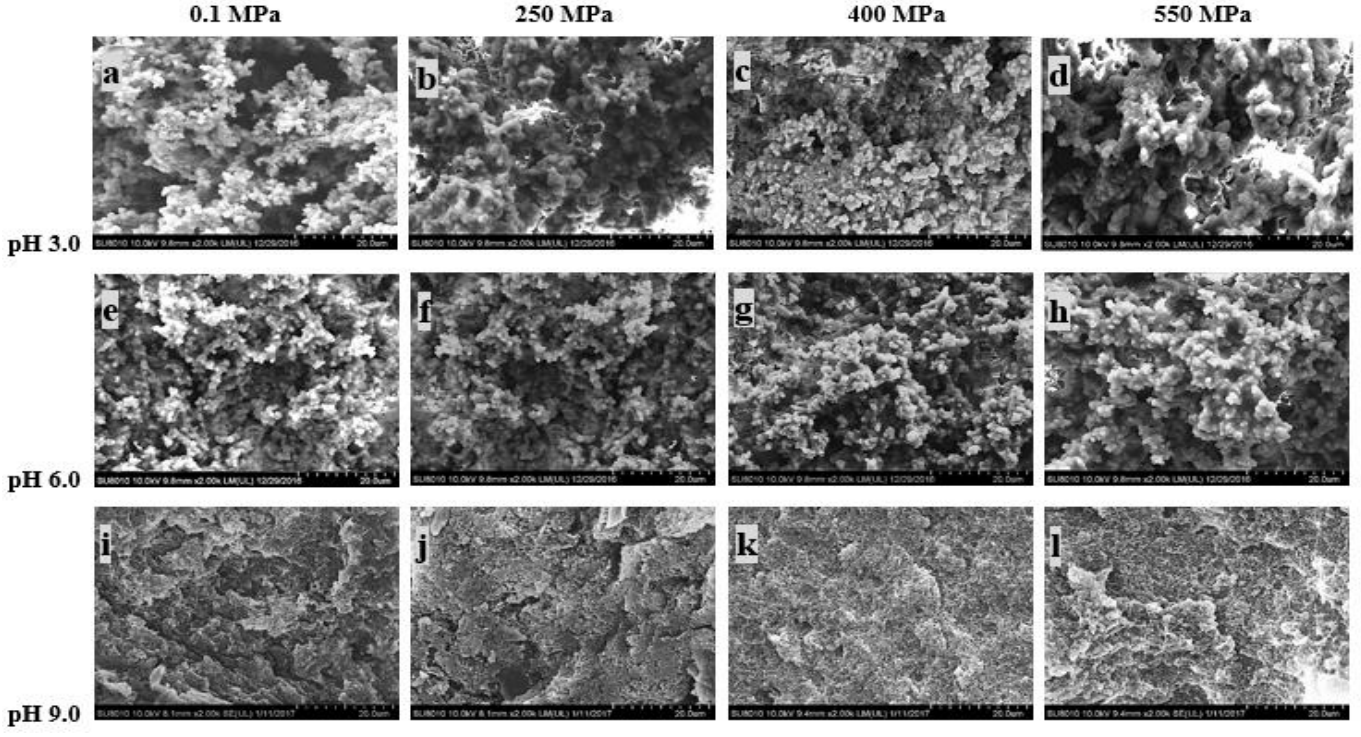

Fig. 3-6. Textural properties (a, b and c) and water-holding capacity (d) of gels from SPP treated by HHP at different pH values.

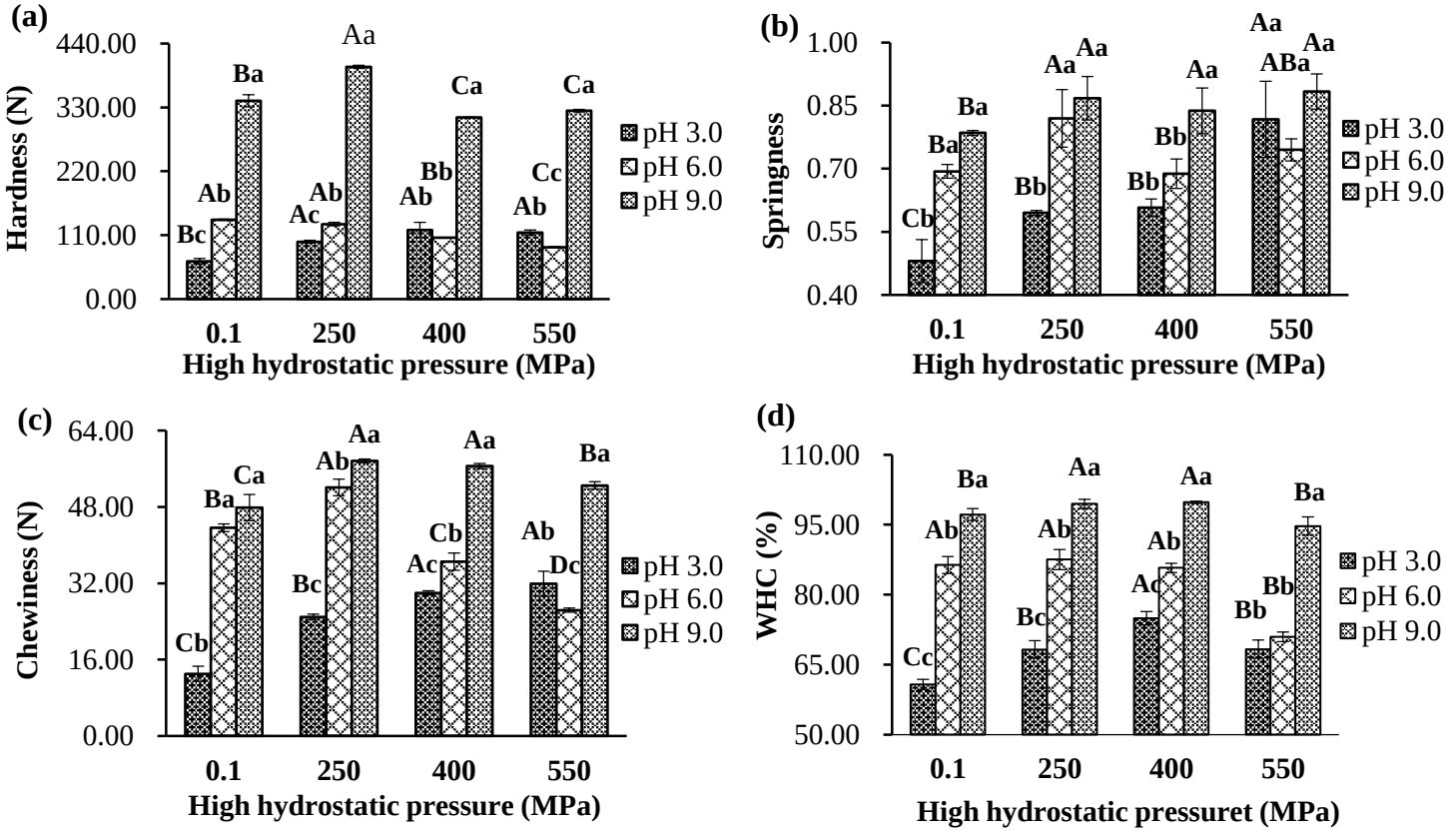

* Bars with different uppercase letters (A-D) indicate significant differences of SPP treated by same pH values but under different pressure; and bars with different lowercase letters (a-c) means significant differences of SPP treated by same pressure but combined with different pH values ($p < 0.05$).

Table 3-2 Changes in distributions of T2 relaxation times (T_{2b}, T_{21}), and proportion of peak area (A_{2b}, A_{21}) of gels from SPP treated by HHP at different pH values.

HHP (MPa)	pH	T_{2b} (ms)	T_{21} (ms)	A_{2b} (%)	A_{21} (%)
0.1	3.0	9.66 ± 0.00^{Ba}	126.04 ± 0.00^{Bb}	2.41 ± 0.16^{Ba}	96.35 ± 0.09^{Ab}
	6.0	8.12 ± 0.40^{Bb}	144.81 ± 0.00^{Ca}	1.17 ± 0.13^{Bb}	98.12 ± 0.03^{Aa}
	9.0	0.23 ± 0.02^{Ac}	95.48±0.00Ac	1.52 ± 0.34^{Ab}	98.48 ± 0.34^{Aa}
250	3.0	12.38 ± 1.82^{Aa}	139.96 ± 6.87^{Aa}	2.71 ± 0.03^{ABa}	96.41 ± 0.52^{Ab}
	6.0	7.32 ± 0.00^{Cb}	144.81 ± 0.00^{Ca}	1.19 ± 0.04^{Bb}	98.20 ± 0.05^{Aa}
	9.0	0.27 ± 0.07^{Ac}	95.48 ± 0.00^{Ab}	1.46 ± 0.17^{Ab}	98.54 ± 0.17^{Aa}
400	3.0	13.21 ± 0.65^{Aa}	144.81 ± 0.00^{Ab}	2.95 ± 0.10^{Aa}	96.38 ± 0.27^{Ab}
	6.0	8.41 ± 0.00^{Bb}	155.22 ± 0.00^{Ba}	1.34 ± 0.02^{Bb}	98.15 ± 0.24^{Aa}
	9.0	0.32 ± 0.08^{Ac}	95.48 ± 0.00^{Ac}	1.14 ± 0.44^{Ab}	98.86 ± 0.44^{Aa}
550	3.0	5.36 ± 0.26^{Cb}	106.02 ± 5.20^{Cb}	1.12 ± 0.15^{Cb}	94.68 ± 0.19^{Bc}
	6.0	11.10 ± 0.00^{Aa}	166.38 ± 0.00^{Aa}	1.85 ± 0.08^{Aa}	96.78 ± 0.06^{Bb}
	9.0	0.26 ± 0.09^{Ac}	95.48 ± 0.00^{Ac}	0.71 ± 0.20^{Ab}	99.29 ± 0.20^{Aa}

* Results are presented as mean ± standard deviation (n=3). Different uppercase (A-C) in the same column means significant differences of SPP treated by same pH values but under different pressure treatment; and different lowercase (a-c) in the same column means significant differences of SPP treated by same pressure but combined with different pH values ($p < 0.05$).

4. Conclusions

HHP treatment exposed interior hydrophobic residues and -SH- groups, modified secondary structure, and promoted the unfolding of protein chains of SPP. The unfolding was responsible for the subsequent aggregation of SPP and leading to the formation of higher molecular weight polymers by the disulfide linkage with the increase of pressure level at pH 6.0 and 9.0. Rheological behavior of SPP was strongly dependent on the pH values, and the G′ was significantly increased after HHP treatment ($p < 0.05$). The hardness, springiness, chewiness and WHC of gels made from SPP treated at moderate pressure (250 and 400 MPa) in an alkaline dispersion system (pH 9.0) were significantly improved, leading to a compact and uniform three-dimensional gel network, which indicated that more immobilized water fractions with a less mobilized state in SPP gels formed at pH 9.0. It was suggested that 400 MPa treated SPP at different pHs, especially at pH 9.0, followed by those at pH 6.0 and 3.0, were reasonable choices in the present study for preparing novelty food products with structural modification. These results would be of great help for understanding the gelling behavior of SPP at different pH levels, and the development of HHP technique in improving gelation properties of SPP in handling of this new protein resource as natural gelatin, adjusting textures of gel-like food in alkali (e.g. baked products), weak acidic (e.g. yogurt, beverages), and acidic (e.g. fruit juice) conditions.

Acknowledgments

The authors gratefully acknowledge the earmarked fund for China Agriculture Research System (CARS-10-B21). We also thank the National Key R&D Program of China (2016YFE0133600).

References

Angioloni, A., Collar, C. (2013). Impact of high hydrostatic pressure on protein aggregation and rheological properties of legume batters. *Food and Bioprocess Technology*, 6, 3576-3584.

Arogundade, L. A., Mu, T. H. (2012a). Influence of oxidative browning inhibitors and isolation techniques on sweet potato protein recovery and composition. *Food Chemistry*, 134, 1374-1384.

Arogundade, L. A., Mu, T. H., Añón, M. C. (2012b). Heat-induced gelation properties of isoelectric and ultrafiltered sweet potato protein isolate and their gel microstructure. *Food Research International*, 49, 216-225.

Barba F. J., Terefe N. S., Buckow R., et al. (2015). New opportunities and perspectives of high pressure treatment to improve health and safety attributes of foods. A review. *Food Research International*, 77, 725-742.

Boutureira, O., Bernardes, G. J. L. (2015). Advances in chemical protein modification. *Chemical Reviews*, 115, 2174-2195.

Cando, D., Herranz, B., Borderías, A. J., et al. (2015). Effect of high pressure on reduced sodium chloride surimi gels. *Food Hydrocolloids*, 51, 176-187.

Chang, C., Tu, S., Ghosh, S., et al. (2015). Effect of pH on the inter-relationships between the physicochemical, interfacial and emulsifying properties for pea, soy, lentil and canola protein isolates. *Food Research International*, 77, 360-367.

Chen, X., Li, P., Nishiumi, T., et al. (2014). Effects of high pressure processing on the cooking loss and gel strength of chicken breast actomyosin containing sodium alginate. *Food and Bioprocess Technology*, 7, 3608-3617.

Cheung, L., Wanasundara, J., Nickerson, M. T. (2014). Effects of pH and NaCl levels on the physicochemical and emulsifying properties of a cruciferin protein isolate. *Food Biophysics*, 9, 105-113.

De Maria, S., Ferrari, G., Maresca, P. (2016). Effects of high hydrostatic pressure on the conformational structure and the functional properties of bovine serum albumin. *Innovative Food Science & Emerging Technologies*, 33, 67-75.

FAOSTAT. (2016). Production quantity [Internet]. Food and Agricultural Organization. http://www.fao.org/faostat/en/#data/QC. Accessed 01/06/18.

Gaspar, A. L. C., De Góes-Favoni, S. P. (2015). Action of microbial transglutaminase (MTGase) in the modification of food proteins: A review. *Food Chemistry*, 171, 315-322.

Grossi A, Olsen K, Bolumar T, et al. (2016). The effect of high pressure on the functional properties of pork myofibrillar proteins. *Food Chemistry*, 196, 1005-1015.

Han, M., Wang, P., Xu, X., et al. (2014). Low-field NMR study of heat-induced gelation of pork myofibrillar proteins and its relationship with microstructural characteristics. *Food Research International*, 62, 1175-1182.

Han, Y., Wang, J., Li, Y., et al. (2015). Circular dichroism and infrared spectroscopic characterization of secondary structure components of protein Z during mashing and boiling processes. *Food Chemistry*, 188, 201-209.

He, R., He, H. Y., Chao, D., et al. (2014). Effects of high pressure and heat treatments on physicochemical and gelation properties of rapeseed protein isolate. *Food and Bioprocess Technology*, 7, 1344-1353.

Jia, Y. J., Liang, X. H., Zhu, W. X. (2010). Separation of β-amylase from sweet potato by different precipitation methods. *Food Science*, 31, 22-25.

Khan N. M., Mu, T. H., Sun, H. N., et al. (2015). Effects of high hydrostatic pressure on secondary structure and emulsifying behavior of sweet potato protein. *High Pressure Research*, 35, 189-202.

Khan, N. M., Mu, T. H., Zhang, M., et al. (2014). The effects of pH and high hydrostatic pressure on the physicochemical properties of a sweet potato protein emulsion. *Food Hydrocolloids*, 35, 209-216.

Khan, N. M., Mu, T. H., Zhang, M., et al. (2013). Effects of high hydrostatic pressure on the physicochemical and emulsifying properties of sweet potato protein. *International Journal of Food Science & Technology*, 48, 1260-1268.

Kim, J. H. J., Varankovich, N. V., Nickerson, M. T. (2016). The effect of pH on the gelling behaviour of canola and soy protein isolates. *Food Research International*, 81, 31-38.

Laemmli, UK. (1970). Cleavage of structural proteins during assembly of head of bacteriophage T4. *Nature*, 227, 680-685.

Liang, Y., Guo, B., Zhou, A., et al. (2016). Effect of high pressure treatment on gel characteristics and gel formation mechanism of bighead carp (Aristichthys nobilis) surimi gels. *Journal of Food Processing and Preservation*, 6, 1-8.

Mu, T. H., Tan, S. S., Chen, J. W., et al. (2009a). Effect of pH and $NaCl/CaCl_2$ on the solubility and emulsifying properties of sweet potato protein. *Journal of the Science of Food and Agriculture*, 89, 337-342.

Mu, T. H., Tan, S. S., Xue, Y. L. (2009b). The amino acid composition, solubility and emulsifying properties of sweet potato protein. *Food Chemistry*, 112, 1002-1005.

Ni, N., Wang, Z. Y., He, F., et al., (2014). Gel properties and molecular forces of lamb myofibrillar protein during heat induction at different pH values. *Process Biochemistry*, 49, 631–636.

Norton, T., Sun, D. W. (2008). Recent advances in the use of high pressure as an effective processing technique in the food industry. *Food and Bioprocess Technology*, 1, 2–34.

Peyrano F., Speroni F., Avanza M. V. (2016). Physicochemical and functional properties of cowpea protein isolates treated with temperature or high hydrostatic pressure. Innovative *Food Science & Emerging Technologies*, 33, 38-46.

Puppo C., Chapleau N., Speroni F., et al. (2004). Physicochemical modifications of high-pressure-treated soybean protein isolates. *Journal of Agricultural and Food Chemistry*, 52, 1564-1571.

Qin, Z., Guo, X., Lin, Y., et al. (2013). Effects of high hydrostatic pressure on physicochemical and functional properties of walnut (Juglans regia L.) protein isolate. *Journal of the Science of Food and Agriculture*, 93, 1105-1111.

Queirós, R. P., Saraiva, J. A., Da Silva, J. A. L. (2018). Tailoring structure and technological properties of plant proteins using high hydrostatic pressure. *Critical Reviews in Food Science and Nutrition*, 58, 1538-1556.

Renkema, J. M. S., Gruppen, H., Van, Vliet. T. (2002). Influence of pH and ionic strength on heat-induced formation and rheological properties of soy protein gels in relation to denaturation and their protein compositions. Journal of Agricultural and *Food Chemistry*, 50, 6064-6071.

San Martin, M. F., Barbosa-Cánovas, G. V., & Swanson, B. G. (2002). Food processing by high hydrostatic pressure. Critical *Reviews in Food Science and Nutrition*, 42, 627-645.

Sun, M. J., Mu, T. H., Sun, H. N., et al. (2014). Digestibility and structural properties of thermal and high hydrostatic pressure treated sweet potato (Ipomoea batatas L.) protein. *Plant Foods for Human Nutrition*, 69, 270-275.

Sun, X. D., Arntfield, S. D. (2012). Molecular forces involved in heat-induced pea protein gelation: effects of various reagents on the rheological properties of salt-extracted pea protein gels. *Food Hydrocolloids*, 28, 325-332.

Tang, C. H., & Ma, C. Y. (2009). Effect of high pressure treatment on aggregation and structural properties of soy protein isolate. *LWT-Food Science and Technology*, 42, 606-611.

Wang, K. Q, Luo, S. Z, Zhong, X. Y., et al. (2017a). Changes in chemical interactions and protein conformation during heat-induced wheat gluten gel formation. *Food Chemistry*, 214, 393-399.

Wang, M., Chen, X., Zou, Y., et al. (2017b). High-pressure processing-induced conformational changes during heating affect water holding capacity of myosin gel. *International Journal of Food Science & Technology*, 52, 724-732.

Wang, P., Xu, X., Huang, M., et al. (2014). Effect of pH on heat-induced gelation of duck blood plasma protein. *Food Hydrocolloids*, 35, 324-331.

Whitmore, L., Wallace, B. A. (2004). DICHROWEB, an online server for protein secondary structure analyses from circular dichroism spectroscopic data. *Nucleic Acids Research*, 32 (suppl 2), 668-673. http://dichroweb.cryst.bbk.ac.uk. Accessed 13. 02. 17

Wihodo, M., Moraru, C. I. (2013). Physical and chemical methods used to enhance the structure and mechanical properties of protein films: A review. *Journal of Food Engineering*, 114, 292-302.

Wu, C., Hua, Y., Chen, Y., et al. (2017). Effect of temperature, ionic strength and 11S ratio on the rheological properties of heat-induced soy protein gels in relation to network proteins content and aggregates size. *Food Hydrocolloids*, 66, 389-395.

Yang, C., Wang, Y., Vasanthan, T., et al. (2014). Impacts of pH and heating temperature on formation mechanisms and properties of thermally induced canola protein gels. *Food Hydrocolloids*, 40, 225-236.

Zhang, M., Mu, T. H., Sun, M. J. (2014). Purification and identification of antioxidant peptides from sweet potato protein hydrolysates by Alcalase. *Journal of Functional Foods*, 7, 191-200.

Zhang, Z., Yang, Y., Tang, X., et al. (2015). Chemical forces and water holding capacity study of heat-induced myofibrillar protein gel as affected by high pressure. *Food Chemistry*, 188, 111-118.

Zhang, Z., Yang, Y., Zhou, P., et al. (2017). Effect of high pressure modification on conformation and gelation properties of myofibrillar protein. *Food Chemistry*, 217, 678-686.

Zhou, A. M., Lin, L. Y., Liang, Y., et al. (2014). Physicochemical properties of natural actomyosin from threadfin bream (Nemipterus spp.) induced by high hydrostatic pressure. *Food Chemistry*, 156, 402–407.

Zhu, Z., Guan, Q., Koubaa, M., et al. (2017). HPLC-DAD-ESI-MS2 analytical profile of extracts obtained from purple sweet potato after green ultrasound-assisted extraction. *Food Chemistry*, 215, 391-400.

Chapter IV

Effects of salts and high hydrostatic pressure on the structure and gelation properties of sweet potato protein

Chapter IV Effects of salts and high hydrostatic pressure on structure and gelation properties of sweet potato protein

This chapter is adapted from the published article:

Effect of salts combined with high hydrostatic pressure on structure and gelation properties of sweet potato protein

*Zhong-Kai Zhao[1,2]· Tai-Hua Mu[*1]· Miao Zhang[1]· Aurore Richel[2]*

1 Laboratory of Food Chemistry and Nutrition Science, Institute of Food Science and Technology, Chinese Academy of Agricultural Sciences; Key Laboratory of Agro-Products Processing, Ministry of Agriculture and Rural Affairs, No. 2 Yuan Ming Yuan West Road, Haidian District, P.O. Box 5109, Beijing 100193, P. R. China.

2 University of Liège, Gembloux Agro-Bio Tech, Biological and Industrial Chemistry Unit, Passage des Déportés, 2, 5030 Gembloux, Belgium

Reference

Zhao, Z. K., Mu, T. H., Zhang, M., & Richel, A. (2018). Effect of salts combined with high hydrostatic pressure on structure and gelation properties of sweet potato protein. *LWT*, 93, 36-44.

DOI

https://doi.org/10.1016/j.lwt.2018.03.007

Abstract

The effects of monovalent (NaCl) and divalent ($CaCl_2$ and $MgCl_2$) salts combined with HHP on structure and gelation properties of SPP were investigated. Surface hydrophobicity and zeta potential of SPP significantly decreased as salts concentration increased. The total amount of -SH- groups in SPP decreased with addition of NaCl, $CaCl_2$ and $MgCl_2$ under HHP, whereas the disulfide bonds (-S-S-) increased from 0.59 to 0.80 and 0.74 μmol/g with addition of 0.1 and 0.2 mol/L of $CaCl_2$ combined with HHP, respectively. The α-helical content of SPP was increased by all three salts, but decreased as salts combined with HHP, while β-sheet content was increased at high ionic strength with HHP, especially in presence of $CaCl_2$ and $MgCl_2$, being increased from 30.40 to 33.45 and 33.55 %, respectively. The storage modulus (G′) of SPP was enhanced by salts and HHP, even though it decreased at high ionic strength. Textural properties and water holding capacity of SPP gels were improved with salt ions by HHP, being attributed to more bound water.

Keywords

Sweet potato protein; High hydrostatic pressure; Salt ions; Structure; Gelation properties

1. Introduction

Protein elements recovered from by-products is mainly environmental and economic concerns, particularly in developing countries where daily dietary protein intake is relatively low. Sweet potato (*Ipomoea batatas* [L.] Lam) in China accounts for 90.32 % of Asia production and 67.11 % of world output (FAOSTAT, 2014). As a major resource of starch in China, a large amount of waste effluent is generated during sweet potato starch processing, which contains approximately 1.5 % crude protein but is normally discarded (Mu, Tan & Xue, 2009). SPP is rich in essential amino acids, and presents higher nutritive value than most other plant proteins (Mu et al., 2009), being potentially applied in functional food.

Salt ions make an essential contribution to the structure, texture, appearance and sensory properties of food (Albarracín et al, 2011; Barat et al, 2013). Due to the electrolytic character, sodium and calcium salts are used to improve the gelation properties of various processed foods, including beverages, jam, cream and sausage (Tobin et al., 2013; Wu et al., 2016). As an essential trace element, magnesium salts have attracted much interest correlated to their protective function in human heart blood vessels and the ability to partially substitute for sodium salts to improve the gel textural properties of proteins (Gupta & Gupta, 2014; Zhang et al., 2016). In general, divalent ions are considered more effective for binding to oppositely charged amino acids and water molecules than monovalent ions, leading to weak electrostatic repulsion interactions between adjacent protein molecules, and finally resulting in physical aggregation and precipitation (Wu et al., 2016; Chen et al., 2017). It was reported that myosin exhibited a higher turbidity and larger particle size with addition of $CaCl_2$ and promoted the unfolding of α-helical units (Cao, et al., 2015). Zhang et al. (2016) suggested that divalent ions ($CaCl_2$ and $MgCl_2$) were contributing to stronger hydrophobic interactions, weaker hydrogen bonding and electrostatic interactions compare to that of monovalent ions (NaCl).

HHP is an efficient non-thermal physical method to cause modification of protein secondary structure, and hence improve protein gelation properties via protein-protein interactions, such as surface hydrophobicity, electrostatic interactions, disulphide linkages and hydrogen bonding (Zhang et al., 2015; De Maria, Ferrari, & Maresca, 2016). The degree of protein denaturation, aggregation and gelation are depended on protein system, applied pressure level, salt additives and even ionic strength (Añón, De Lamballerie, & Speroni, 2011). It had been reported that HHP could induce the aggregation of myosin and further promote its gel-strength (Xue et al., 2017). Moreover, Cando et al. (2015) indicated that HHP could be potentially applied on reduced NaCl surimi gels to get similar structure, mechanical and sensory properties as the ones with a high level of NaCl. In our previous study, the effects of HHP in improving physicochemical and emulsifying properties of SPP had been confirmed (Khan et al, 2015). The in vitro digestibility and gelation properties of SPP at atmospheric pressure were also investigated (Sun et al., 2012; Arogundade, Mu, & Añón, 2012).

SPP exhibits satisfactory water-solubility and gelation properties ((Mu, Tan & Xue, 2009; Arogundade et al., 2012), showing potential utilization in gel-like foods, such as mince, yogurt and soft beverages products, etc. As salt ions can affect the gelation behavior of protein which varied by protein types and might contribute to the formation of food characteristics. However, no study on effect of salts combined with HHP on structure and gelation properties of SPP is currently available. Hence, the objective of this study was to determine the effect of HHP on chemical forces, structure and rheological properties of SPP in the presence of monovalent (NaCl) or divalent salts ($CaCl_2$, $MgCl_2$), as well as textural properties, water holding capacity, mobility and water distribution of SPP gels after HHP treatment.

2. Materials and methods

2.1. Materials

Sweet potato cultivar Shang Shu No.19 was supplied by Shangqiu Academy of Agriculture and Forestry Sciences (Henan province, China). Tris Base, glycine and 5,5-dithio-bis-[2-nitrobenzoic acid] (DTNB) were purchased from Sigma–Aldrich, Inc. (St. Louis, Mo, USA). Other chemicals and reagents were of analytical grade.

2.2. SPP preparation

SPP preparation was carried out according to Arogundade, Mu, & Añón (2012) with slight modification. Briefly, fresh peeled sweet potato tubers were ground with sodium bisulfite solution (0.1 %, for color protection) at a solid to solvent ratio of 1:2, centrifuged at 10,000 g for 45 min, and the supernatant was collected and adjusted to pH 4.0 to generate a precipitate. The precipitate was dissolved in distilled water at a ratio of 1:3, the pH was adjusted to pH 7.0, centrifugation was repeated as previously described, and the supernatant was concentrated using an ultrafiltration device with a 10 kDa molecular weight cut-off ultrafiltration membrane, then lyophilized. The final SPP sample was 92.95 % dry weight basis as measured by the Kjeldahl method (N% × 6.25).

2.3. HHP treatment

HHP treatment was performed using a 0.6 L laboratory-scale HHP units (model HHP-L3, HuaTaiSenMiao Engineering & Technique Ltd. Co., Tianjin, China) equipped with both temperature control and pressure regulation. Each SPP dispersion (4 %) in 50 mmol/L Tris-HCl buffer at pH 7.0 was vacuum-packed in food-grade polyethylene bags with or without added NaCl (0.2 and 0.4 mol/L), $CaCl_2$ (0.1 and 0.2 mol/L) or $MgCl_2$ (0.1 and 0.2 mol/L), then subjected to HHP at 400 MPa (selected pressure stage, data not shown) for 30 min before release within 5 s. The pressurization was maintained at 25 °C with a water jacket for temperature control. SPP samples with the same salt additives but not pressure treated were used as reference. After HHP treatment, each protein solution was freeze dried, and then stored at -18 °C for subsequent analysis.

2.4. Ho

Ho of SPP samples was determined using 1-anilinonaphthalene-8-sulphonic acid (ANS) as a hydrophobic fluorescence probe. SPP treated by HHP combined with different salts were solubilized in 10 mmol/L Tris-HCl buffer (pH 7.0) to get a concentration of 0.1 % (w/v), then serially diluted to a final concentration of 0.004-0.02 %. Each diluted solution (4.0 mL) was mixed with 20 μL of ANS (8.0 mmol/L) in the same buffer. The relative fluorescence intensity (FI) was measured using a fluorescence spectrometer (Hitachi, F2500, Tokyo, Japan) at wavelengths of 390 nm (excitation) and 470 nm (emission) with slit widths of 5 nm. Ho was obtained from the initial slope of the plot of FI versus protein concentration calculated by linear regression analysis (data not shown).

2.5. Zeta potential

Zeta potential was measured by a Zetasizer (Nano-ZS90, Malvern Instruments Ltd., Worcestershire, UK) equipped with an avalanche photodiode detector. SPP solutions (1.0 mg/mL, w/v) were prepared by dissolving protein powder into Milli-Q water. An aliquot (1.0 mL) of SPP solution (1.0 mg/mL) was then injected into the clear disposable test cell (DTS1060C, Malvern Instruments Ltd.) and equilibrated at 25 °C for 2 min before testing. Electrostatic interactions were inferred from the absolute value of the zeta potential.

2.6. -SH- groups

Total and free -SH- group content were determined according to the method of He et al. (2014). An aliquot (1.0 mL) of SPP (1.0 mg/mL) was dissolved in Tris-glycine buffer (0.086 mol/L Tris, 0.09 mol/L glycine, 0.004 mol/L EDTA, 8.0 mol/L urea, pH 8.0), mixed with 50 μL of Ellman's reagent (4.0 mg/mL DTNB) and incubated for 20 min at room temperature, followed by centrifugation at 10,000 *g* for 20 min. The absorbance of the supernatant was measured at 412 nm by a UV-Vis spectrophotometer (TU-1810, Puxi instrument Ltd. Co., Beijing, China) using a molar extinction coefficient of 13,600 $mol^{-1} \cdot cm^{-1}$. The free -SH- groups content was measured in the absence of 8.0 mol/L urea. The disulfide bond (-S-S-) content was calculated as half the difference between the total and free -SH- group content.

2.7. CD

Secondary structure changes of SPP (1.0 mg/mL) were monitored using a MOS-450/AF-CD spectrophotometer (Bio-Logic Science Instruments, Vaucanson, France) with a 0.1 cm optical path length quartz cell. Far-UV spectra (190 to 250 nm) were averaged over three consecutive scans at a speed of 1000 nm per min, a bandwidth of 1.0 nm, a response time of 0.5 s, and a step resolution of 0.5 nm. Data were expressed as mean residue ellipticity (θ, $deg \cdot cm^2 \cdot dmol^{-1}$) according to Whitmore & Wallace. (2004).

2.8. Gelation properties

2.8.1. Dynamic shear rheology-temperature relationship

Dynamic shear rheological properties were investigated by dissolving SPP (10 %) in 10 mM phosphate buffer (pH 7.0) at a constant angular frequency of 10 s^{-1} and a strain of 0.5 % (within the linear viscoelasticity range, LVER). Measurements were made using an Anton Paar rheometer (Physica MCR 301, Graz, Austria) equipped with a temperature controlled Peltier system. A 2.3 mL SPP dispersion was continually injected onto the parallel plate geometry (PP-50 probe, 50 mm diameter, 1.0 mm plate gap). SPP samples were heated at a linear temperature rate of 2 °C/min from 25 to 95 °C. The exposed perimeter was attached with a small amount of silicon oil to avoid sample drying during heating. Rheological parameters of storage modulus (G′) were then recorded during a heating-cooling cycle for each sample.

2.8.2. Preparation of SPP gel model

SPP gels were prepared with SPP dispersion (10 %) in 10 mmol/L phosphate buffer (pH 7.0). The SPP dispersion were injected into glass mold with 2.3 cm internal diameters, covered with aluminum foil, placed in water bath, heated from 25 to 95 °C, and maintained at 95 °C for 30 min. Then, SPP gels in glass molds were immediately cooled under running water, and stored at 4 °C for 12 h. The cylindrical gels were used for texture analysis, measurement of low-field nuclear magnetic resonance (NMR) and water-holding capacity (WHC).

2.8.3. Textural properties

Textural analysis was performed by uniaxial compression tests using a TA-XT2i texture analyser (Stable Micro System Ltd., Godalming, UK) equipped with a 12.0 mm diameter probe (P 0.5R). Cylindrical SPP gels were prepared as described in preceding section of 2.8.2 and compressed to 30 % of the original height at a speed of 1.0 mm/s with 5 s waiting time. Values were measured in triplicate at 25 °C by Texture Expert analysis software (Stable Micro Systems Ltd., Godalming, UK). Hardness, springiness and chewiness were obtained to evaluate the texture behaviours of SPP gels.

2.8.4. Low-field NMR

The measurement of the transverse relaxation time (T2) were performed by using a Niumag pulsed NMR analyzer (MesoMR23-060H-I, Niumag Electric Corporation, Shanghai, China) operating at 32 °C and 23 MHz (resonance frequency, RF). SPP gel sample as described in Section 2.8.2 was freshly prepared and placed inside the cylindrical glass tubes (2.3 cm internal diameters). The T2 was measured using the Carr-Purcell-Meiboom-Gill (CPMG) sequence with spectral width (SW) of 250 kHz and receiver gain (RG) of 10 db. A total of 10,000 echoes were recorded, and the low-field NMR relaxation curve was fitted to a multi-exponential curve with the MultiExp Inv Analysis software (Niumag Electric Corporation, Shanghai, China). The following parameters were presented: T_{2b} and T_{21}were presented as the relaxation components, and A_{2b} and A_{21} were the corresponding area fractions.

2.8.5. WHC

The determination of WHC was performed according to the method of Ercili-Cura et al. (2013) with minor modifications. Approximately 2.0 g of SPP gel was centrifuged at 10,000 *g* for 15 min (4 °C). Subsequently, the supernatant was carefully removed and used for calculation of the free water component or un-bound water released by loose structural units. The centrifuge tube was weighed before addition of the SPP gel, and the tube containing the SPP gel was weighed before and after centrifugation. WHC (%) was expressed as the ratio of SPP gel weight after centrifugation relative to the initial weight using the following equation:

$$\text{WHC (\%)} = (W_2 - W_0) / (W_1 - W_0) \times 100 \qquad (1)$$

Where W_2 and W_1 are the weight (g) of the centrifuge tube containing the SPP gel after and before centrifugation, respectively, and, W_0 is the weight (g) of the empty centrifuge tube.

2.9. Statistical analysis

All experiments were performed in triplicate and expressed as means ± SD. One-way analysis of variance was performed using SAS 8.1 software (SAS institute Inc., Cary, NC, USA). Differences were evaluated by the Duncan's multiple range test using a 95 % confidence interval.

3. Results and discussion

3.1. Ho

Ho values of untreated (0.1 MPa) and HHP-treated (400 MPa) SPP with different salts are shown in Fig. 4-1. A significant decrease in Ho was observed for untreated and HHP-treated SPP with the addition of NaCl, $CaCl_2$ and $MgCl_2$ ($p < 0.05$, Fig. 4-1 A–C). The reduction of Ho was attributed to competition between salt ions and proteins for binding to water molecules, leading to a weak electrostatic repulsion between SPP molecules and an inhibition of contact between the ANS molecules and hydrophobic amino acid residues (Bryant & McClements, 2000). Compared with the untreated SPP, Ho of HHP-treated SPP was increased at the same concentration of salt ions, except that at 0.2 mol/L of NaCl. Qin et al. (2013) indicated that the quaternary structure maintained by hydrophobic interactions is the most sensitive to HHP, and HHP resulted in an increased exposure of the tryptophan residues of walnut protein isolate. This could be used to explain the enhancement of Ho in SPP induced by HHP. However, Cao et al. (2015) reported that $CaCl_2$ (10-40 mmol/L) increased the aggregation and surface hydrophobicity of myosin. Jiang et al. (2015) also found that Ho of soy protein isolate tended to generally increase with the ionic strength, but negatively correlated with its solubility as ionic strength increased. These findings indicated that Ho was dependent on salt type, inherent properties of proteins, and was strongly affected by the ionic strength.

3.2. Zeta potential

The zeta potential of untreated (0.1 MPa) and HHP-treated (400 MPa) SPP with different salts are shown in Fig. 4-2. The absolute value of zeta potential represent as the strength of electrostatic interactions between protein molecules. In general, high absolute zeta potential values indicate electrical stabilization, while low zeta potential values are correlated with coagulation or flocculation (Buell et al., 2013). As shown in Fig. 4-2, the zeta potential of SPP decreased significantly after adding salt ions ($p < 0.05$), especially with $CaCl_2$ (Fig. 2B) and $MgCl_2$ (Fig. 2C), indicating increased aggregation or precipitation, which was possibly due to electrostatic interactions (repulsion and/or attraction) and/or protein conformation changes. Highly charged salt ions might bind to oppositely charged amino acid residues exposed at the protein surface, forming an electric double layer that weakens the electrostatic repulsion between protein chains, and strengthening interactions within the protein dispersion system, such as protein-protein and protein-solvent interactions (Wu et al., 2016).

Moreover, a slight decrease in zeta potential was observed upon HHP treatment in the presence of NaCl (Fig. 4-2A), but no significant difference occurred upon HHP treatment with $CaCl_2$ (Fig. 4-2B) and the difference with $MgCl_2$ was minimal (Fig. 4-2C). HHP treatment did enhance the conformation flexibility of SPP (Tabilo-Munizaga et al., 2014), which might enable the salt ions to access the protein interior and bind to charged amino acids, thereby neutralising negatively charged amino acids and positively charged salt ions. This would weaken the performance at high ionic concentrations, especially in the presence of divalent ions ($CaCl_2$ and $MgCl_2$). Zhang et al. (2014b) indicated that electrostatic repulsive forces of globulin fibrils decreased gradually with increasing ionic strength, which suggested a more aggregated state of protein molecules at high ionic strength based on the weak electrostatic forces.

3.3. -SH- groups

Sulfhydryl (-SH-) groups make an essential contribution to the gelation properties of SPP. The total -SH- group content includes both those exposed -SH- groups on the protein surface and buried -SH- groups in internal structures (Hamada, Ishizaki & Nagai, 1994).

The effects of NaCl, $CaCl_2$ and $MgCl_2$ on the sulfhydryl group (-SH-) and disulphide bond (-S-S-) content of SPP under HHP treatment are shown in Table 4-1. The total and free -SH- group contents of SPP were decreased with the addition of salt ions in a concentration dependent manner, especially in the case of divalent ions ($CaCl_2$ and $MgCl_2$). The total -SH- was deceased by HHP treatment in the presence of the same salt ions at the same concentrations. By contrast, free -SH- groups were increased by HHP treatment. The decrease in total -SH- groups might be due to aggregation and/or the formation of disulphide bonds, which was contributed to protein-protein interactions (De Maria, Ferrari & Maresca, 2016). The increase in free -SH- groups induced by HHP treatment could result from the exposure of the interior -SH- groups during unfolding and extension processing (Zhang et al., 2015).

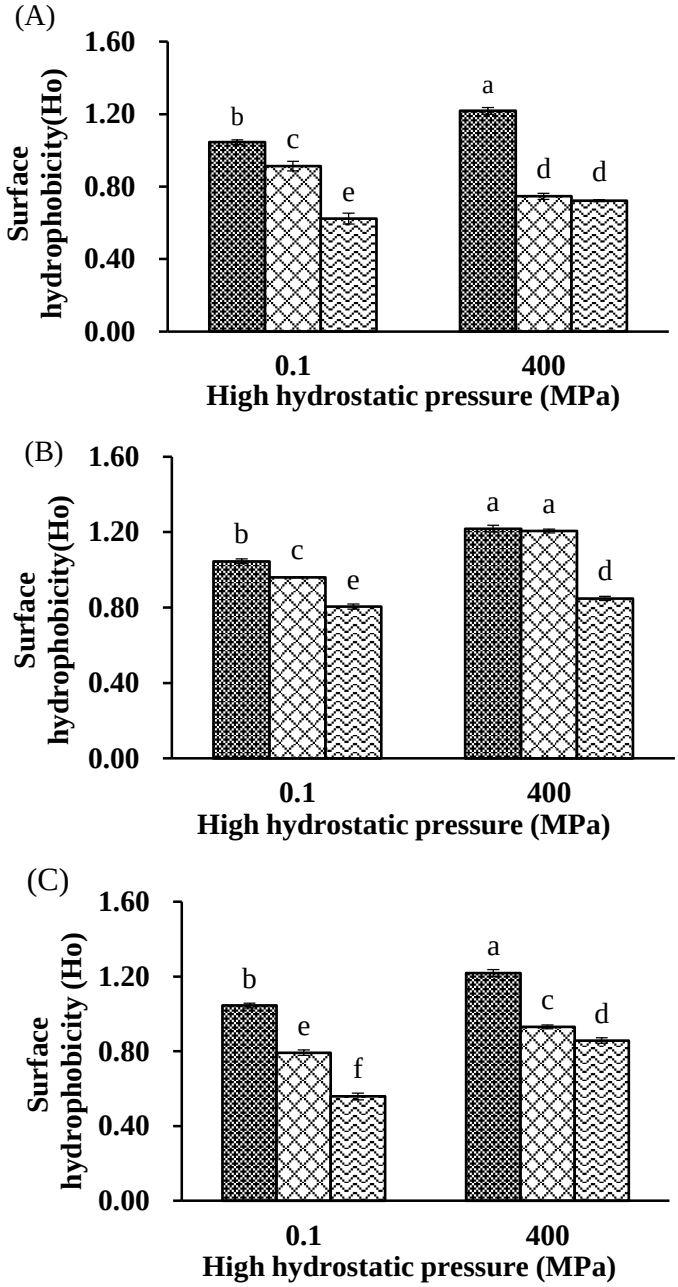

Fig. 4-1. Surface hydrophobicity (Ho) of SPP treated by HHP with addition of NaCl (A): 0 mol/L (■), 0.2 mol/L (▩), 0.4 mol/L (▨); $CaCl_2$ (B) and $MgCl_2$ (C): 0 mol/L (■), 0.1 mol/L (▩), 0.2 mol/L (▨). Different lowercase letters over the bars indicate significant differences ($p < 0.05$).

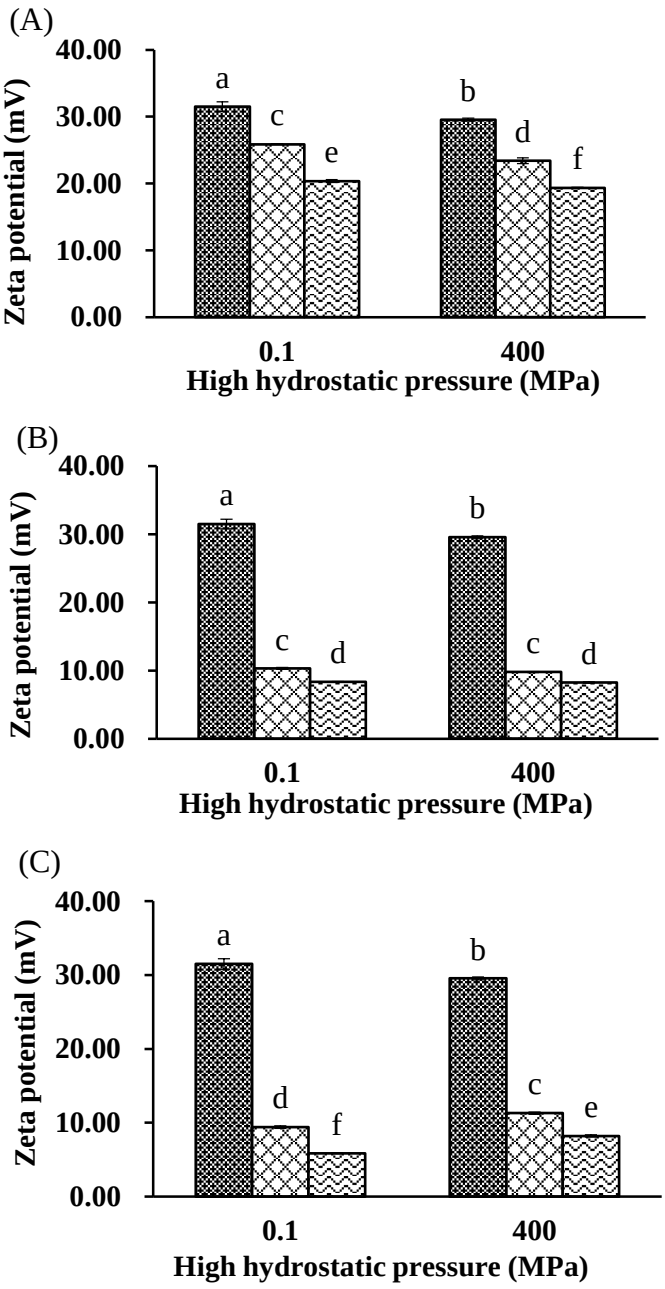

Fig. 4-2. Zeta potential of SPP treated by HHP with addition of NaCl (A): 0 mol/L (■), 0.2 mol/L (▩), 0.4 mol/L (▨); $CaCl_2$ (B) and $MgCl_2$ (C): 0 mol/L (■), 0.1 mol/L (▩), 0.2 mol/L (▨). Different lowercase letters over the bars indicate significant differences ($p < 0.05$).

Table 4-1 Sulfhydryl groups and disulfide bond content of SPP treated by HHP with different salt.

Salt	HHP (MPa)	Concentration (mol/L)	total -SH- (μmol/g protein)	free -SH- (μmol/g protein)	-S-S- (μmol/g protein)
No-salt	0.1	0	10.33±0.13^{a}	9.15±0.06^{a}	0.59±0.06^{ef}
	400	0	9.93±0.06^{c}	8.85±0.06^{d}	0.54±0.01^{f}
NaCl	0.1	0.2	10.12±0.11^{b}	8.80±0.04^{d}	0.66±0.07^{d}
		0.4	9.96±0.04^{c}	8.73±0.06^{e}	0.62±0.01^{de}
	400	0.2	9.94±0.02^{c}	9.04±0.07^{b}	0.45±0.03^{g}
		0.4	9.84±0.09^{c}	8.95±0.04^{c}	0.45±0.03^{g}
$CaCl_2$	0.1	0.1	8.24±0.06^{d}	6.20±0.02^{k}	1.02±0.04^{a}
		0.2	7.84±0.08^{fg}	6.16±0.02^{k}	0.84±0.05^{b}
	400	0.1	7.95±0.09^{ef}	6.35±0.02^{j}	0.80±0.06^{bc}
		0.2	7.71±0.11^{hi}	6.23±0.06^{k}	0.74±0.07^{c}
$MgCl_2$	0.1	0.1	8.03±0.02^{e}	6.99±0.00^{g}	0.52±0.01^{f}
		0.2	7.60±0.11^{ij}	6.54±0.04^{i}	0.53±0.06^{f}
	400	0.1	7.79±0.04^{gh}	7.13±0.04^{f}	0.33±0.02^{h}
		0.2	7.50±0.04^{j}	6.64±0.02^{h}	0.43±0.01^{g}

*Results are presented as mean ± standard deviation (n=3). Values followed by the different lowercase letters in the same column indicate significant differences ($p < 0.05$).

In addition, the content of -S-S- in SPP was increased upon the addition of NaCl and CaCl2, no significant difference was observed with MgCl2, while it was decreased by HHP treatment at the same ionic concentration (Table 4-1). The increase in -S-S- content was contributed to the salt bridging that might strengthen the molecular interactions (Mecit, et al., 2014), while its decrease might be due to the unfolding of SPP structure by HHP, which would expose key hydrophobic and charged amino acids and more internal functional areas, changing the surface of SPP molecules and eventually making disulfide bonds more vulnerable to attack during pressure treatment.

3.4. CD

Changes in secondary structure of SPP are shown in Fig. 4-3 and Table 4-2. As shown in Fig. 4-3, untreated (0.1 MPa) SPP exhibited a positive peak near 190 200 nm, and a negative peak near 210 nm. After the addition of salts, a "blue shift" (to lower wavelength) was clearly observed for SPP with NaCl, $CaCl_2$ and $MgCl_2$ (Fig. 3A, B and C). The ellipticity decreased with increasing of ions concentration, indicating an increase in α-helical content compared with the untreated protein (He et al., 2014). Moreover, a further reduction of ellipticity was promoted by higher ionic strength combined with HHP.

As shown in Table 4-2, the α-helical content of untreated SPP was increased, the β-sheet content was altered slightly, while the β-turn and random coil content were decreased after adding NaCl (0.2 mol/L), $CaCl_2$ (0.1 mol/L) and $MgCl_2$ (0.1 mol/L). According to Zhang et al. (2015), α-helices and β-sheets were respectively stabilized by intra- and inter-molecular hydrogen bonds, which were strongly affected by hydrophobicity and electrostatic interactions. Salt ions could weaken electrostatic repulsion, promoting hydrophobic aggregation and enhancing the protein–protein interactions through intra-molecular hydrogen binding, leading to an increase in α-helices. With ions concentration increasing, the α-helical content of SPP was significantly decreased ($p < 0.05$), while the β-sheet and β-turn content were both increased, due to weak hydrogen bonding between SPP and water molecules at high ionic strength, which might be contribute to the unfolding and stretching of SPP chains (De Maria, Ferrari & Maresca, 2016).

Furthermore, the α-helical content of SPP treated with HHP in the absence of salt ions was significantly increased, while the β-turn and random coil content were decreased ($p < 0.05$). This might be due to that HHP enhancing the stability of intra-molecular hydrogen bonds within protein chains (Grossi, 2016). However, a lower α-helical content and increased β-sheet and β-turn content were observed following HHP treatment at the same ion concentrations, which was attributed to the unfolding of SPP structure and conformational changes induced by HHP. In addition, the secondary structure modification by divalent salt ions (CaCl2 and MgCl2) at lower ion concentrations (0.1 mol/L) was tended to similar to that by monovalent ions (NaCl) at high concentrations (0.2 mol/L). This suggested that divalent salts acted as effective modifiers of protein secondary structure, and could be used to partially replace monovalent ions as salt additives in food systems to decrease the overall salt content (Kuhn, Cavallieri & Da Cunha, 2011).

3.5. Gelation properties

3.5.1. Dynamic shear rheology-temperature relationship

The storage modulus represents the elastic component and strength of the gel structure, both of which make an essential contribution to the three-dimensional gel network of proteins (Arogundade, Mu & Añón, 2012). As shown in Fig. 4-4, G′ values of SPP were significantly increased after adding NaCl, $CaCl_2$ and $MgCl_2$, while it decreased with increasing ionic strength for all three salts ($p < 0.05$, Fig. 4A-C). Similar result was also reported by Lakemond et al., (2003), who found that G′ values of soy glycinin significantly increased after adding salt from 0.03 to 0.2 mol/L but decreased with further increasing ionic strength (0.5 mol/L). Compared with monovalent ions (NaCl), SPP with divalent ions ($CaCl_2$ and $MgCl_2$) displayed much lower G′ values (Fig. 4A, B and C), which was possibly due to the larger atomic radius of Ca^{2+} and Mg^{2+} compared with Na^{+}, resulting in a stronger attraction of water molecules and further reduced the hydration of proteins (Bryant & McClements, 2000). These results were in agreement with those of Arakawa & Timasheff (1984), who suggested that divalent salt ions binding to proteins overcame salt exclusion effects and increased the surface tension, resulting in a decrease in preferential hydration. As expected, HHP treatment resulted in higher G′ value (Fig. 4A-C). The findings suggested that HHP could significantly improve the elastic properties of SPP by inducing unfolding and modifying the structure of protein molecules (Wang et al., 2016; Zhou et al., 2015).

3.5.2. Textural analysis

The textural properties of gels made by untreated and HHP treated SPP in presence of different salt ions are shown in Table 4-3. The hardness, springiness and chewiness of gels made from untreated SPP were decreased after adding NaCl, $CaCl_2$ and $MgCl_2$, and the reduction was larger with increasing ionic concentration. Notably, gels made from HHP-treated SPP at the same ionic strength displayed higher hardness, springiness and chewiness. This result confirmed the functional role of HHP treatment in improving the gelation properties of SPP, especially textural behavior. Liang et al. (2016) demonstrated that HHP treatment induced the electrostriction of charged amino acid groups, leading to water structuring around exposed nonpolar groups, and promoted the solvation of polar groups through hydrogen bonding, which enhanced protein gel behavior.

Fig. 4-3. Circular dichroism (CD) spectrum of SPP treated by HHP (HHP) with addition of NaCl (A): 0.1 MPa (—), 0.1 MPa-0.2 mol/L (—), 0.1 MPa-0.4 mol/L (—), 400 MPa (—), 400 MPa-0.2 mol/L (—), 400 MPa-0.4 mol/L (—); $CaCl_2$ (B) and $MgCl_2$ (C): 0.1 MPa (—), 0.1 MPa-0.1 mol/L (—), 0.1 MPa-0.2 mol/L (—), 400 MPa (—), 400 MPa-0.1 mol/L (—), 400 MPa-0.2 mol/L (—), respectively.

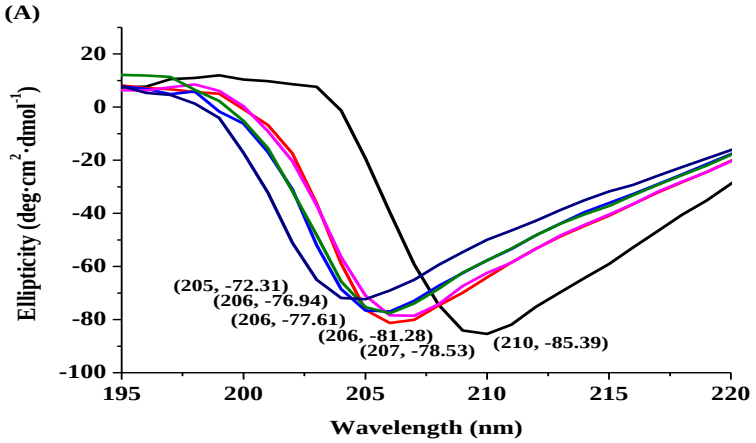
(A)
Ellipticity (deg·cm^2·dmol^{-1})
Wavelength (nm)
(205, -72.31)
(206, -76.94)
(206, -77.61)
(206, -81.28)
(207, -78.53)
(210, -85.39)

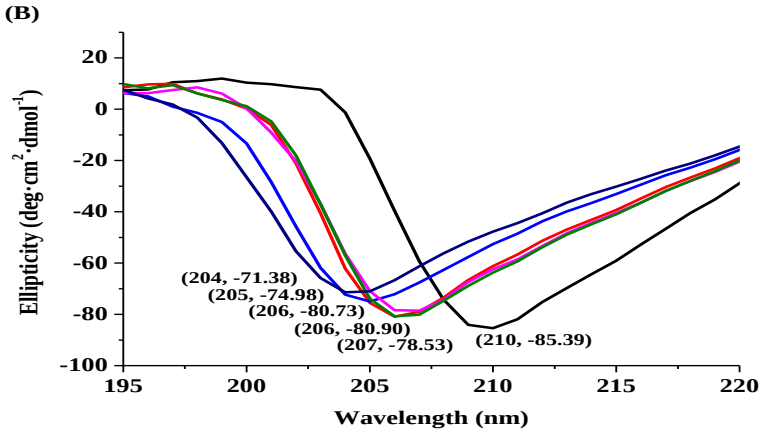
(B)
Ellipticity (deg·cm^2·dmol^{-1})
Wavelength (nm)
(204, -71.38)
(205, -74.98)
(206, -80.73)
(206, -80.90)
(207, -78.53)
(210, -85.39)

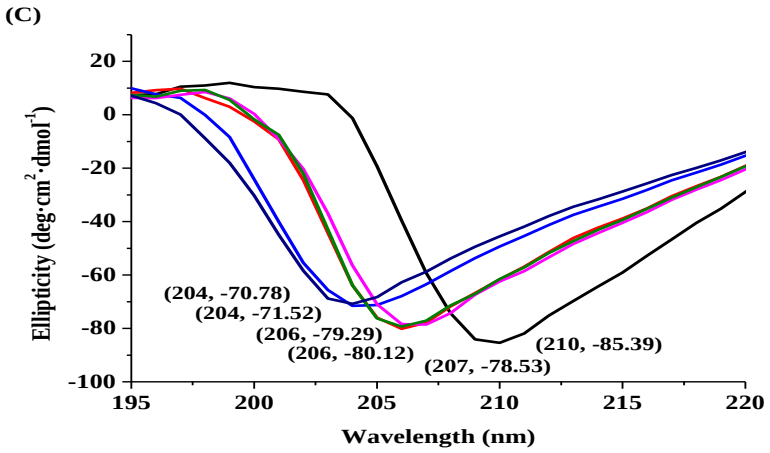
(C)
Ellipticity (deg·cm^2·dmol^{-1})
Wavelength (nm)
(204, -70.78)
(204, -71.52)
(206, -79.29)
(206, -80.12)
(207, -78.53)
(210, -85.39)

Table 4-2 Secondary structure composition (%) of SPP treated by HHP with different salt.

Salt	HHP (MPa)	Concentration (mol/L)	α-helix	β-sheet	β-turn	random coil
No-salt	0.1	0	11.15±0.64^{h}	30.40±0.42^{fg}	22.90±0.00^{ab}	35.55±0.21^{a}
	400	0	19.10±0.28^{ab}	30.90±0.14^{fg}	21.00±0.14^{d}	29.10±0.00^{de}
NaCl	0.1	0.2	19.55±0.21^{a}	30.25±0.21^{g}	20.85±0.07^{d}	29.35±0.07^{de}
		0.4	17.45±0.64^{c}	32.05±0.92^{cd}	21.30±0.71^{d}	29.20±0.42^{de}
	400	0.2	17.80±0.14^{c}	31.80±0.14^{de}	21.30±0.00^{d}	29.05±0.35^{de}
		0.4	14.90±0.28^{e}	33.30±0.14^{ab}	22.35±0.21^{c}	29.50±0.28^{d}
$CaCl_2$	0.1	0.1	19.15±0.21^{ab}	31.05±0.21^{ef}	20.95±0.07^{d}	28.85±0.07^{e}
		0.2	15.65±0.49^{d}	32.65±0.07^{cd}	22.45±0.21^{bc}	29.25±0.49^{de}
	400	0.1	19.30±0.00^{ab}	30.35±0.07^{fg}	21.00±0.28^{d}	29.35±0.07^{de}
		0.2	13.40±0.28^{f}	33.45±0.21^{a}	23.00±0.14^{ab}	30.10±0.28^{c}
$MgCl_2$	0.1	0.1	18.80±0.28^{b}	30.80±0.28^{fg}	21.15±0.35^{d}	29.15±0.35^{de}
		0.2	13.75±0.07^{f}	33.30±0.28^{ab}	22.80±0.14^{bc}	30.20±0.14^{c}
	400	0.1	18.80±0.28^{b}	31.10±0.57^{ef}	21.00±0.28^{d}	29.15±0.07^{de}
		0.2	12.05±0.21^{g}	33.55±0.07^{a}	23.40±0.00^{a}	31.10±0.14^{b}

*Results are presented as mean ± standard deviation (n=3). Values followed by the different lowercase letters in the same column indicate significant differences ($p < 0.05$).

Compared to the addition of monovalent (NaCl) salt ions, SPP gels with the addition of divalent salt ions ($CaCl_2$ and $MgCl_2$) showed lower hardness, springiness and chewiness (Table 4-3). It might attribute to weak inter-molecular interactions (e.g. electrostatic interaction (Fig. 4-2), and also indicate a stronger ability of divalent salt ions to induce salting out effects at relatively low ionic concentrations (Table 4-3). Moreover, excessive ions might result in much net positive charges in SPP dispersion system, leading to an increase in repulsion or dissociation between protein molecules (Ganasen & Benjakul, 2011), thereby weakening cross-links between protein chains, and resulting in a softening of gel structure and a decrease in compactness.

3.5.3. Low field NMR

Water in food system exists as bound, immobilized and even free water components (Han et al., 2014). The mobility, distribution and binding state of water molecules with proteins in gel system were essential to evaluating the quality of gel products, since it could be monitored by non-destruction testing (NDT) of low-field NMR without destroying gel structures (Zhang et al., 2015).

The distribution and proportion of T2 relaxation times of SPP treated by HHP combined with different salt are shown in Fig. 4-5 and Table 4-4. There are two distinct water populations be located at approximately 0.1-1 ms (T_{2b}) and 100-1000 ms (T_{21}), which was corresponded to bound and immobilized water fractions (Fig. 4-5A-C). The relaxation time of T_{2b} and T_{21} increased after adding NaCl, $CaCl_2$ and $MgCl_2$, while they were decreased by HHP treatment (Table 4). It is believed that T_{2b} reflects water closely associated with proteins, T_{21} indicates the part of water fractions trapped within the gel three dimensional (3D) networks (Zhang et al., 2015), respectively. Moreover, a shorter relaxation time (T2) indicated water bound more closely to proteins than that with longer relaxation time. This suggested that HHP induced the hydration of SPP and reduced the mobility of water, which might be due to the increase in unfolding of SPP protein structure. However, the broader distribution of T2 upon adding different salt was probably due to the more inhomogeneous and soft gel structures, resulting in a greater variation within the gel network of the water proton population.

The proportion of T_{2b} distribution (A_{2b}) of SPP was increased from 1.15 % (untreated) to 1.62 % after HHP treatment, indicating that more bound water molecules were closely associated with SPP molecules. In addition, in the case of untreated SPP, A_{2b} was decreased by monovalent salt (NaCl) but increased upon addition with divalent salts ($CaCl_2$ and $MgCl_2$), while the proportion of T_{21} distributions (A_{21}) was inversely decreased by divalent salts ($CaCl_2$ and $MgCl_2$), which indicated the loss of immobilized water trapped in the gel structure. The findings were in accord with the strong surface hydrophobicity (Fig. 4-1) and weak electrostatic interactions (Fig. 4-2) after adding salts, which might led to loss of homogeneous structure and loose gel networks compare to HHP-treated SPP, and even untreated SPP without salt ions.

3.5.4. WHC

As shown in Table 4-3, WHC of SPP gels varied with the types and concentrations of added salt ions. Compared with untreated SPP without salt ions, WHC of SPP gels initially decreased (78.16 %) at 0.2 mol/L salt, then increased (80.34 %) at higher ionic strength (0.4 mol/L). Upon addition of $CaCl_2$, WHC of SPP gels decreased with increasing ionic strength, which was lower than those with NaCl. No significant changes were observed in SPP gels with addition of $MgCl_2$. The lowering of WHC values indicated the loss of hydrogen bonding in the gel networks (Arakawa & Timasheff, 1984; Cando et al., 2015). This could be due to that salt ions promoted the random accumulation and arrangement of gel structure, and as a consequence, SPP gels might release a greater number of free water molecules, which would decrease the stiffness of networks. The same reductions in WHC and gel coarseness with increasing ionic concentration were also reported by Lakemond et al., (2003). In addition, WHC of gels made from HHP-treated SPP (87.38 %) were slightly higher than those of untreated SPP gels (85.72 %). Interestingly, WHC of gels from SPP with monovalent ions (NaCl) was significantly promoted by HHP treatment at both low (0.2 mol/L) and high (0.4 mol/L) salt concentrations, whereas no significant difference was observed with gels from SPP with $CaCl_2$ and $MgCl_2$ under HHP treatment. These findings suggested that HHP was more effective at promoting the formation of hydrogen bonding between SPP and water molecules in the presence of monovalent ions (NaCl) than divalent ions ($CaCl_2$, $MgCl_2$), even at relatively high ionic strength.

4. Conclusion

Both of monovalent (NaCl) and divalent ($CaCl_2$ and $MgCl_2$) salts modified structure and altered chemical forces of SPP (e.g. Ho, electrostatic interaction, -SH-groups), which could be enhanced by HHP (400 MPa) for strengthening the gel formation. Interestingly, G′ of SPP was significantly dependent on ionic strength and partially improved by HHP. Low field NMR measurement indicated the loss of immobilized water trapped in gel structure with divalent salt, but the increase of bound water was induced by HHP. Moreover, weak WHC and diminished textural properties of SPP gels in the presence of all three types of salts were also strengthened by HHP treatment. These findings would be of great help for understanding the gelling behavior of SPP with different type of salts, and the development of HHP technique in improving gelation properties of SPP might be useful in the handling of this new protein resource as functional ingredients in gel-like foods (such as sausage, yogurt, beverages and ice cream, etc.) or in the formulating of novel foods.

Fig. 4-4. Thermomechanical spectrum of SPP treated by HHP with addition of NaCl (A): 0.1 MPa (), 0.1 MPa-0.2 mol/L (), 0.1 MPa-0.4 mol/L (), 400 MPa (), 400 MPa-0.2 mol/L (), 400 MPa-0.4 mol/L (); CaCl2 (B) and MgCl2 (C): 0.1 MPa (), 0.1 MPa-0.1 mol/L (), 0.1 MPa-0.2 mol/L (), 400 MPa (), 400 MPa-0.1 mol/L (), 400 MPa-0.2 mol/L (), respectively.

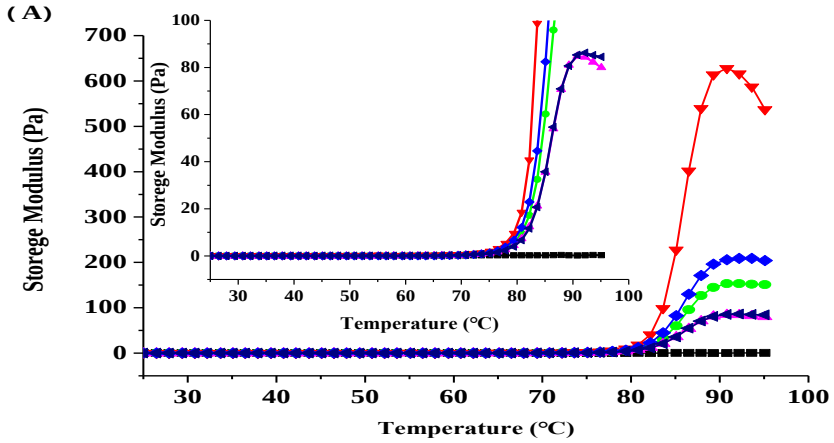
(A)
Storege Modulus (Pa)
Temperature (°C)
Storege Modulus (Pa)
Temperature (°C)

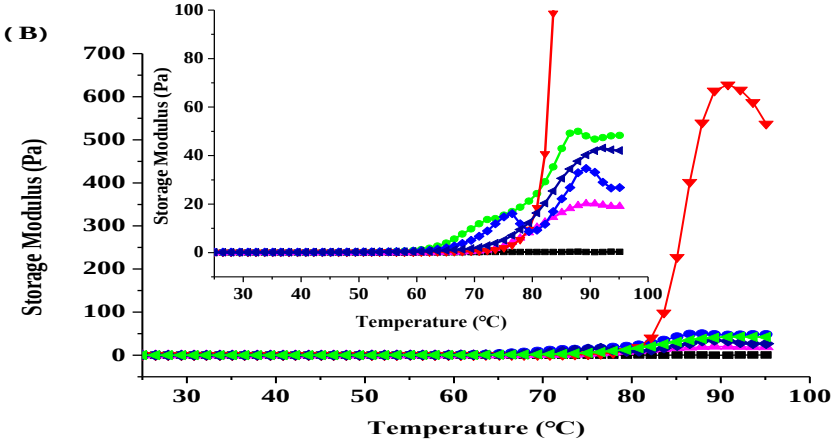
(B)
Storage Modulus (Pa)
Temperature (°C)
Storage Modulus (Pa)
Temperature (°C)

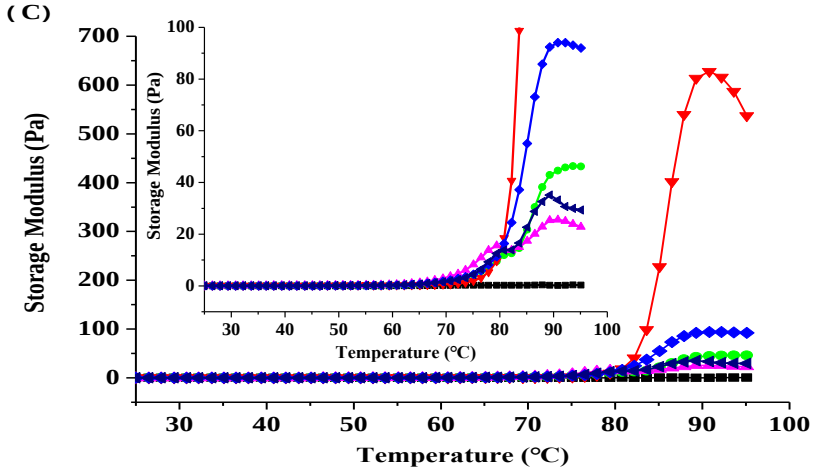
(C)
Storage Modulus (Pa)
Temperature (°C)
Storage Modulus (Pa)
Temperature (°C)

Table 4-3 Textural properties and water holding capacity of gels from SPP treated by HHP with different salt.

Salt	HHP (MPa)	Concentration (mol/L)	Hardness (N)	Springness	Chewiness	WHC (%)
No-salt	0.1	0	163.62±1.78^{a}	0.89±0.00^{b}	61.41±1.69^{a}	85.72±1.81^{b}
	400	0	116.43±1.03^{b}	0.95±0.01^{a}	49.74±0.00^{b}	87.38±1.01^{b}
NaCl	0.1	0.2	85.73±1.59^{d}	0.84±0.05^{cd}	33.16±2.63^{d}	78.16±6.25^{de}
		0.4	45.28±3.07^{i}	0.80±0.03^{d}	17.21±2.32^{gh}	80.34±3.63^{cd}
	400	0.2	90.05±3.08^{c}	0.88±0.03^{bc}	36.52±0.95^{c}	94.43±2.51^{a}
		0.4	51.23±2.46^{h}	0.82±0.04^{d}	19.05±2.21^{fg}	84.69±1.84^{bc}
$CaCl_2$	0.1	0.1	59.99±1.44^{g}	0.51±0.02^{g}	12.22±1.10^{ij}	73.03±3.64^{ef}
		0.2	26.42±1.44^{l}	0.51±0.03^{g}	5.05±0.13^{l}	61.89±1.46^{g}
	400	0.1	65.78±1.94^{f}	0.58±0.01^{f}	14.98±0.96^{hi}	71.10±4.62^{f}
		0.2	28.60±0.04^{kl}	0.48±0.02^{g}	4.94±0.49^{l}	64.63±2.85^{g}
$MgCl_2$	0.1	0.1	65.93±2.01^{f}	0.65±0.02^{e}	21.74±1.40^{ef}	77.39±3.01^{de}
		0.2	31.11±0.83^{k}	0.59±0.01^{g}	8.76±0.57^{k}	76.44±1.39^{de}
	400	0.1	73.65±1.50^{e}	0.67±0.00^{e}	23.83±0.54^{e}	76.09±0.13^{def}
		0.2	38.49±2.50^{j}	0.65±0.01^{e}	11.77±0.82^{j}	79.13±1.38^{d}

*Results are presented as mean ± standard deviation (n=3). Values followed by the different lowercase letters in the same column indicate significant differences ($p < 0.05$). WHC: water holding capacity.

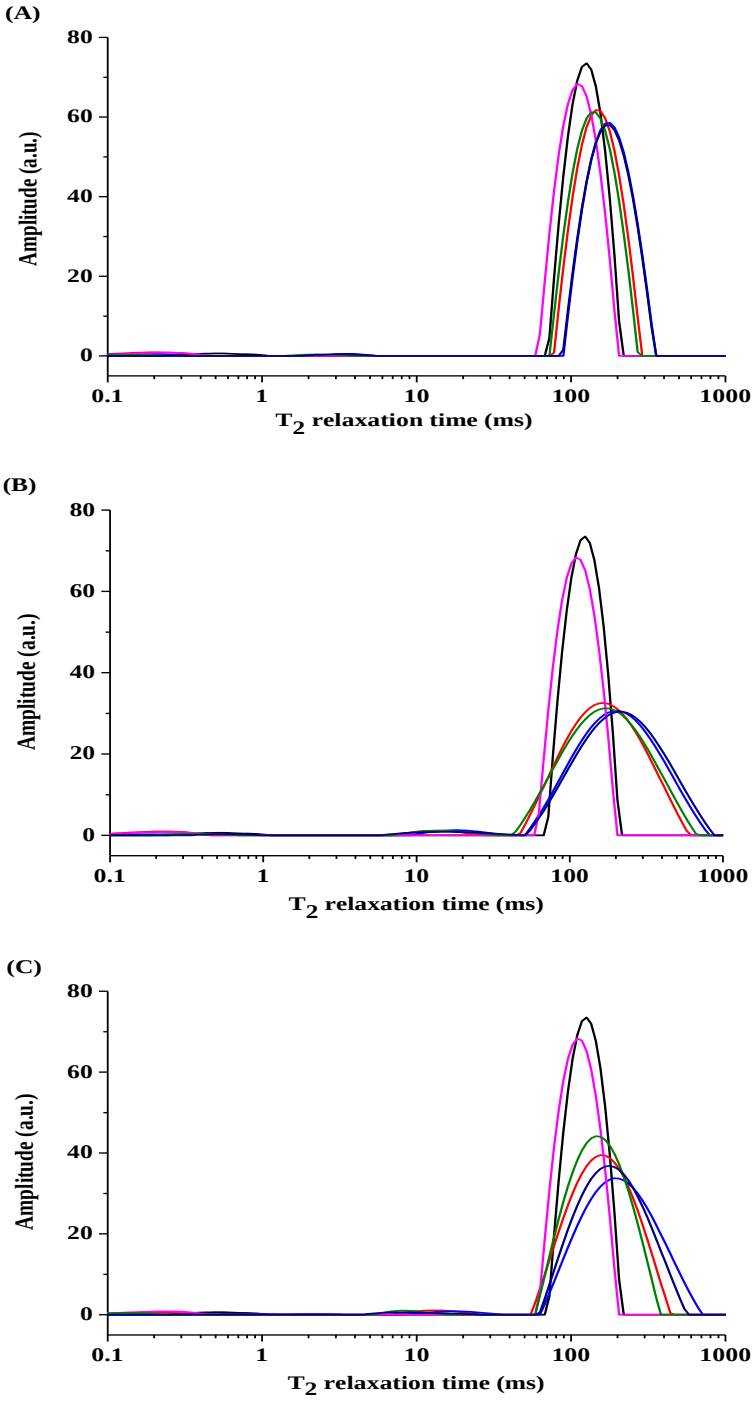
(A)
Amplitude (a.u.)
80
60
40
20
0
0.1
1
10
100
1000
T2 relaxation time (ms)
(B)
Amplitude (a.u.)
80
60
40
20
0
0.1
1
10
100
1000
T2 relaxation time (ms)
(C)
Amplitude (a.u.)
80
60
40
20
0
0.1
1
10
100
1000
T2 relaxation time (ms)

Fig. 4-5. Distributions of T2 relaxation times of gels from SPP treated by HHP with addition of NaCl (A): 0.1 MPa (—), 0.1 MPa-0.2 mol/L (—), 0.1 MPa-0.4 mol/L (—), 400 MPa (—), 400 MPa-0.2 mol/L (—), 400 MPa-0.4 mol/L (—); $CaCl_2$ (B) and $MgCl_2$ (C): 0.1 MPa (—), 0.1 MPa-0.1 mol/L (—), 0.1 MPa-0.2 mol/L (—), 400 MPa (—), 400 MPa-0.1 mol/L (—), 400 MPa-0.2 mol/L (—), respectively.

Table 4-4 Distributions of T2 relaxation times (T_{2b}, T_{21}), and proportion of peak area (A_{2b}, A_{21}) of gels from SPP treated by HHP with different salt.

Salt	HHP (MPa)	Concentration (mol/L)	T_{2b} (ms)	T_{21} (ms)	A_{2b} (g/100g)	A_{21} (g/100g)
No-salt	0.1	0	0.72 ± 0.27^{e}	126.04 ± 0.00^{h}	1.15 ± 0.03^{d}	98.71 ± 0.17^{ab}
	400	0	0.23 ± 0.02^{e}	109.70 ± 0.00^{i}	1.62 ± 0.34^{c}	98.38 ± 0.34^{ab}
NaCl	0.1	0.2	2.06 ± 0.50^{e}	144.81 ± 0.00^{fg}	0.38 ± 0.10^{e}	98.56 ± 1.41^{ab}
		0.4	3.09 ± 0.45^{e}	178.34 ± 0.00^{c}	0.61 ± 0.05^{e}	98.71 ± 0.63^{ab}
	400	0.2	$2.42\pm0.24_{e}$	139.96 ± 6.87^{g}	0.39 ± 0.13^{e}	98.46 ± 0.75^{ab}
		0.4	$2.97\pm0.29_{e}$	178.34 ± 0.00^{c}	0.62 ± 0.02^{e}	99.38 ± 0.02^{a}
$CaCl_2$	0.1	0.1	13.21 ± 0.65^{bcd}	166.38 ± 0.00^{d}	1.87 ± 0.02^{bc}	95.05 ± 1.31^{def}
		0.2	16.35 ± 2.40^{ab}	204.91 ± 0.00^{ab}	2.26 ± 0.02^{a}	94.62 ± 0.76^{f}
	400	0.1	14.16 ± 0.69^{abc}	178.34 ± 0.00^{c}	2.14 ± 0.03^{ab}	95.14 ± 0.13^{def}
		0.2	17.52 ± 2.57^{a}	212.27 ± 10.42^{a}	2.22 ± 0.10^{a}	94.88 ± 0.46^{ef}
$MgCl_2$	0.1	0.1	12.75 ± 0.00^{bcd}	155.22 ± 0.00^{e}	1.69 ± 0.12^{c}	96.38 ± 0.37^{cd}
		0.2	16.27 ± 0.80^{ab}	198.04 ± 9.72^{b}	1.63 ± 0.12^{c}	94.88 ± 0.51^{ef}
	400	0.1	11.04 ± 3.72^{cd}	150.02 ± 7.36^{ef}	1.11 ± 0.24^{d}	97.68 ± 0.61^{bc}
		0.2	10.30 ± 3.47^{d}	178.34 ± 0.00^{c}	1.33 ± 0.01^{d}	96.17 ± 0.43^{de}

*Results are presented as mean ± standard deviation (n=3). Values followed by the different lowercase letters in the same column indicate significant differences ($p < 0.05$).

Acknowledgments

The authors gratefully acknowledge the earmarked fund for China Agriculture Research System (CARS-10-B21) and National Key R & D Program of China (2016YFE0133600).

References

Albarracín, W, Sánchez, I. C., Grau, R., et al. (2011). Salt in food processing; usage and reduction: a review. *International Journal of Food Science & Technology*, 46 (7), 1329-1336.

Añón, M. C., De Lamballerie, M., & Speroni, F. (2011). Influence of NaCl concentration and high pressure treatment on thermal denaturation of soybean proteins. *Innovative Food Science & Emerging Technologies*, 12 (4), 443–450.

Arakawa, T., Timasheff, S. N. (1984). Mechanism of protein salting in and salting out by divalent cation salts: balance between hydration and salt binding. *Biochemistry*, 23 (25), 5912–5923.

Arogundade, L. A., Mu, T. H., & Añón, M. C. (2012). Heat-induced gelation properties of isoelectric and ultrafiltered sweet potato protein isolate and their gel microstructure. *Food Research International*, 49 (1), 216–225.

Barat, J. M., Pérez-Esteve, E., Aristoy, M. C., et al. (2013). Partial replacement of sodium in meat and fish products by using magnesium salts. A review. *Plant and Soil*, 368 (1-2), 179-188.

Bryant, C. M., & McClements, D. J. (2000). Influence of NaCl and CaCl2 on cold-set gelation of heat-denatured whey protein. *Journal of Food Science*, 65 (5), 801–804.

Buell, A. K., Hung, P., Salvatella, X., Welland, M. E., Dobson, C. M., & Knowles, T. P. (2013). Electrostatic effects in filamentous protein aggregation. *Biophysical Journal*, 104 (5), 1116–1126.

Cando, D., Herranz, B., Borderías, A. J., & Moreno, H. M. (2015). Effect of high pressure on reduced sodium chloride surimi gels. *Food Hydrocolloids*, 51, 176–187.

Cao, L., Su, S., Regenstein, J. M., et al. (2015). Ca^{2+}-induced conformational changes of myosin from silver carp (Hypophthalmichthys molitrix) in gelation. *Food Biophysics*, 10 (4), 447–455.

Chen, N., Zhao, M., Chassenieux, C., & Nicolai, T. (2017). The effect of adding NaCl on thermal aggregation and gelation of soy protein isolate. *Food Hydrocolloids*, 70, 88–95.

De Maria, S., Ferrari, G., & Maresca, P. (2016). Effects of high hydrostatic pressure on the conformational structure and the functional properties of bovine serum albumin. *Innovative Food Science & Emerging Technologies*, 33, 67–75.

Ercili-Cura, D., Lille, M., Legland, D., Gaucel, S., Poutanen, K., Partanen, R., & Lantto, R. (2013). Structural mechanisms leading to improved water retention in

acid milk gels by use of transglutaminase. *Food Hydrocolloids*, 30 (1), 419-427.

Ganasen, P., & Benjakul, S. (2011). Chemical composition, physical properties and microstructure of pidan white as affected by different divalent and monovalent cations. *Journal of Food Biochemistry*, 35 (5), 1528–1537.

Grossi, A., Olsen, K., Bolumar, T., et al. (2016). The effect of high pressure on the functional properties of pork myofibrillar proteins. *Food Chemistry*, 196, 1005–1015.

Gupta, U. C., & Gupta, S. C. (2014). Sources and deficiency diseases of mineral nutrients in human health and nutrition: a review. *Pedosphere*, 24 (1), 13–38.

Hamada, M., Ishizaki, S., & Nagai, T. (1994). Variation of SH content and kamaboko-gel forming ability of shark muscle protein by electrolysis. J. *Shimonoseki University of Fisheries*, 42, 131–135.

Han, M., Wang, P., Xu, X., et al. (2014). Low-field NMR study of heat-induced gelation of pork myofibrillar proteins and its relationship with microstructural characteristics. *Food Research International*, 62, 1175-1182.

He, R., He, H. Y., Chao, D., Ju, X., & Aluko, R. (2014). Effects of high pressure and heat treatments on physicochemical and gelation properties of rapeseed protein isolate. *Food and Bioprocess Technology*, 7 (5), 1344–1353.

Jiang, L., Wang, Z., Li, Y., Meng, X., Sui, X., Qi, B., & Zhou, L. (2015). Relationship between surface hydrophobicity and structure of soy protein isolate subjected to different ionic strength. *International Journal of Food Properties*, 18 (5), 1059–1074.

Khan N. M., Mu, T. H., Sun, H. N., et al. (2015). Effects of high hydrostatic pressure on secondary structure and emulsifying behavior of sweet potato protein. *High Pressure Research*, 35 (2), 189-202.

Kuhn, K. R., Cavallieri, Â. L. F., & Da Cunha, R. L. (2011). Cold-set whey protein-flaxseed gum gels induced by mono or divalent salt addition. *Food Hydrocolloids*, 25 (5), 1302–1310.

Lakemond, C. M., de Jongh, H. H., Paques, M., van Vliet, T., Gruppen, H., & Voragen, A. G. (2003). Gelation of soy glycinin; influence of pH and ionic strength on network structure in relation to protein conformation. *Food Hydrocolloids*, 17 (3), 365–377.

Liang, Y., Guo, B., Zhou, A., et al. (2016). Effect of high pressure treatment on gel characteristics and gel formation mechanism of bighead carp (Aristichthys nobilis) surimi gels. *Journal of Food Processing and Preservation*, 40, 1–8.

Mecit, H. O., Kathryn, L. M., Michael, J. M., Moshe R. (2014). Monitoring the effects of divalent ions (Mn^{+2} and Ca^{+2}) in heat-set whey protein gels. *LWT-Food Science and Technology*, 56, 93–100.

Mu, T. H., Tan, S. S., Xue, Y. L., (2009). The amino acid composition, solubility and emulsifying properties of sweet potato protein. *Food Chemistry*, 112 (4), 1002–1005.

Qin, Z., Guo, X., Lin, Y., Chen, J., Liao, X., Hu, X., & Wu, J. (2013). Effects of

high hydrostatic pressure on physicochemical and functional properties of walnut (Juglans regia L.) protein isolate. *Journal of the Science of Food and Agriculture*, 93 (5), 1105–1111.

Sun, M. J., Mu, T. H., Zhang, M., et al. (2012). Nutritional assessment and effects of heat processing on digestibility of Chinese sweet potato protein. *Journal of Food Composition and Analysis*, 26 (1), 104-110.

Tabilo-Munizaga, G., Gordon, T. A., Villalobos-Carvajal, R., Moreno-Osorio, L., Salazar, F. N., Pérez-Won, M., & Acuña, S. (2014). Effects of high hydrostatic pressure (HHP) on the protein structure and thermal stability of Sauvignon blanc wine. *Food Chemistry*, 155, 214–220.

Tobin, B. D., O'Sullivan, M. G., Hamill, R. M., & Kerry, J. P. (2013). The impact of salt and fat level variation on the physiochemical properties and sensory quality of pork breakfast sausages. *Meat Science*, 93 (2), 145–152.

Wang, M., Chen, X., Zou, Y., Chen, H., Xue, S., Qian, C., & Zhou, G. (2016). High‐pressure processing‐induced conformational changes during heating affect water holding capacity of myosin gel. *International Journal of Food Science & Technology*, 52, 724‐732.

Whitmore, L., & Wallace, B. A. (2004). DICHROWEB, an online server for protein secondary structure analyses from circular dichroism spectroscopic data. *Nucleic Acids Research*, 32 (suppl 2), W668–W673.

Wu, L., Wu, T., Wu, J., Chang, R., Lan, X., Wei, K., & Jia, X. (2016). Effects of cations on the “salt in” of myofibrillar proteins. *Food Hydrocolloids*, 58, 179–183.

Xue, S. W., Yang, H. J., Wang, H. H., et al. (2017). High-pressure effects on the molecular aggregation and physicochemical properties of myosin in relation to heat gelation. *Food Research International*, 99, 413-418.

Zhang, Y. H., Huang, L. H., Tang, S. X., et al. (2014), Effect of ionic strength on formation and microstructure of self-assembly globulin nanofibrils and gels. *Digest Journal of Nanomaterials and Biostructures*, 9 (3), 951–957.

Zhang, Z., Yang, Y., Tang, X., Chen, Y., & You, Y. (2015). Chemical forces and water holding capacity study of heat-induced myofibrillar protein gel as affected by high pressure. *Food Chemistry*, 188, 111–118.

Zhang, Z., Yang, Y., Tang, X., Chen, Y., & You, Y. (2016). Chemical forces study of heat-induced myofibrillar protein gel as affected by partial substitution of NaCl with KCl, $MgCl_2$ and $CaCl_2$. *CyTA-Journal of Food*, 14 (2), 239–247.

Zhou, J. Z., Zhang, H., Gao, L., Wang, L., & Qian, H. F. (2015). Influence of pH and ionic strength on heat-induced formation and rheological properties of cottonseed protein gels. *Food and Bioproducts Processing*, 96, 27–34.

Chapter V

Effects of microbial transglutaminase and high hydrostatic pressure on structure and gelation properties of sweet potato protein

Chapter V Effects of microbial transglutaminase and high hydrostatic pressure on structure and gelation properties of sweet potato protein

This chapter is adapted from the article (under review):

Effects of high hydrostatic pressure and microbial transglutaminase treatment on structure and gelation properties of sweet potato protein

*Zhong-Kai Zhao[1,2], Tai-Hua Mu[*1], Miao Zhang[1], Aurore Richel[2]*

1 Laboratory of Food Chemistry and Nutrition Science, Institute of Food Science and Technology, Chinese Academy of Agricultural Sciences; Key Laboratory of Agro-Products Processing, Ministry of Agriculture and Rural Affairs, No. 2 Yuan Ming Yuan West Road, Haidian District, P.O. Box 5109, Beijing 100193, P. R. China.

2 University of Liège, Gembloux Agro-Bio Tech, Laboratory of Biomass and Green Technologies, Passage des Déportés, 2, 5030 Gembloux, Belgium

Abstract

The effects of HHP combined with MTGase on structure and gelation properties of SPP were investigated. MTGase induced the formation of high molecular mass aggregates of SPP by the inter-molecular cross-linking. The average particle size of SPP increased by HHP at 250-550 MPa, being increased from 249.5 nm (0.1 MPa) to 270.2 nm (550 MPa). While it was decreased by the subsequent MTGase catalysis that showed the lowest value of 200.3 nm at 550 MPa, indicating the formation of intra-molecular linkages. The amount of sulfhydryl groups and thermal denaturation temperature were increased by HHP and MTGase, with the highest value of 3.5 μmol/g protein and 80.4 °C in MTGase catalyzed SPP with 400 MPa pretreatment. Textural properties of the gels made from HHP treated SPP or those with further MTGase catalysis were both enhanced due to the covalent linkage of disulfide bonds (-S-S-) and ε-(γ-glutaminyl) lysine isopeptide bonds. In addition, low-field NMR results showed an increase in corresponding area fractions of A2b and A_{21}, being attributed to more bound or immobilized water fractions were trapped in the SPP gel matrix.

Keywords

Sweet potato protein; High hydrostatic pressure; Enzymatic catalysis; Texture; Low field NMR

1. Introduction

Proteins are one of the main classes of structural components, which are generally modified via chemical, physical or enzymatic methods for the development of new functional properties (Lam & Nickerson, 2014; Hwang, Lai & Hsu, 2007; Jia, Huang & Xiong, 2016). Among them, HHP and enzymatic treatment have gradually attracted the attention of researchers, due to the fact that they are performed by mild conditions, and can generate profound changes in structural and techno-functional properties of food proteins, leading to the improvement in gelation, emulsifying and/or textural or qualities of products (Ardelean, Otto, Jaros, & Rohm, 2012; Qin, et al., 2016; Liu, Damodaran & Heinonen, 2018).

As a non-thermal processing technique, HHP treatment has been widely used to modify protein secondary structure, induce the exchange of chemical forces and interaction between protein molecules, including surface hydrophobicity, electrostatic interaction and hydrogen bonding (He, He, Chao, Ju & Aluko, et al., 2014). Notably, the functionality of HHP in promoting the protein molecule aggregation provides a new sight to carry out the novelty approach of HHP in improving the gelation properties of protein resources, being attributed to the formation of disulfide linkages (Angioloni & Collar, 2013; Zhao, Mu, Zhang & Richel, 2018a).

MTGase is an extracellular enzyme of the transferases class with a molecular weight of 38 kDa, commercially produced through traditional fermentation by the microorganism Streptoverticillium moboarense (Kieliszek & Misiewicz, 2014; Gaspar & De Góes-Favoni, 2015). It has been used to promote covalent cross-linking by catalyzing acyl-transfer reactions between γ-carboxamide groups of glutamine residues and ε-amino groups of lysine residues, resulting in the formation of ε-(γ-glutaminyl) lysine isopeptide bonds (Heck, Faccio, Richter & Thöny-Meyer, 2013; Zeeb, Fischer & Weiss, 2014). MTGase catalysis affected the structural unfolding and chemical forces between peanut protein molecules, corresponding to the exposure of sulfhydryl groups and the increase in surface hydrophobicity (Qiu, et al., 2017). MTGase also efficiently enhanced the stability of soy protein emulsion gels (Tang, Yang, Liu & Chen, 2013).

China accounts for 63.8 % of sweet potato (*Ipomoea batatas* [L.] Lam) total output in the world (FAOSTAT, 2017), which could not only be utilized for starch processing, but also being a new protein source that can be recycled from the effluent after extraction (Arogundade & Mu, 2012a). Compared to other plant proteins, the major storage protein in sweet potato root, which accounts for about 60-80 % of the total root protein called “Sporamin”, has a molecular mass of approximately 25 kDa under reducing SDS–PAGE conditions, while it shows molecular masses of 31 kDa (sporamin A) and 22 kDa (sporamin B) under non-reducing SDS–PAGE conditions respectively (Sun, Mu, Zhang & Arogundade, 2012; Zhao, Mu, Zhang & Richel, 2018a). This specific structural character may lead to the differences in physicochemical and functional properties of SPP correlated with other plant proteins. SPP presented certain antioxidant capacity (*in vitro*), anticancer activity (*in vivo and vitro*) and emulsifying properties (Zhang, Mu

& Sun, 2014; Li, Mu & Deng, 2013; Khan, Mu, Zhang & Arogundade, 2014). Moreover, the gelation behavior of SPP under HHP treatment combined with different pH conditions or different salt ion additives has also been detected in our previous studies (Zhao, Mu, Zhang & Richel, 2018a; Zhao, Mu, Zhang & Richel, 2018b). According to Sun, Mu, Zhang & Arogundade (2012), SPP is rich in glutamic and lysine acid residues. Thus, SPP might be an interesting substrate for MTGase catalysis in handling the novelty food processing. However, limited information about structural changes and gelation behaviors of SPP affected by enzyme of MTGase is currently available, as well as the simultaneous treatment of HHP and MTGase.

The present research is designed to investigate the effects of HHP and MTGase treatment on secondary structure, molecular weight characteristics, particle size distribution and thermal properties of SPP, as well as the textural properties, water mobility and distribution of SPP gels for a better understanding of the development of HHP in improving the gelation of SPP, and enrich the invaluable information of MTGase as functional additive to adjust SPP matrix quality.

2. Materials and methods

2.1. Materials

Sweet potato cultivar Shang Shu No.19 was supplied by Shangqiu Academy of Agriculture and Forestry Sciences (Henan province, China). Microbial transglutaminase (MTGase, 1000 U/g) was purchased from Solarbio Co. Ltd. (Beijing, China). Tris base, β-mercaptoethanol, glycine and 5,5′-dinitrobis-[2-nitrobenzoic acid] (DTNB) were purchased from Sigma-Aldrich, Inc. (St. Louis, Mo, USA). Other chemicals and reagent were of analytical grade.

2.2. SPP preparation

SPP was prepared according to our previous method by Arogundade, Mu, & Añón, (2012b). Briefly, fresh peeled tubers were grounded with sodium bisulfite buffer solution (0.1 %) at a solid-to-solvent ratio of 1:2 for color protection, sieved with 0.15 mm pore diameter mesh and centrifuged at 10,000 g for 45 min to collect the supernatant. The pH of the supernatant was subsequently adjusted to 4.0 (isoelectric point of SPP) to collect the protein precipitate, then re-solubilized with distilled water at pH 7.0 by using 2 mol/L NaOH. After the same centrifugation, the supernatant was concentrated and purified by using an ultrafiltration device (model Ro-NF-UF-4010, Diqing filtration technology Co., Ltd., Shanghai, China) with a 10 kDa molecular weight cut-off membrane, then lyophilized to get SPP powder with 92.95 % purity as measured by the Kjeldahl method (N % × 6.25).

2.3. SDS–PAGE

MTGase catalyzed SPP was prepared by adding enzyme of MTGase at the concentrations of 0, 15, 25, 50 and 100 U/g protein, respectively. Simply, MTGase in different concentrations were mixed with protein dispersion (10 %) and incubated

in water bath (Peiying Electric Appliance Co., Ltd., Suzhou, Jiangsu, China) at 40 °C for 1 h by a constant shaking, then immediately inactivated at 75 °C for 10 min (Gaspar & De Góes-Favoni, 2015) and diluted to the final concentration of 5 mg/mL.

Next, molecular weight distribution of MTGase catalyzed SPP samples were investigated using SDS-PAGE electrophoresis system (model AE-6450, ATTO Co., Japan) both under reducing and non-reducing conditions (with or without 1 % β-mercaptoethanol), in order to select the suitable amount of enzyme addition for present studies. An aliquot 40 μL of above SPP sample solution and 10 μL of sample solubilizing buffer solution (containing SDS [1 %], Tris–HCl buffer [50 mmol/L, pH 6.8], EDTA–2Na [60 mmol/L], and sucrose [12 %]) with or without addition of β-mercaptoethanol were mixed well. After that, a 10-μL aliquot of the mixture was loaded on each gel lane. For gel preparation, acrylamide separating gel (12.5 %) and acrylamide stacking gel (5 %) were freshly prepared, and the mixture prepared for reducing SDS-PAGE condition should be boiling for 5 min before loading. Gel electrophoresis was then conducted at 30 mA for 1.5 h. The molecular weight of the protein bands was compared with a color-mixed protein marker within a broad range of 11-245 kDa (pre-stained marker, Solarbio Science & technology Co., Ltd. Beijing, China).

2.4. HHP treatment and MTGase catalyzed cross-linking

HHP was performed by a laboratory-scale HHP unit (model HHP-L3; HuaTaiSenMiao Engineering & Technique Ltd. Co., Tianjin, China) with a 0.6-L cylindrical pressure vessel (60 × 210 mm) and an operational pressure range of 0.1-600 MPa. The target pressure condition was reached at a rate of about 250 MPa/min, and released at about 300 MPa/min, respectively. Distilled water was regarded as pressure transfer medium. SPP dispersion (10 %, w/v) in 10 mmol/L phosphate buffer (pH 7.0) was vacuum-packed in food-grade polyethylene bags, then subjected severally at 250, 400 and 550 MPa for 30 min before release the pressure within 5 s. The pressurization was maintained at 25 °C with a circulating water jacket for temperature control. Sample without pressurization (0.1 MPa) was set as a reference. Each sample was divided into two parts after HHP processing. MTGase (50 U/g protein) was subsequently added to one part of HHP-treated samples (pH 7.0) for enzymatic catalysis as described in section 2.3. Both of HHP-treated and MTGase further catalyzed SPP samples were freeze dried, then stored at -18 °C for further analysis.

2.5. -SH- groups

Free -SH- content was determined according to our previous literature (Zhao, Mu, Zhang & Richel, 2018a) by using a UV-Vis spectrophotometer (TU-1810; Puxi Instrument Co. Ltd. Beijing, China) with a molar extinction coefficient value of 13,600 mol/cm^{-1}. An aliquot (1.0 mL) of pressure-treated or further cross-linked SPP solution (1.0 mg/mL) was prepared by dissolving sample in Tris–glycine buffer (containing 0.086 mol/L Tris, 0.09 mol/L glycine, 0.004 mol/L EDTA, and 8.0 mol/L urea; pH 8.0), then mixed with 50 μL DTNB (5,5′-dinitrobis [2-nitrobenzoic acid],

4.0 mg/mL) and incubated for 20 min at room temperature (25 °C), followed with centrifugation at 10,000 *g* for 20 min. After that, the absorbance of the supernatant was immediately read at 412 nm.

2.6. Particle size distribution

Particle size distribution was measured using a Malvern Zetasizer Nano instrument (Malvern Instruments Ltd., Malvern, UK) with a 1.0 cm optical path length sample cell. Each of 1.0 mL pressure-treated or further cross-linked SPP sample solution (1.0 mg/mL) was prepared in phosphate buffer (10 mmol/L, pH 7.0), then mixed well and injected into the working cells, followed by continuously scanning 3 times before equilibration at 25 ℃ for 2 min. The main results were presented as the average particle size (d/nm).

2.7. DSC

DSC was performed by a thermal calorimeter of Q200 DSC (TA Instruments, Inc., New Castle, USA) in the temperature range of 25-110 ℃ and a heating speed of 10 °C/min. Pressure-treated or further cross-linked SPP samples of approximately 3.00 mg were weighted into aluminum pan and hermetically sealed with phosphate buffer (10 mmol/L, pH 7.0) at a solid-to-solvent ratio of 1:3, then equilibrated for 2 h before scanning. The instrument was calibrated by indium and a sealed empty crucible was used as reference. The onset (To, °C), peak (Tp, °C), final (Td, °C) temperature and the enthalpy (ΔH, J/g) associated with the denaturation were determined from the thermograms by using the accompanied software (Universal Analysis 2000, Version 4.1 D, TA Instruments).

2.8. CD

Secondary structure changes of pressure-treated or further cross-linked SPP sample solution (1.0 mg/mL) were monitored using a MOS-450/AF-CD spectrophotometer (Bio-Logic Science Instruments, Vaucanson, France) equipped with a 0.1 cm optical path length quartz cell. Far-UV spectra (190 to 250 nm) were averaged over three consecutive scans at a speed of 1000 nm/min and a step resolution of 0.5 nm. The bandwidth and response time was of 1.0 nm and 0.5 s, respectively. Data were expressed as mean residue ellipticity (θ, $deg \cdot cm^2 \cdot dmol^{-1}$) according to Whitmore & Wallace (2004). Typically, secondary structure units were consisted of α-helix, β-sheet, β-turn and random coil.

2.9. FTIR

FTIR spectra were obtained using an FTIR spectrometer (Bruker Tensor 27 system, Bruker Optics, Germany) with attenuated total reflection (ATR) mode at room temperature (25 °C) according to the method of Liu, Chiou & Avena-Bustillos, et al (2017). An aliquot of 0.1 mL pressure-treated or further cross-linked SPP sample solution was used for each test, and a total of 64 consecutive scans were recorded in the range of 400-2000 cm^{-1} with a resolution of 4 cm-1. Further reveal information of spectra was analyzed via assorted Bruker Optik GmbH OPUS (OPUS) data collection software program.

2.10. Preparation of SPP gel model

For SPP gel model preparation, 10 mL pressure-treated or further cross-linked SPP dispersion were injected into the cylindrical glass mold (2.3 cm internal diameters), heated from 25 to 95 °C in water bath and maintained at 95 °C for further 30 min, then immediately cooled with running water and set at 4 °C overnight. The cylindrical gel model was used for texture analysis and low-field nuclear magnetic resonance (NMR) measurement.

2.11. Textural properties

Textural analysis of fresh SPP gels was assessed by using a TA-XT2i texture analyser (Stable Micro System Ltd., Godalming, UK) according to uniaxial compression tests and equipped with a 12.0 mm diameter probe (P 0.5R). The test was compressed to 30 % of the original height of gel models at a speed of 1.0 mm/s and a 5 s waiting time at 25 °C by Texture Expert analysis software (Stable Micro Systems Ltd., Godalming, UK), and the parameters of hardness, springiness, cohesiveness, gumminess and chewiness were recorded.

2.12. Low-field NMR

The NMR was performed by using a Niumag pulsed NMR analyzer (MesoMR23-060H-I, Niumag Electric Corporation, Shanghai, China) with resonance frequency of 23 MHz, spectral width of 250 kHz and receiver gain of 10 db at 32 °C. Fresh heat-induced SPP gel was placed inside the cylindrical glass tubes (2.3 cm internal diameters). Transverse relaxation time was then measured using the Carr-Purcell-Meiboom-Gill (CPMG) sequence with a total 10,000 echoes. The low-field NMR relaxation curve was fitted to a multi-exponential curve with the MultiExp Inv Analysis software (Niumag Electric Corporation, Shanghai, China). T2b and T21 were presented as relaxation time components, and A_{2b} and A_{21} were of corresponding area fractions.

2.13. Statistical analysis

Experiments were conducted in triplicate. Statistical analysis was subjected to one-way analysis of variance using SAS 8.1 software (SAS institute Inc., Cary, NC, USA). Data was expressed as means ± SD. And the Duncan multiple range test was applied with a confidence interval of 95 %.

3. Results and discussion

3.1. MTGase-catalyzed cross-linking of SPP

MTGase-catalyzed covalent cross-linking of SPP with different enzyme concentrations are investigated both under non-reducing (Fig. 5-1A) and reducing (Fig. 5-1B) conditions. MTGase was located at 38 kDa and presented as a single band (Fig. 5-1A and B, lane 1). This information is consistent with the previous study reported by Kieliszek & Misiewicz (2014). As shown in Fig. 5-1 A, both of untreated and MTGase-catalyzed SPP samples exhibited similar molecular weight

distribution under non-reducing SDS-PAGE conditions, with three main band located at about 25-35 kDa, 20 kDa and between 17-20 kDa, which can be identified for 31 kDa, 22 kDa and 19 kDa, respectively. Among, the bands of 31 and 22 kDa was denoted the two subfamilies of SPP, namely sporamins A and B (Yeh, Chen, Lin, Chen, & Lin, 1997; Sun, Mu, Zhang & Arogundade, 2012). Moreover, the band at about 19 kDa and another minor band observed at about 42 kDa might correlated to the trypsin inhibitor protein fractions (Hou, & Lin, 1997). Notably, compared to the untreated SPP (lane 2), the high molecular weight protein aggregates larger than 245 kDa was marked with the presence of MTGase, and become more intense with the increasing of MTGase addition (lane 3-6). This phenomenon could be ascribed to the enzymatic cross-linking of SPP by the formation of covalent bonds. Similar aggregation also had been detected by Tang, Sun, Yin & Ma (2008) for kidney protein isolate and Feng et al., (2014) for peanut protein fractions.

For reducing SDS-PAGE image (Fig. 5-1 B), a main band with molecular weight of approximately 25 kDa was exhibited, corresponding to the monomer of SPP (Maeshima, Sasaki & Asahi, 1985). Interestingly, the high molecular weight aggregates were similarly observed at the top of the gel, forcefully indicated the inter-molecular linkages of SPP catalyzed by MTGase, being attributed to the covalent ε-(γ-glutaminyl) lysine isopeptide bonds. According to our previous reports, the covalent bonding of disulfide linkage induced by HHP treatment was detected under non-reducing SDS-PAGE conditions, while it can be destroyed under reducing SDS-PAGE conditions by reducing agent of β-mercaptoethanol (Zhao, Mu, Zhang & Richel, 2018a). This phenomenon also suggested that the MTGase catalyzed covalent isopeptide bonds were much stronger than the reported disulfide linkages, which might lead to improved gel properties. Furthermore, a slight band was appeared after 50 and 100 U/g MTGase addition (Fig. 5-1 A and B, lane 5-6), belonging to the extra enzyme additives. Thus, MTGase at a concentration of 50 U/g SPP was selected for further experiment and analysis, both with catalytic efficiency and economic concerns.

3.2. -SH- groups

The -SH- groups make an essential contribution to the three- dimensional gel network according to the oxidation during the formation of disulfide bonds (-S-S-). The content of free -SH- groups of SPP treated by HHP with further MTGase catalysis are shown in Table 5-1. Compared to SPP at 0.1 MPa, the content of free -SH- group was increased by HHP from 250 MPa but no significant difference was observed at 400 and 550 MPa, while the subsequent MTGase treatment led to a higher content of free -SH- groups compared to HHP-treated ones. The increase in free -SH- groups induced by pressurization could result from the exposure of interior part of -SH- due to partially unfolding (Zhang, Yang, Tang, Chen, & You, 2015). The protein unfolding induced by HHP allowed the buried -SH- groups to be exposed, and probably contributed to the cross-linking of protein molecules by the formation of disulfide bonds with an improved gel behavior (De Maria, Ferrari, & Maresca, 2016). Tang, Sun, Yin & Ma, (2008) indicated that MTGase treatment could be similarly altered the native structure changes of kidney bean protein isolates and

induced the exposure of -SH- groups. Meanwhile, Jia, Huang & Xiong (2016) also has been declared the positively effect of MTGase on promoting the unfolding of actomyosin, owe to the reduction or disruption of non-covalent interactions, such as non-specific association (e.g., electrostatic adsorption) and hydrophobic interactions.

Fig. 5-1. SDS-PAGE of SPP catalyzed by MTGase under both non-reducing (A) and reducing (B) conditions. *Lane M, standard marker, Lane 1, MTGase, Lanes 2-6, SPP catalyzed with MTGase at the concentrations of 0, 15, 25, 50 and 100 U/g protein.

(A)

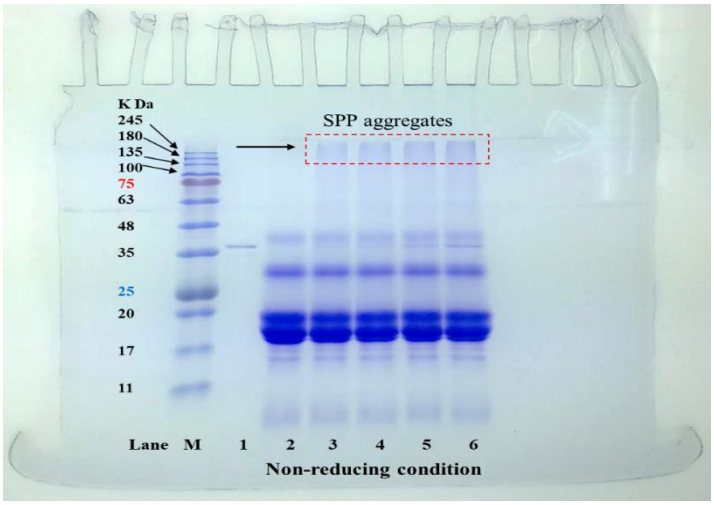

(B)

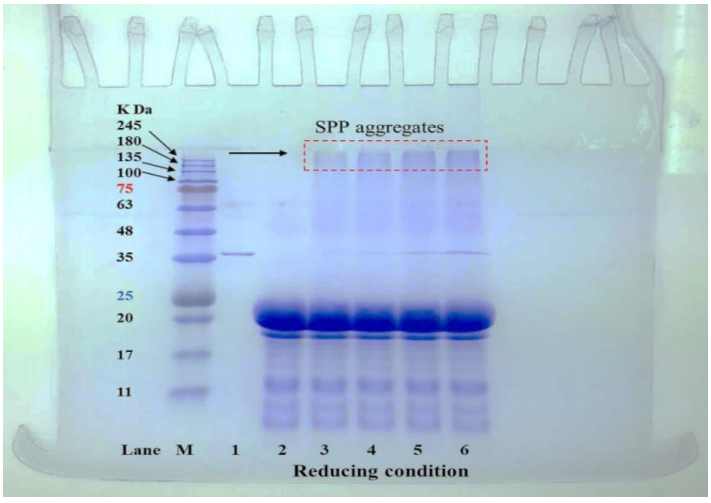

3.3. Particle size analysis

Average particle size of SPP treated by HHP with further MTGase catalysis are presented in Table 5-1. The average particle size of untreated SPP (0.1 MPa) was around 249.5 nm. No significant difference was observed at 250 MPa, while it gradually increased at 400 (254.9 nm) and 550 MPa (270.2 nm), which could be explained by the partial aggregation of SPP molecular chains. This result was consistent with that in our previous studies under the same pressure levels (Zhao, Mu, Zhang & Richel, 2018a). Similar aggregation had also been reported in soy protein isolate by Tang & Ma, (2009), who suggested that HHP caused formation of soy protein aggregates including both insoluble and soluble parts at 200-600 MPa.

Compare to untreated SPP (0.1 MPa), no significant change was observed in average particle size of MTGase-catalyzed SPP samples, while those of SPP treated by HHP with further MTGase catalysis significantly decreased at pressure level of 250, 400 and 550 MPa. Normally, the unfolding of protein molecules was accompanied by the exposure of hydrophobic, hydrophilic residues or non-polar active binding sites from interior structure area, which might lead to the intensive molecular interactions, including protein inter-molecular and protein-solvent interactions, and even presenting positively effect on further MTGase catalysis (He, He, Chao, Ju & Aluko, 2014; Wang, et al., 2017). The inverse decrease in average particle size of HHP treated SPP with further enzymatic catalysis was probably owing to the covalent bonds formed within the same SPP molecules, and also might be partially explained the intra- and inter-molecular cross-linking reactions (Mariniello, Giosafatto, Di Pierro, Sorrentino, & Porta, 2007). Similar intra-molecular cross-linking of pea albumin protein also has been observed by Djoullah, Krechiche, Husson & Saurel (2016), who suggested that the intra-ε-(γ-glutaminyl) lysine isopeptide bonds of protein fractions were able to be favored than the inter-molecular ones, due to the accessibility of the functional binding site.

3.4. DSC

Thermal characteristics of SPP treated by HHP with further MTGase catalysis were determined by DSC test. As shown in Table 5-1, the onset denaturation temperature (To) of SPP was increased by HHP from 78.8 (0.1 MPa) to 79.3 °C (550 MPa), the final denaturation temperature (Td) was reduced from 94.8 (0.1 MPa) to 93.3 °C (550 MPa), no significant difference was observed in peak denaturation temperature (Tp), and the denaturation enthalpy (ΔH) value was markedly decreased from 19.2 (0.1 MPa) to 17.4 J/g (550 MPa). Moreover, a shorter denaturation temperature range (R) was also observed in SPP undergoing with pressurization from 16.0 °C (0.1 MPa) to 14.0 °C (550 MPa). The increase in To induced by HHP treatment was attributed to the formation of SPP aggregates, being connected by -S-S- bonding. Whereas the decrease in ΔH indicated the loss of protein structure and gradual unfolding of SPP during the pressurization (Feng, et al., 2014). And, a narrow denaturation temperature range might probably reflect the improvement in thermal stability of SPP by HHP treatment. The reduction in ΔH and shifting of denaturation temperature of SPP induced by HHP had been similarly reported by Khan, Mu, Zhang, & Chen, (2013). And the results were also agreed with those

detected by Puppo et al., (2004) for soybean protein isolates and Peyrano, Speroni & Avanza, (2016) for cowpea protein isolates respectively, but with a much lower denaturation degree under different pressure levels (200-600 MPa). This difference suggested that HHP induced denaturation of protein was strongly depend on the applied pressure condition and varied by the protein resource. Correlated to the native and HHP treated SPP, further MTGase cross-linked SPP exhibited higher To, Tp, and Td, lower ΔH, and narrow denaturation temperature ranges (Table 1). The increase in To, Tp and Td of MTGase cross-linked SPP suggested the delay of the thermal transition and a higher denaturation values, especially for the cross-linked SPP with HHP pretreatment, simultaneously enhanced by disulfide bonds and isopeptide bonds between the glutamine and lysine residues (Gaspar & De Góes-Favoni, 2015).

3.5. CD

Secondary structure changes of SPP samples treated by HHP with further MTGase catalysis are summarized in Table 5-2. The α-helical content of untreated SPP (11.8 %) was continuously decreased by the pressure increasing from 0.1 to 550 MPa, especially for 250 (11.0 %), 400 (10.6 %) and 550 MPa (9.9 %) treatment. An increase tendency was observed in β-sheet unit of SPP after 250 MPa (31.3 %) treatment compared to the untreated ones (30.0 %), but no differences were detected at higher pressure of 400 and 550 MPa. Meanwhile, no significant changes were observed in β-turn and random coil structure unit, respectively. It has been suggested that α-helical and β-sheet were severally stabilized by intra- and inter-molecular hydrogen bonds (Zhang, Yang & Tang, et al., 2015). The decrease in α-helical and the increase in β-sheet therefore indicated the disruption of intra-molecular hydrogen bonds and the strengthening of inter-molecular hydrogen bonds between SPP molecules by HHP, respectively. Cando, Herranz, Borderías, & Moreno (2015) reported that hydrogen bonds were formed at pressures below 150 MPa, but ionic and hydrophobic interactions were dominant at higher pressures (>200 MPa). Thus, the increase in β-sheet content implied the functionality of HHP in stabilizing the inter-molecular hydrogen bonds within protein chains.

Compared to the native SPP (0.1 MPa), no significant differences were detected in SPP with the addition of MTGase in α-helical, β-sheet and β-turn, while a reduction in random coil content was observed. For pressure-treated samples, subsequent MTGase catalysis similarly alter the secondary structure changes of SPP. Particularly, the enzymatic catalysis decreased the α-helical content of SPP at 400 MPa but increased it at 550 MPa. Meanwhile, minimum changes were observed in β-sheet unit, β-turn was only reduced at 550 MPa, and the random coil content was varied by different HHP pretreatment. Actually, MTGase induced secondary structure changes was probably attributed to the specific covalent cross-linking reactions (Yang, et al., 2017). In addition, HHP induced unfolding was accompanied with the stretching of protein molecular chains, which could facilitate the exposure of functional groups and positively offer more chance or access for following MTGase catalysis (Herranz, Tovar, Borderias & Moreno, 2013).

Table 5-1 Sulfhydryl groups (-SH-), average particle size (d/nm) and thermal properties of SPP treated by HHP with further MTGase catalysis.

Samples		-SH- μmol/g	Average particle size	To /°C	Tp /°C	Td /°C	ΔH J/g	Range /°C
HHP (MPa)	0.1	2.85±0.13^{d}	249.45±1.63^{bc}	78.76±0.15^{d}	86.08±0.06^{b}	94.77±0.18^{b}	19.23±0.15^{a}	16.01±0.30^{a}
	250	3.11±0.03^{b}	243.25±4.03^{c}	78.92±0.21^{cd}	86.10±0.15^{b}	94.47±0.24^{b}	18.55±0.32^{b}	15.54±0.32^{ab}
	400	3.14±0.03^{b}	254.85±4.45^{b}	79.17±0.16^{bc}	86.12±0.21^{b}	93.31±0.51^{c}	17.81±0.20^{c}	14.14±0.47^{c}
	550	3.03±0.03^{bc}	270.20±9.62^{a}	79.30±0.08^{b}	85.82±0.38^{b}	93.27±0.24^{c}	17.44±0.28^{c}	13.97±0.23^{c}
HHP (MPa) + MTGase	0.1 + MTG	2.92±0.08^{cd}	247.55±2.76^{bc}	80.16±0.10^{a}	86.79±0.32^{a}	95.43±0.41^{a}	17.03±0.09^{d}	15.27±0.32^{b}
	250 + MTG	3.40±0.13^{a}	217.50±1.84^{d}	80.26±0.20^{a}	86.70±0.11^{a}	95.35±0.18^{a}	16.44±0.28^{e}	15.10±0.38^{b}
	400 + MTG	3.51±0.03^{a}	211.85±4.88^{d}	80.40±0.23^{a}	86.69±0.12^{a}	95.55±0.18^{a}	16.15±0.03^{e}	15.15±0.26^{b}
	550 + MTG	3.44±0.08^{a}	200.25±1.06^{e}	80.32±0.05^{a}	86.69±0.12^{a}	94.39±0.29^{b}	14.76±0.20^{f}	14.07±0.32^{c}

*Different letters in the same column indicate significant differences ($p < 0.05$).

Table 5-2 Secondary structure component of SPP treated by HHP with further MTGase catalysis.

Samples		Secondary structure composition (%)			
		α-helix	β-sheet	β-turn	Random coil
HHP (MPa)	0.1	11.80±0.28^{bc}	30.00±0.14^{b}	23.05±0.35^{abc}	35.15±0.21^{ab}
	250	10.95±0.07^{cd}	31.30±0.42^{a}	23.05±0.07^{abc}	34.70±0.28^{bc}
	400	10.60±0.14^{de}	30.75±0.21^{ab}	23.35±0.07^{ab}	35.25±0.07^{a}
	550	9.85±0.64^{ef}	31.40±0.14^{a}	23.15±0.35^{ab}	35.55±0.35^{a}
HHP (MPa) + MTGase	0.1 + MTG	11.95±0.35^{b}	31.05±0.78^{ab}	22.75±0.35^{bc}	34.25±0.07^{cd}
	250 + MTG	11.05±0.49^{bcd}	31.45±0.49^{a}	22.90±0.00^{abc}	34.60±0.14^{c}
	400 + MTG	9.60±0.57^{f}	31.55±1.06^{a}	23.40±0.42^{a}	35.50±0.00^{a}
	550 + MTG	13.05±0.49^{a}	30.65±0.49^{ab}	22.45±0.21^{c}	33.85±0.21^{d}

*Different letters in the same column indicate significant differences ($p < 0.05$).

3.6. FTIR

FTIR spectroscopy of SPP treated by HHP with further MTGase catalysis are exhibited in Fig. 5-2, being used to illustrate the structural conformation changes and the stretching vibration of functional groups. The amide I region (1600–1700 cm^{-1}) of FTIR spectra mainly be attributed to the C=O stretching vibration and to a small degree to the C–N stretching vibration of the peptide backbones, with regard to the protein secondary structure (Qin, et al., 2016). For the corresponding relationships between the absorption peak and secondary structure, α-helical was appeared at 1650-1660 cm^{-1}, β-sheet was at 1610-1640 cm^{-1}, β-turn and random coil unit were at 1660-1670 and 1640-1650 cm^{-1} respectively (Herranz, Tovar, Borderias & Moreno, 2013). Compared to SPP at 0.1 MPa, the absorbance intensity of Amide I region in HHP treated SPP was decreased with pressure level from 250 to 550 MPa (Fig 5-2 A). Han, et al. (2015) indicated that the degree of protein unfolding was increased observably with the applied pressure. In addition, MTGase catalysis produced a similar decrease in the absorbance of cross-linked SPP (Fig. 5-2 B). According to Herranz, Tovar, Borderias & Moreno (2013), the absorbance intensity of a protein molecule depends on the net change undergone by the dipole moment through the interaction with infrared radiation. Thus, the weak band of further cross-linked SPP was inferred at a lower level of internal organization and symmetry, even compared to HHP treated samples. HHP treatment might change the molecular structure of SPP and enhance the accessibility of pressure-treated SPP to MTGase catalytic cross-linking.

3.7. Textural properties

Textural properties of gels made from SPP treated by HHP with further MTGase catalysis are given in Table 5-3. The hardness, springiness, cohesiveness and chewiness were significantly affected by HHP, which increased from 0.1 to 400 MPa then decreased at 550 MPa. This might be due to the SPP aggregation via disulfide bonds formation (Zhao, Mu, Zhang & Richel, 2018a). The hardness and chewiness of the gel prepared from SPP by HHP with further MTGase catalysis were higher than those of non-HHP and HHP treated SPP samples, but no significant differences were detected in springiness and cohesiveness. Actually, textural behavior was attributed to the quality of protein gels, and closely related to the gel network construction and holding capacities (Cheung, Wanasundara & Nickerson, 2014). The subsequent enzymatic treatment further enhanced the covalent cross-linking of SPP by the specific isopeptide bonds (Herranz, Tovar, Borderias, & Moreno, 2013). These results confirmed the functional role of HHP and the following MTGase catalysis in improving the gelation properties of SPP, especially on textural behaviors. In this case, both of HHP treatment and MTGase catalysis could be applied in gel-like food processing with an improved quality.

Fig. 5-2. FTIR spectroscopy of SPP treated by HHP (A) and further MTGase catalysis (B). *Attaching spectroscopy is belonging to the amide I region (1600–1700 cm^{-1}) of SPP samples with different treatment.

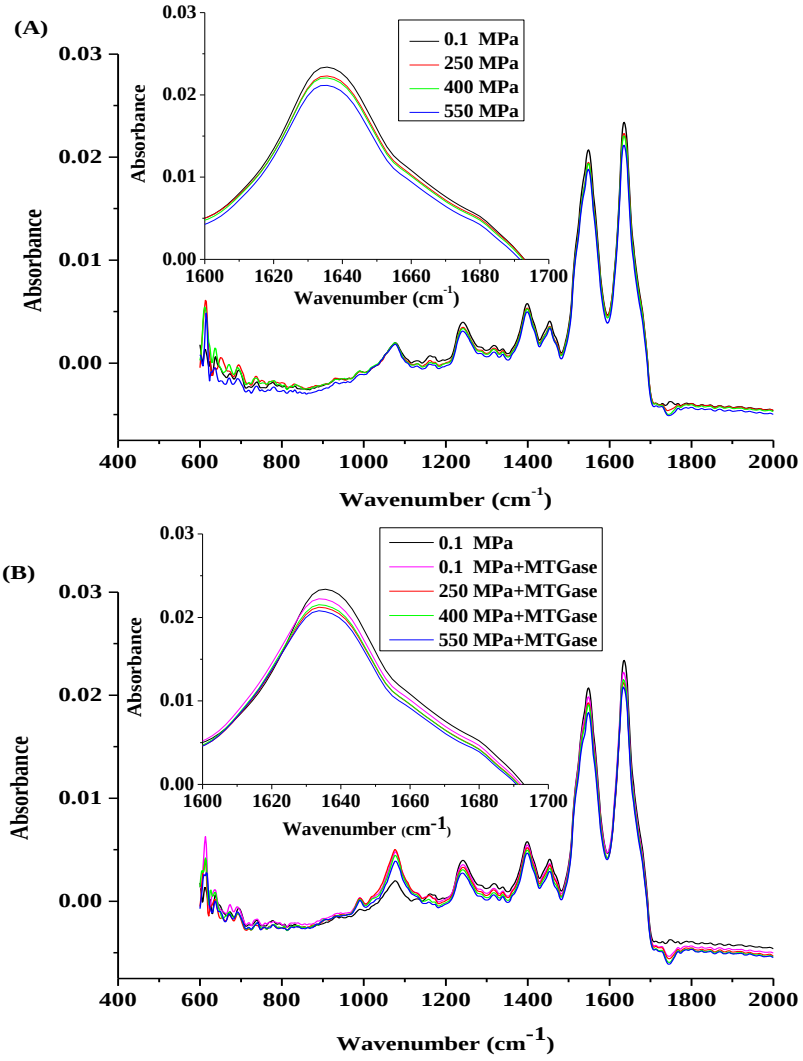

3.8. Low-field NMR

The mobility, distribution and holding behavior of water fractions in protein gel system is closely related to its functional properties, which could be nondestructive monitored by NMR (Wang, Xu, Huang, Huang, & Zhou, 2014). The distribution and proportion of T2 relaxation time of gels made from SPP treated by HHP with further MTGase catalysis are shown in Table 4. Two relaxation time ingredients were detected at approximately 1–10 ms (T_{2b}) and 10–100 ms (T_{21}), corresponding to the bonded and immobilized water fractions. T_{2b} suggested that water fractions were closely associated with proteins, whereas T_{21} indicated the part of water trapped within the gel matrix (Grossi, et al., 2016). Compared to gel from SPP at 0.1 MPa, no significant differences were observed in T_{2b} of gels from HHP treated SPP, while

T_{21} was gradually increased with pressure increasing from 0.1 to 550 MPa. A longer relaxation time (T2) was indicated water bound more loosely to macromolecules than that with shorter relaxation time (Zhang, Yang, Tang, Chen, &You, 2015). Thus, the increase in T_{21} values implied a little weak in water bonding status, which was connected to the unfolding of SPP molecular chains by HHP. Notably, the proportion of peak area of A_{2b} after HHP treatment was little decreased at 250 MPa then increased at 400 and 550 MPa, and A_{21} increased obviously. The increase in proportion of peak area suggested that both of more bonded and immobilized water fractions were trapped in the gel networks after HHP.

Compared to HHP treated SPP, following MTGase catalysis reduced the T_{2b} values of the gels made from SPP treated at 400 and 550 MPa, while T_{21} was increased from 250 to 550 MPa. A_{2b} showed an increase especially at 400 and 550 MPa, whereas A_{21} was decreased at 550 MPa. The reduction in T_{2b} suggested that bound water had lower water mobility and was more closely associated with proteins, which might be due to the increase in negative electric charges (Zhang, Yang & Tang, et al., 2015). And a broad relaxation time of cross-linked SPP in T_{21} could be attributed to the elastic network formed by part of SPP aggregates during HHP treatment with subsequent covalent linkages. A higher proportion peak area of A2b and A_{21} detected with further MTGase catalysis was due to the fact that more free water was attracted by cross-linked SPP or trapped in the gel structure, and might transfer to bound or immobilized water as pressure increased (Han, Wang, Xu, & Zhou, et al., 2014).

3.9. Hypothetic mechanism explanation

The hypothetic illustration of the reactions induced by HHP and further MTGase catalysis on SPP are presented in Fig. 5-3, including disulfide linkage (Fig. 5-3 a), intra-/inter-molecular covalent cross-linking (Fig. 5-3 b and c), and associative reactions (Fig. 5-3 d). Unfolding of SPP structure induced by HHP allowed the inaccessible free -SH- groups to be exposed (Table 5-1), which consequently contributed to the -SH-/-SS- exchange reactions and the formation of disulfide bonds (Fig. 5-3 a). As pressure increased, the decrease in α-helical and the increase in β-sheet content (Table 2) were presented, suggesting a weak intra-hydrogen bond but a strong inter-hydrogen bond, which might strengthen the interactions between SPP molecules. For the following enzymatic treatment, high molecular aggregates were formed (Fig. 5-1), suggesting the formation of inter- and intra- molecular covalent cross-linking via ε-(γ-glutaminyl) lysine isopeptide bond (Fig. 5-3 b and c). In this case, the gelation behavior of SPP was significant improved by the associative reactions of HHP and MTGase (Fig. 5-3 d), corresponding to the increases in hardness and chewiness of SPP gels (Table 5-3), as well as more bound and immobilized water fractions trapped in SPP gel networks (Table 5-4).

Table 5-3 Textural profile analysis of SPP treated by HHP with further MTGase catalysis

Samples		Hardness (g)	Springiness	Cohesiveness	Chewiness
HHP (MPa)	0.1	54.77±2.06^{e}	0.89±0.02^{c}	0.59±0.03^{c}	31.11±0.52^{f}
	250	58.61±2.38^{e}	0.92±0.02^{bc}	0.62±0.02^{bc}	34.65±1.01^{f}
	400	67.20±1.91^{d}	0.94±0.00^{ab}	0.67±0.01^{a}	42.71±2.40^{e}
	550	40.61±2.51^{f}	0.93±0.02^{ab}	0.60±0.02^{c}	24.11±2.18^{g}
HHP (MPa) + MTGase	0.1 + MTG	99.55±0.71^{c}	0.95±0.02^{ab}	0.59±0.00^{c}	57.72±1.22^{d}
	250 + MTG	111.07±1.40^{b}	0.96±0.00^{a}	0.60±0.01^{c}	63.80±1.96^{c}
	400 + MTG	127.21±3.08^{a}	0.96±0.01^{a}	0.65±0.03^{ab}	75.33±0.13^{b}
	550 + MTG	123.27±2.37^{a}	0.97±0.01^{a}	0.59±0.03^{c}	82.05±2.50^{a}

*Different letters in the same column indicate significant differences ($p < 0.05$).

Table 5-4 Distributions of T2 relaxation time (T_{2b}, T_{21}), and proportion of peak area (A_{2b}, A_{21}) of SPP treated by HHP with further MTGase catalysis.

Samples		T_{2b} (ms)	T_{21} (ms)	A_{2b} (%)	A_{21} (%)
HHP (MPa)	0.1	1.28±0.27^{ab}	89.07±0.00^{c}	0.80±0.06^{cd}	98.58±0.41^{bc}
	250	1.60±0.20^{a}	93.34±3.70^{b}	0.77±0.09^{d}	98.81±0.00^{ab}
	400	1.60±0.18^{a}	95.48±0.00^{b}	0.97±0.14^{abc}	99.10±0.20^{a}
	550	1.52±0.16^{ab}	100.05±3.96^{a}	0.90±0.12^{abcd}	99.14±0.14^{a}
HHP (MPa) + MTGase	0.1 + MTG	1.56±0.13^{a}	95.46±0.03^{b}	0.87±0.00^{bcd}	99.04±0.09^{ab}
	250 + MTG	1.50±0.26^{ab}	102.31±0.02^{a}	0.89±0.05^{bcd}	99.08±0.05^{ab}
	400 + MTG	1.18±0.05^{b}	102.34±0.00^{a}	1.09±0.18^{a}	99.14±0.03^{a}
	550 + MTG	1.19±0.25^{b}	102.34±0.00^{a}	1.04±0.13^{ab}	98.25±0.68^{c}

*Different letters in the same column indicate significant differences ($p < 0.05$).

Fig. 5-3. The hypothetic illustration of covalent linkages of disulfide bond (a), intra- (b) or inter-molecular cross-linking (c) of SPP induced by HHP and MTGase, respectively.

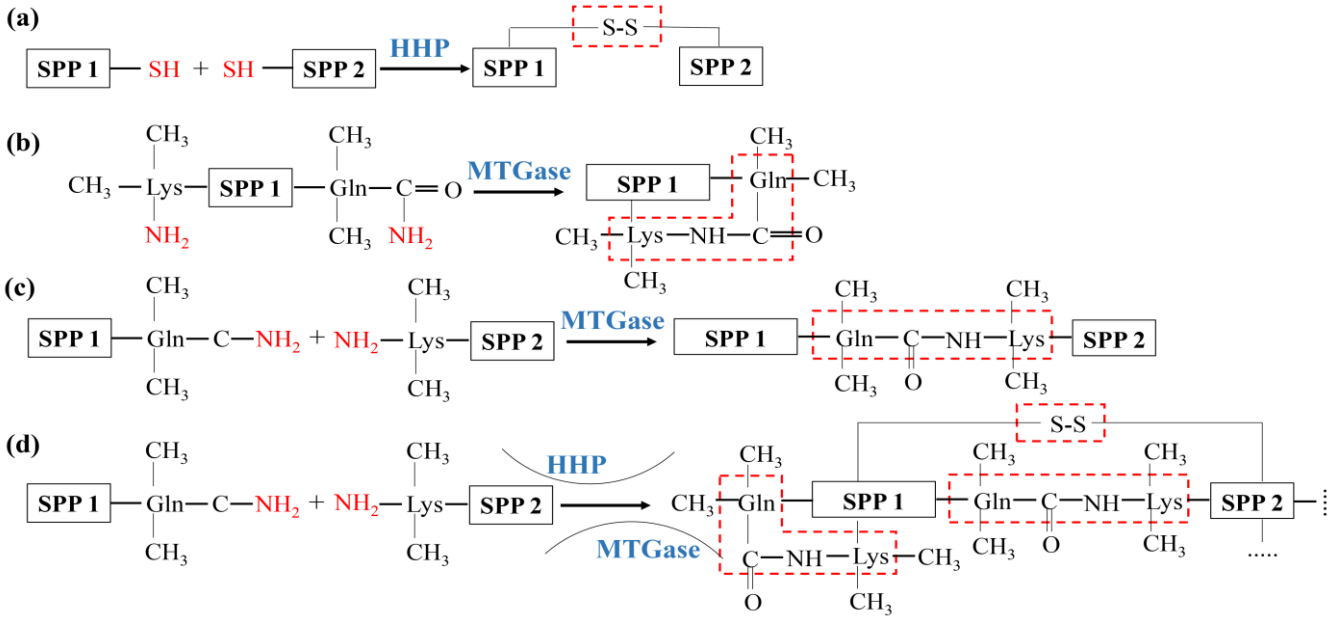

4. Conclusion

The structural changes and gelation properties of SPP treated by HHP with further MTGase catalysis were evaluated. Both of HHP and MTGase modified secondary structure of SPP and induced inter-molecular covalent cross-linking, according to the disulfide bond and ε-(γ-glutaminyl) lysine isopeptide bond, respectively. As a result, the denaturation temperature was increased, especially for cross-linked SPP with HHP pretreatment. Meanwhile, the average particle size was similarly increased by HHP but inversely decreased with following MTGase catalysis, owing to the intra-molecular linkages. HHP and MTGase simultaneously strengthened the gel formation, and significantly improved the textural behaviors. Low field NMR measurement indicated the increase of bound and immobilized water fractions trapped in the gel structure. Our findings would be useful for understanding the gelation properties of SPP treated by HHP and MTGase, and the development of cross-linked SPP in gel-like food fabrication (e.g. yogurt, jelly and minced meat) for a better quality.

Acknowledgments

The authors gratefully acknowledge the earmarked fund for China Agriculture Research System (CARS-10-B21) and National Key R & D Program of China (2016YFE0133600).

Reference

Angioloni, A., Collar, C. (2013). Impact of high hydrostatic pressure on protein aggregation and rheological properties of legume batters. *Food and Bioprocess Technology*, 6, 3576-3584.

Ardelean, A. I., Otto, C., Jaros, D., & Rohm, H. (2012). Transglutaminase treatment to improve physical properties of acid gels from enriched goat milk. *Small Ruminant Research*, 106, 47-53.

Arogundade, L. A., Mu, T. H. (2012a). Influence of oxidative browning inhibitors and isolation techniques on sweet potato protein recovery and composition. *Food Chemistry*, 134, 1374-1384.

Arogundade, L. A., Mu, T. H., Añón, M. C. (2012b). Heat-induced gelation properties of isoelectric and ultrafiltered sweet potato protein isolate and their gel microstructure. *Food Research International*, 49, 216-225.

Cando, D., Herranz, B., Borderías, A. J., & Moreno, H. M. (2015). Effect of high pressure on reduced sodium chloride surimi gels. *Food Hydrocolloids*, 51, 176-187.

Cheung, L., Wanasundara, J., Nickerson, M. T. (2014). Effects of pH and NaCl levels on the physicochemical and emulsifying properties of a cruciferin protein isolate. *Food Biophysics*, 9, 105-113.

De Maria, S., Ferrari, G., & Maresca, P. (2016). Effects of high hydrostatic pressure on the conformational structure and the functional properties of bovine

serum albumin. *Innovative Food Science & Emerging Technologies*, 33, 67-75.

Djoullah, A., Krechiche, G., Husson, F., & Saurel, R. (2016). Size measuring techniques as tool to monitor pea proteins intramolecular crosslinking by transglutaminase treatment. *Food Chemistry*, 190, 197-200.

FAOSTAT. (2017). Production quantity [Internet]. *Food and Agricultural Organization*. http://www.fao.org/faostat/en/#data/QC. Accessed 01/06/19.

Feng, X. L., Liu, H. Z., Shi, A. M., Liu, L., Wang, Q., & Adhikari, B. (2014). Effects of transglutaminase catalyzed crosslinking on physicochemical characteristics of arachin and conarachin-rich peanut protein fractions. *Food Research International*, 62, 84-90.

Gaspar, A. L. C., & de Góes-Favoni, S. P. (2015). Action of microbial transglutaminase (MTGase) in the modification of food proteins: A review. *Food Chemistry*, 171, 315-322.

Grossi, A., Olsen, K., Bolumar, T., Rinnan, Å., Øgendal, L. H., & Orlien, V. (2016). The effect of high pressure on the functional properties of pork myofibrillar proteins. *Food Chemistry*, 196, 1005-1015.

Han, M., Wang, P., Xu, X., & Zhou, G. (2014). Low-field NMR study of heat-induced gelation of pork myofibrillar proteins and its relationship with microstructural characteristics. *Food Research International*, 62, 1175-1182.

Han, Y., Wang, J., Li, Y., Hang, Y., Yin, X., & Li, Q. (2015). Circular dichroism and infrared spectroscopic characterization of secondary structure components of protein Z during mashing and boiling processes. *Food Chemistry*, 188, 201-209.

He, R., He, H. Y., Chao, D., Ju, X., & Aluko, R. (2014). Effects of high pressure and heat treatments on physicochemical and gelation properties of rapeseed protein isolate. *Food and Bioprocess Technology*, 7 (5), 1344-1353.

Heck, T., Faccio, G., Richter, M., & Thöny-Meyer, L. (2013). Enzyme-catalyzed protein crosslinking. *Applied Microbiology and Biotechnology*, 97 (2), 461-475.

Herranz, B., Tovar, C. A., Borderias, A. J., & Moreno, H. M. (2013). Effect of high-pressure and/or microbial transglutaminase on physicochemical, rheological and microstructural properties of flying fish surimi. *Innovative Food Science & Emerging Technologies*, 20, 24-33.

Hou, W. C., & Lin, Y. H. (1997). Dehydroascorbate reductase and monodehydroascorbate reductase activities of trypsin inhibitors, the major sweet potato (*Ipomoea batatas* [L.] Lam) root storage protein. *Plant Science*, 128 (2), 151-158.

Hwang, J. S., Lai, K. M., & Hsu, K. C. (2007). Changes in textural and rheological properties of gels from tilapia muscle proteins induced by high pressure and setting. *Food Chemistry*, 104 (2), 746-753.

Jia, D., Huang, Q., & Xiong, S. (2016). Chemical interactions and gel properties of black carp actomyosin affected by MTGase and their relationships. *Food Chemistry*, 196, 1180-1187.

Khan, N. M., Mu, T. H., Zhang, M., & Arogundade, L. A. (2014). The effects of

pH and high hydrostatic pressure on the physicochemical properties of a sweet potato protein emulsion. *Food Hydrocolloids*, 35, 209-216.

Khan, N. M., Mu, T. H., Zhang, M., & Chen, J. W. (2013). Effects of high hydrostatic pressure on the physicochemical and emulsifying properties of sweet potato protein. *International Journal of Food Science & Technology*, 48 (6), 1260-1268.

Kieliszek, M., & Misiewicz, A. (2014). Microbial transglutaminase and its application in the food industry. A review. *Folia Microbiologica*, 59 (3), 241-250.

Lam, R. S., & Nickerson, M. T. (2014). The properties of whey protein–carrageenan mixtures during the formation of electrostatic coupled biopolymer and emulsion gels. *Food Research International*, 66, 140-149.

Li, P. G., Mu, T. H., & Deng, L. (2013). Anticancer effects of sweet potato protein on human colorectal cancer cells. *World Journal of Gastroenterology: WJG*, 19 (21), 3300.

Liu, C., Damodaran, S., & Heinonen, M. (2018). Effects of microbial transglutaminase treatment on physiochemical properties and emulsifying functionality of faba bean protein isolate. *LWT - Food Science and Technology*, 99, 396–403.

Liu, F., Chiou, B. S., Avena-Bustillos, R. J., Zhang, Y., Li, Y., McHugh, T. H., & Zhong, F. (2017). Study of combined effects of glycerol and transglutaminase on properties of gelatin films. *Food Hydrocolloids*, 65, 1-9.

Maeshima, M., Sasaki, T., & Asahi, T. (1985). Characterization of major proteins in sweet potato tuberous roots. *Phytochemistry*, 24 (9), 1899-1902.

Mariniello, L., Giosafatto, C. V. L., Di Pierro, P., Sorrentino, A., & Porta, R. (2007). Synthesis and resistance to in vitro proteolysis of transglutaminase cross-linked phaseolin, the major storage protein from Phaseolus vulgaris. *Journal of Agricultural and Food Chemistry*, 55 (12), 4717-4721.

Peyrano, F., Speroni, F., & Avanza, M. V. (2016). Physicochemical and functional properties of cowpea protein isolates treated with temperature or high hydrostatic pressure. *Innovative Food Science & Emerging Technologies*, 33, 38-46.

Puppo, C., Chapleau, N., Speroni, F., de Lamballerie-Anton, M., Michel, F., Añón, C., & Anton, M. (2004). Physicochemical modifications of high-pressure-treated soybean protein isolates. *Journal of Agricultural and Food Chemistry*, 52 (6), 1564-1571.

Qin, X. S., Luo, S. Z., Cai, J., Zhong, X. Y., Jiang, S. T., Zhao, Y. Y., & Zheng, Z. (2016). Transglutaminase-induced gelation properties of soy protein isolate and wheat gluten mixtures with high intensity ultrasonic pretreatment. *Ultrasonics Sonochemistry*, 31, 590-597.

Qiu, C., Hu, X., Li, L., Yang, X., Zhao, M., & Ren, J. (2017). Effect of transglutaminase cross-linking on the conformational and emulsifying properties of peanut arachin and conarachin fractions. *European Food Research and Technology*, 243 (6), 913-920.

Sun, M. J., Mu, T. H., Zhang, M., & Arogundade, L. A. (2012). Nutritional

assessment and effects of heat processing on digestibility of Chinese sweet potato protein. *Journal of Food Composition and Analysis*, 26 (1-2), 104-110.

Tang, C. H., & Ma, C. Y. (2009). Effect of high pressure treatment on aggregation and structural properties of soy protein isolate. *LWT-Food Science and Technology*, 42 (2), 606-611.

Tang, C. H., Sun, X., Yin, S. W., & Ma, C. Y. (2008). Transglutaminase-induced cross-linking of vicilin-rich kidney protein isolate: influence on the functional properties and in vitro digestibility. *Food Research International*, 41 (10), 941-947.

Tang, C. H., Yang, M., Liu, F., & Chen, Z. (2013). A novel process to efficiently form transglutaminase-set soy protein isolate-stabilized emulsion gels. *LWT-Food Science and Technology*, 53 (1), 15-21.

Wang, M., Chen, X., Zou, Y., Chen, H., Xue, S., Qian, C., ... & Zhou, G. (2017). High-pressure processing-induced conformational changes during heating affect water holding capacity of myosin gel. *International Journal of Food Science & Technology*, 52 (3), 724-732.

Wang, P., Xu, X., Huang, M., Huang, M., & Zhou, G. (2014). Effect of pH on heat-induced gelation of duck blood plasma protein. *Food Hydrocolloids*, 35, 324-331.

Whitmore, L., & Wallace, B. A. (2004). DICHROWEB, an online server for protein secondary structure analyses from circular dichroism spectroscopic data. *Nucleic Acids Research*, 32 (suppl 2), W668–W673.

Yang, A., Xia, J., Gong, Y., Deng, H., Wu, Z., Li, X., ... & Chen, H. (2017). Changes in the structure, digestibility and immunoreactivities of glycinin induced by the cross‐linking of microbial transglutaminase following heat denaturation. *International Journal of Food Science & Technology*, 52 (10), 2265-2273.

Yeh, K. W., Chen, J. C., Lin, M. I., Chen, Y. M., & Lin, C. Y. (1997). Functional activity of sporamin from sweet potato (Ipomoea batatas Lam.): a tuber storage protein with trypsin inhibitory activity. *Plant Molecular Biology*, 33 (3), 565-570.

Zeeb, B., Fischer, L., & Weiss, J. (2014). Stabilization of food dispersions by enzymes. *Food & Function*, 5 (2), 198-213.

Zhang, M., Mu, T. H., Sun, M. J. (2014). Purification and identification of antioxidant peptides from sweet potato protein hydrolysates by Alcalase. *Journal of Functional Foods*, 7, 191-200.

Zhang, Z., Yang, Y., Tang, X., Chen, Y., & You, Y. (2015). Chemical forces and water holding capacity study of heat-induced myofibrillar protein gel as affected by high pressure. *Food Chemistry*, 188, 111-118.

Zhang, Z., Yang, Y., Zhou, P., Zhang, X., & Wang, J. (2017). Effects of high pressure modification on conformation and gelation properties of myofibrillar protein. *Food Chemistry*, 217, 678-686.

Zhao, Z. K., Mu, T. H., Zhang, M., & Richel, A. (2018a). Chemical forces, structure, and gelation properties of sweet potato protein as affected by pH and high hydrostatic pressure. *Food and Bioprocess Technology*, 11 (9), 1719-1732.

Zhao, Z. K., Mu, T. H., Zhang, M., & Richel, A. (2018b). Effect of salts combined with high hydrostatic pressure on structure and gelation properties of sweet potato protein. *LWT - Food Science and Technology*, 93, 36-44

Chapter VI

Effects of sulfur-containing amino acids and high hydrostatic pressure on structure and gelation properties of sweet potato protein

Chapter VI Effects of sulfur-containing amino acids and high hydrostatic pressure on structure and gelation properties of sweet potato protein

This chapter is adapted from the article (under review):

Effects of sulfur-containing amino acids and high hydrostatic pressure on structure and gelation properties of sweet potato protein

*Zhong-Kai Zhao[1,2], Tai-Hua Mu[*1], Miao Zhang[1], Aurore Richel*[*2]*

1 Laboratory of Food Chemistry and Nutrition Science, Institute of Food Science and Technology, Chinese Academy of Agricultural Sciences; Key Laboratory of Agro-Products Processing, Ministry of Agriculture and Rural Affairs, No. 2 Yuan Ming Yuan West Road, Haidian District, P.O. Box 5109, Beijing 100193, P. R. China.

2 University of Liège, Gembloux Agro-Bio Tech, Laboratory of Biomass and Green Technologies, Passage des Déportés, 2, 5030 Gembloux, Belgium

Abstract

The structural modification and gelation properties of SPP affected by sulfur-containing amino acids (L-cysteine or L-cystine) and HHP were investigated. Additives altered the denaturation temperature and reduced the denaturation enthalpy of SPP. Higher α-helical contents were observed in untreated or HHP-treated SPP with L-cysteine or L-cystine, while β-sheet and random coil structure unit were decreased. FTIR spectra showed a weak absorbance in HHP-treated SPP with L-cysteine and L-cystine. Storage modulus (G′) of untreated or HHP-treated SPP was enhanced by L-cysteine and L-cystine. Textural properties of SPP gels were improved by sulfur-containing amino acids and HHP, especially for L-cysteine. Decrease in T_{2b} relaxation time and increase in A_{21} proportion peak area by Low-field NMR suggested that water bound more closely to SPP molecules in the presence of L-cysteine and L-cystine, and more immobilized water fraction was trapped in SPP gel matrix.

Keywords

Sweet potato protein; High hydrostatic pressure; Sulfur-containing amino acids; Gelation; Low-field NMR

1. Introduction

Plant protein is received increasing interests based on the customer demands due to their various health beneficial functions, e.g., nutritional supplement (Sun, Mu, Zhang & Arogundade, 2012), intervention of obesity-induced metabolic dysfunction (Wanezaki, Tachibana & Nagata, et al., 2015), as well as antioxidant activities (Zhang & Mu, 2017). High acceptability and desirable workability make plant protein commonly used in dairy beverage and baking sweets, even gradually replacing some meat ingredient for reconstituted meat products or sea food (Lin, Lu & Kelly, et al., 2017). For complicated food matrix, interactions between protein fractions, additives or different component are inevitable, which derive significant influence on protein structure and functionality (Akin & Ozcan, 2017). Utilization of plant proteins combined with additive amino acids is innovatively regarded as a beneficial way to improve the functionalities and nutrition of food complexes (Cando, Herranz, Borderías & Moreno, 2016).

As a construction unit, amino acid sequence constitutes the primary structure of proteins, which partially define the acting site of protein interacting with other components (O'sullivan, Murray, Flynn & Norton, 2016). The dominant concept of protein nutrition mainly refers to the balance of amino acids composition (Sun, Mu, Zhang & Arogundade, 2012). Sulfur-containing amino acids (e.g., methionine, cysteine and cysteine) are considered to have essential contributions in maintaining the conformation of protein molecules (Zhao & Jiang, 2018). The key role of sulfur-containing amino acids against free radicals and heavy metal has been highly evaluated (Colovic, Vasic, Djuric & Krstic, 2018). The thiol group of sulfur-containing amino acids can participate in oxidation reaction during the formation of disulfide bonding, resulting in covalent cross-linking between plant protein molecules (Zhao, Mu, Zhang & Richel, 2018a). Particularly, cystine and lysine were found useful for unfolding and further aggregation of myofibrillar protein, which could be as effective additives applied to improve the gelation of surimi gel with reduced sodium content (Cando, Herranz, Borderías & Moreno, 2016).

As a non-thermal promising technology, HHP has been reported to modify the secondary structure of protein, alter the chemical forces and molecular interactions within the dispersion system, and used to improve the gelation behaviors of different food proteins (Tabilo-Munizaga, Gordon & Villalobos-Carvajal, et al., 2014; Grossi, Olsen & Bolumar, et al., 2016). HHP treatment is efficiently in promoting the unfolding of protein ingredient and inducing the formation of disulfide linkages (-S-S-) due to the exposure of sulfhydryl groups (-SH-), thus produce a better gel construction (De Maria, Ferrari & Maresca, 2016). In general, sulfur has a low propensity to hydrogen bond, as a consequence, the sulfur-containing amino acids in almost exhibit nonpolar and hydrophobic properties, and frequently buried in the interior of proteins (Visschers & De Jongh, 2005). HHP could induce unfolding and denaturation, followed by the further aggregation of protein molecular chain, which can strengthened protein surface interactions and lead to the improved mechanical properties (Ma, Chen, Zheng & Zhou, et al., 2013). For instance, the combination of pressure processing and additive cystine resulted in a significant increase of

breaking force and breaking deformation in surimi gels (Cando, Moreno, Borderías & Skåra, 2016).

Sweet potato (*Ipomoea batatas* [L.] Lam) accounts for 90.49 % of Asian production, being utilized for starch processing and food consuming (FAOSTAT, 2017). Laudably, SPP recovered from starch processing effluent has earned both environmental and economic concerns, being developed for a new protein resource potentially applied in gel-like food, such as mince, yogurt and soft beverages, etc. SPP showed high nutritional values and certain gelation potential (Arogundade, Mu & Añón, 2012), while the sulfur-containing amino acids were detected as the first limiting amino acid (Sun, Mu, Zhang & Arogundade, 2012), which might have influence on gelation properties of SPP. The effects of salt ions combined with HHP treatment on gelation behavior of SPP have been explored in our previous studies (Zhao, Mu, Zhang & Richel, 2018b). However, no information about the functional role of sulfur-containing amino acids on structure and gelation properties of SPP under HHP is available.

The objective of the present study was to identify the changes in structural modification and gelation behavior of SPP affected by L-cysteine and L-cystine under HHP for a better understand of the essential and functional role of additive sulfur-containing amino acids on SPP gelation behaviors, thus to provide valuable information on the application of SPP and HHP technique in the food industry.

2. Materials and methods

2.1. Materials

Sweet potato cultivar Shang Shu No.19 was supplied by Shangqiu Academy of Agriculture and Forestry Sciences (Henan province, China). L-cysteine and L-cystine were purchased from Sigma-Aldrich, Inc. (St. Louis, Mo, USA). All other reagents were of analytical grade.

2.2. SPP preparation

SPP was extracted by the isoelectric precipitation method according to our previous report (Zhao, Mu, Zhang & Richel, 2018b). Briefly, fresh peeled sweet potato tubers were ground at solid to solvent ratio of 1:2 with 0.1 % sodium bisulfite for color protection. The supernatant was collected by centrifugation at 10,000 g for 45 min, and further precipitated at pH 4.0 (isoelectric point of SPP). After that, the precipitate was re-dissolved in distilled water with a ratio of 1:3 and adjusted to pH 7.0. The centrifugation was then repeated to obtain the water-soluble fractions, followed by the ultrafiltration equipped with a 10 kDa molecular weight cut-off membrane. The concentrated dispersion was finally lyophilized and stored at -18 °C for further testing. SPP with 92.95 % purity was obtained as measured by the Kjeldahl method with a nitrogen conversion coefficient of 6.25.

2.3. HHP treatment

HHP treatment was performed using a 0.6 L laboratory-scale HHP units (model HHP-L3, HuaTaiSenMiao Engineering & Technique Ltd. Co., Tianjin, China) equipped with both of temperature and pressure regulation. Each SPP dispersion (4 %, w/v) was prepared in 10 mmol/L phosphate buffer (pH 7.0) and vacuum-packed in food-grade polyethylene bags with the addition of 0.1, 0.5, 1.0 % L-cysteine or L-cystine respectively, then subjected to 400 MPa (selected pressure stage, data not shown) for 30 min at 25 °C before release the pressure within 5 s. After HHP, each protein solution was freeze dried and stored at -18 °C for subsequent analysis.

2.4. DSC

Thermal properties were detected using a calorimeter of Q200 DSC (TA Instruments, Inc., New Castle, USA) in the temperature range of 25-110 °C with a heating speed of 10 °C/min. Approximately 3.00 mg SPP samples with different sulfur-containing amino acids additive were weighted into an aluminum pan, then hermetically sealed with 10 mmol/L phosphate buffer (pH 7.0) at a solid to solvent ratio of 1:3. The instrument was calibrated by indium, and the samples were equilibrated at 25 °C for 2 h before scanning. The onset (To, °C), peak (Tp, °C) and final (Td, °C) denaturation temperature, as well as denaturation enthalpy (ΔH, J/g) were determined according to thermogram by using the accompanied software (Universal Analysis 2000, Version 4.1 D, TA Instruments). A sealed empty crucible was used as reference.

2.5. CD

Secondary structure components of α-helix, β-sheet, β-turn and random coil were monitored using a MOS-450/AF-CD spectrophotometer (Bio-Logic Science Instruments, Vaucanson, France) equipped with a 0.1 cm optical path length quartz cell. The testing was conducted at a speed of 1000 nm/min, a step resolution of 0.5 nm, a bandwidth of 1.0 nm and a response time of 0.5 s, respectively. The far-UV spectra at 190-250 nm of SPP (1.0 mg/mL, phosphate buffer, pH 7.0) were averaged over the three consecutive scans. And the data were expressed as mean residue ellipticity (θ, $deg \cdot cm^2 \cdot dmol^{-1}$).

2.6. FTIR

FTIR spectra of SPP samples were obtained by a spectrometer (Bruker Tensor 27 system, Bruker Optics, Germany) with an attenuated total reflection (ATR) mode. An aliquot of 0.1 mL sample solution was consecutively scaned in the range of 400-4000 cm^{-1} for 64 times with a resolution of 4 cm^{-1}. The spectra was recorded and further analyzed via assorted Bruker Optik GmbH OPUS (OPUS) data collection software program.

2.7. Gelation properties

2.7.1. Dynamic shear rheological properties

Dynamic shear rheological properties were investigated using Anton Paar rheometer (Physica MCR 301, Graz, Austria) equipped with a temperature controlled Peltier system. Measurements were conducted within the linear viscoelasticity range at an angular frequency of 10 s^{-1} and strain of 0.5 %, respectively. A constant 2.3 mL mixed SPP dispersion (10 %, w/v) was prepared in 10 mM phosphate buffer (pH 7.0), continually injected onto the parallel plate geometry (PP-50 probe, 50 mm diameter) with 1.0 mm plate gap, heated at a linear temperature rate of 2 °C/min from 25 to 95 °C, and then cooled down to 25 °C. The exposed perimeter was covered with a small amount of silicon oil to avoid sample drying during heating. Rheological parameters of storage modulus (G′) were recorded during the heating process, followed by the frequency sweeping test in the range of 0.1-100 s^{-1} after the heating and cooling process mentioned above.

2.7.2. Preparation of SPP gel model

An aliquot of 10 mL SPP sample dispersion (10 %, w/v) was injected into the cylindrical glass mold (2.3 cm internal diameters), heated from 25 to 95 °C in water bath and maintained at 95 °C for 30 min, then immediately cooled down to room temperature (25 °C) with running water. The cylindrical gel model was stored at 4 °C overnight for further textural analysis and low-field nuclear magnetic resonance (NMR) measurement.

2.7.3. Textural analysis

Textural properties of freshly prepared SPP gels were analyzed by using a TA-XT2i texture analyzer (Stable Micro System Ltd., Godalming, UK) based on the uniaxial compression test and equipped with a 12.0 mm diameter probe (P 0.5R). The operation was compressed to 30 % of the original height of the gel model (as described in section 2.6.2) with pre-test speed of 1.5 mm/s, test speed of 1.0 mm/s and a 5 s waiting time. Data were measured in triplicate and recorded by Texture Expert analysis software (Stable Micro Systems Ltd., Godalming, UK). The parameters of hardness, springiness, gumminess and chewiness were elaborately selected and recorded to evaluate the texture behaviors.

2.7.4. Low-field NMR

The low-field NMR was predicted using a Niumag pulsed NMR analyzer (MesoMR23-060H-I, Niumag Electric Corporation, Shanghai, China) with resonance frequency of 23 MHz, spectral width of 250 kHz, receiver gain of 10 db and working temperature of 32 °C. Fresh prepared SPP gel models (as described in section 2.6.2) was placed inside the cylindrical glass tubes (2.3 cm internal diameters), then tested by Carr-Purcell-Meiboom-Gill (CPMG) sequence with a total 10,000 echoes. The low-field NMR relaxation curve was fitted with a multi-exponential curve by MultiExp Inv Analysis software (Niumag Electric Corporation, Shanghai, China). The transverse relaxation time (T2) components of T_{2b} and T_{21}, as well as the corresponding area fractions of A2b and A21 were recorded, respectively.

2.7.5. Microstructure

Microstructure of SPP gels were determined by using a scanning electron microscope (SEM, Hitachi S-3400n, Japan). Gels were cut into small cubes, fixed with 30 % (w/v) glutaraldehyde in phosphate buffer (10 mM, pH 7.0), and continuously dehydrated in a series of ethanol solution (30, 50, 70, 80 and 100 %). After that, the gel samples were further dehydrated by critical-point drying method with CO_2 as the transition fluid, pasted on a copper stub with double-sided tabs, rendered conductive by coating with platinum, and photographed at an accelerating voltage of 15.0 kV with ×2000 magnifications.

2.7.6. Statistical analysis

All tests were conducted in triplicate, and the data were expressed as means ± SD. Statistical analysis was subjected to one-way analysis of variance using SAS 8.1 software (SAS institute Inc., Cary, NC, USA). Images were designed and graphed by Origin 8.5 software (OriginLab Co., Northampton, MA, USA). Duncan multiple range test was applied with a confidence interval of 95 %.

3. Results and discussion

3.1. DSC

Thermal characteristics of untreated (0.1 MPa) and HHP-treated SPP (400 MPa) with the addition of L-cysteine and L-cystine are shown in Table 6-1. Compared to untreated SPP without additives, To was increased in SPP with the presence of 1.0 % L-cysteine, and it was significantly enhanced by HHP even at low concentration of L-cysteine at 0.1 % ($p < 0.05$). The highest To value was detected in 400 MPa treated SPP with 1.0 % of L-cysteine, which increased from 78.54 to 79.30 °C. While no changes were observed in Tp by additives or HHP. A slight decrease of Td was observed in SPP after adding 0.1 and 0.5 % L-cysteine, respectively. Moreover, ΔH was similarly decreased by sulfur-containing amino acids with or without HHP treatment. The increase of To was ascribed to the protein partially aggregation, which was probably due to that the additive L-cysteine was the active mercapto donor for the covalent bonding (Colovic, Vasic, Djuric & Krstic, 2018). Meanwhile, HHP induced disulfide bonds could strengthen the cross-links of SPP, thus leading to a higher denaturation temperature (Zhao, Mu, Zhang & Richel, 2018a). Similar observation was also reported by Tang & Ma (2009) in soy protein isolate, who found that HHP higher than 200 MPa could resulted in formation of insoluble aggregates. ΔH was related to the balance between endothermic reactions (e.g. the breakup of hydrogen bonds) and exothermic reactions (e.g. protein aggregation and the breakup of hydrophobic interactions) (Peyrano, Speroni & Avanza, 2016). The reduction in ΔH was involved in the denaturation of SPP, which could be correlated to the conformational changes modified by sulfur-containing amino acids and HHP (Tabilo-Munizaga, Gordon & Villalobos-Carvajal, et al., 2014).

Table 6-1 Thermal properties of untreated (0.1 MPa) and HHP-treated (400 MPa) SPP with addition of L-cysteine and L-cystine.

HHP (MPa)	Additive	Percentage (%)	To/°C	Tp/°C	Td/°C	ΔH (J/g)
0.1	No additive		78.54±0.14^{d}	86.17±0.22^{a}	94.93±0.00^{bc}	18.42±0.36^{a}
	L-cysteine	0.1	78.75±0.39^{cd}	86.08±0.06^{a}	94.06±0.41^{d}	15.09±0.18^{bcd}
		0.5	79.07±0.09^{bcd}	86.41±0.14^{a}	93.89±0.00^{d}	15.50±0.00^{b}
		1.0	79.48±0.18^{ab}	86.36±0.28^{a}	94.47±0.00^{cd}	15.18±0.04^{bc}
	L-cystine	0.1	78.86±0.49^{bcd}	86.50±0.37^{a}	95.16±0.17^{b}	15.16±1.15^{bc}
		0.5	78.83±0.06^{bcd}	86.16±0.19^{a}	95.05±0.16^{bc}	14.20±0.14^{d}
		1.0	78.97±0.28^{bcd}	86.29±0.33^{a}	95.04±0.00^{bc}	14.71±0.00^{bcd}
400	No additive		78.89±0.04^{bcd}	86.07±0.13^{a}	94.47±0.33^{cd}	14.26±0.61^{d}
	L-cysteine	0.1	79.16±0.03^{abcd}	86.48±0.10^{a}	94.99±0.08^{bc}	15.08±0.17^{bcd}
		0.5	79.28±0.28^{abc}	86.51±0.18^{a}	94.99±0.08^{bc}	15.28±0.00^{bc}
		1.0	79.30±0.12^{abc}	86.46±0.20^{a}	94.76±0.25^{bc}	15.07±0.36^{bcd}
	L-cystine	0.1	78.91±0.14^{bcd}	86.46±0.04^{a}	94.99±0.41^{bc}	15.48±0.61^{b}
		0.5	78.87±0.11^{bcd}	86.36±0.01^{a}	94.76±0.25^{bc}	14.72±0.15^{bcd}
		1.0	79.80±0.95^{a}	86.16±0.27^{a}	96.03±0.74^{a}	14.52±0.01^{cd}

*Results are presented as mean ± standard deviation (n=3). Values followed by the different lowercase letters in the same column indicate significant differences ($p < 0.05$).

Table 6-2 Secondary structure composition of untreated (0.1 MPa) and HHP-treated (400 MPa) SPP with addition of L-cysteine and L-cystine.

HHP (MPa)	Additive	Percentage (%)	α- helix	β-sheet	β-turn	Random coil
0.1	No additive		11.50±0.42^{h}	30.90±0.57^{a}	22.75±0.07^{bcd}	34.80±0.00^{a}
	L-cysteine	0.1	14.80±0.14^{cd}	28.85±0.49^{d}	22.80±0.28^{bc}	33.65±0.07^{cdef}
		0.5	14.35±0.78^{def}	29.45±0.49^{cd}	22.45±0.21^{cde}	33.75±0.49^{cdef}
		1.0	14.10±0.28^{def}	30.50±0.14^{ab}	22.20±0.00^{efg}	33.15±0.21^{efg}
	L-cystine	0.1	16.80±0.14^{a}	29.05±0.49^{d}	21.90±0.14^{g}	32.25±0.35^{h}
		0.5	14.65±0.21^{cde}	29.60±0.14^{bcd}	22.40±0.14^{def}	33.35±0.35^{efg}
		1.0	14.00±0.57^{def}	29.65±0.64^{bcd}	22.55±0.35^{cde}	33.80±0.28^{cde}
400	No additive		13.15±0.07^{g}	29.65±0.21^{bcd}	22.95±0.07^{b}	34.30±0.14^{abc}
	L-cysteine	0.1	15.25±0.07^{bc}	29.10±0.42^{d}	22.55±0.07^{cde}	33.10±0.42^{fg}
		0.5	14.40±0.57^{def}	29.65±0.21^{bcd}	22.50±0.00^{cde}	33.45±0.35^{defg}
		1.0	13.60±0.28^{fg}	29.65±0.07^{bcd}	22.75±0.21^{bcd}	34.05±0.49^{bcd}
	L-cystine	0.1	15.95±0.21^{b}	29.20±0.57^{cd}	22.05±0.07^{fg}	32.85±0.35^{gh}
		0.5	13.85±0.21^{efg}	29.80±0.28^{bcd}	22.55±0.07^{cde}	33.70±0.28^{cdef}
		1.0	11.60±0.42^{h}	30.15±0.78^{abc}	23.60±0.28^{a}	34.65±0.07^{ab}

*Results are presented as mean ± standard deviation (n=3). Values followed by the different lowercase letters in the same column indicate significant differences ($p < 0.05$).

Fig. 6-1. FTIR spectroscopy of untreated (0.1 MPa) and HHP-treated (400 MPa) SPP with the addition of L-cysteine (A and C) or L-cystine (B and D), respectively.

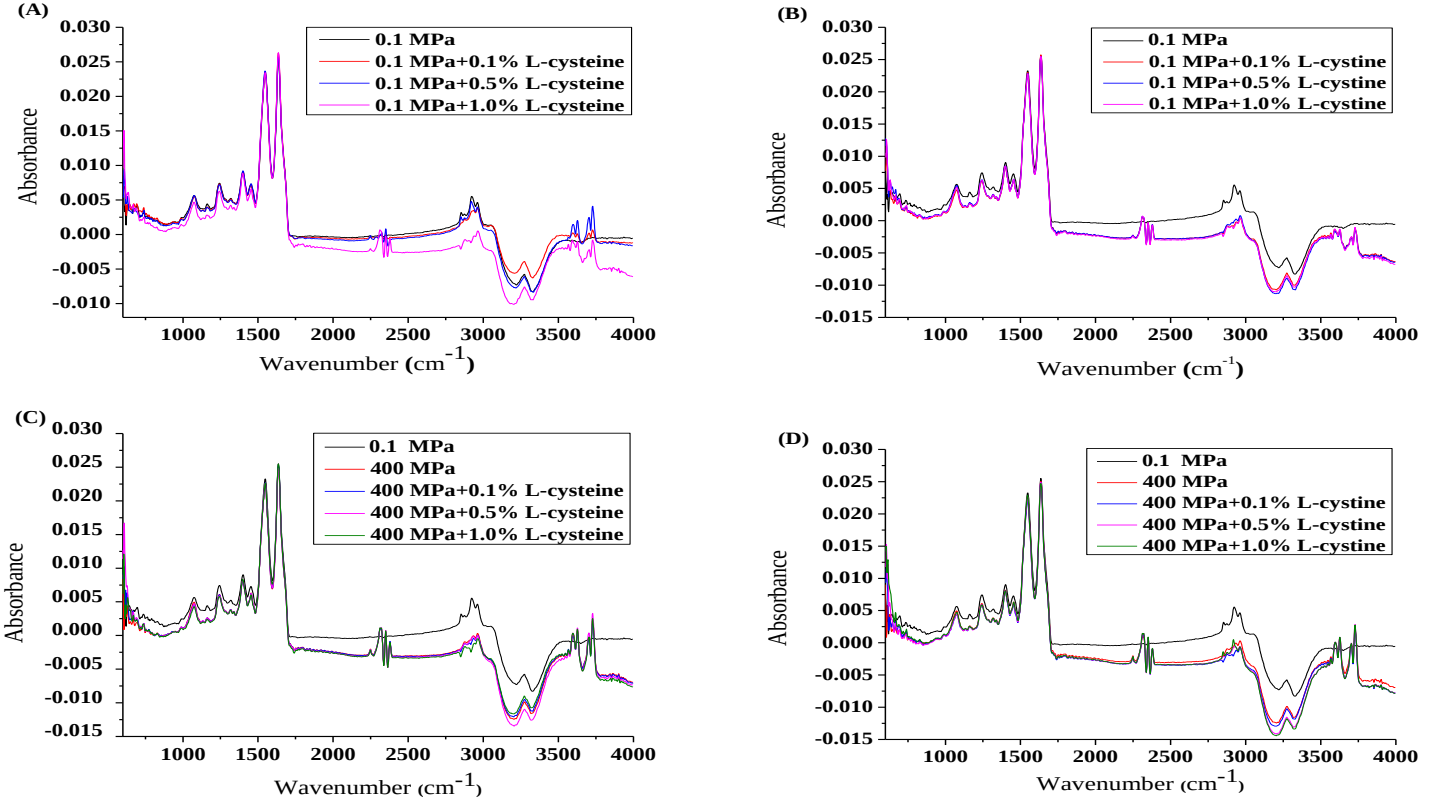

3.2. CD

Secondary structure changes in untreated (0.1 MPa) and HHP-treated SPP (400 MPa) with the addition of L-cysteine and L-cystine are shown in Table 6-2. According to CD spectrum analysis, α-helical content of SPP was significantly increased, β-sheet was tended to decrease, β-turn was slightly changed, and the random coil structure unit was also reduced after adding L-cysteine and L-cystine (Table 6-2). Compared to untreated SPP (0.1 MPa), the increase of α-helical content and the decrease of random coil units was similarly observed in HHP-treated SPP with the presence of sulfur-containing amino acids. Moreover, β-sheet and β-turn content was varied by the additive concentrations.

The α-helical and β-sheet structure component was stabilized by intra- and inter-molecular hydrogen bonds, respectively. The increase in α-helical indicated the enhancement of intra-molecular hydrogen bonds of proteins (Wei, Zhang, Cai & Peng, 2018). HHP-induced compression effect would be shortening the lengths of non-covalent bond, leading to the intensive protein-protein interactions (Chao, Jung & Aluko, 2018). Moreover, HHP-induced increase of α-helical content was attributed to the denaturing effect of pressurization (Tabilo-Munizaga, Gordon & Villalobos-Carvajal, et al., 2014). This might partially explain the secondary structure changes by adding sulfur-containing amino acids. In addition, the increase of α-helical units was similarly found in SPP with salt ions, suggesting the functionality of salt in weakening the electrostatic repulsion and strengthening the hydrophobic aggregation (Zhao, Mu, Zhang & Richel, 2018b). Thus, observation in present studies implied that sulfur-containing amino acids might have influence on protein structure by altering the electrostatic interaction and promoting protein-protein interactions through the intra-molecular hydrogen bonding of SPP.

3.3. FTIR

The spectroscopic properties of the SPP were evaluated to ascertain the effect of additive sulfur-containing amino acids combined with HHP on backbone and functional groups of SPP. As shown in Fig. 6-1, the absorbance intensity of SPP was weakened by two sulfur-containing amino acids in a concentration dependent manner form 0.1 to 1.0 % (Fig. 6-1A and B), particularly in samples with L-cysteine and L-cystine under HHP (Fig. 6-1C and D). The spectral of amide I region (1600-1700 cm-1) was reduced by sulfur-containing amino acids or HHP, which were the most sensitive region to the protein secondary structure. The addition of sulfur-containing amino acids could change the electrostatic forces around the charged groups and the solvation of polar groups, which would induced the destabilization of the proteins (Visschers & De Jongh, 2005).

On the other hand, HHP induced reduction in protein spectrum was associated with the loss of native structural state (Wei, Zhang, Cai & Peng, 2018). The results in the current study were consistent with the decrease in enthalpy values detected by DSC (Table 6-1), suggesting the gradual denaturation of SPP. Free sulfur-containing amino acids might interact with SPP as functional substrates, thus could alter the stretching vibration of backbone and functional groups.

Moreover, L-cystine was a weak oxidant that might maximize the cross-linkages of SPP and result in the weakness of absorbance intensity. A more unfolded protein structure had been reported in surimi dough after adding cystine and pyrophosphate, similarly refer from the formation of a network with a higher density of protein cross-links (Cando, Herranz, Borderías & Moreno, 2016). In addition, as non-thermal and promising treatment, HHP presented significant effects on non-covalent interactions (e.g. hydrophobic interaction and physical aggregations) and the following reformation of intra- or inter-molecular bonds, both of those reactions could arise the stretching vibration of functional groups and further conformation changes (Chao, Jung & Aluko, 2018).

3.4. Gelation properties

3.4.1. Dynamic shear rheological properties

The storage modulus (G′) of SPP contain 0.5 % L-cysteine and L-cystine with or without HHP treatment was typically selected and monitored for a clear describing the influence of sulfur-containing amino acids on gelling behaviors of SPP during the thermal processing (from 25 to 95 °C). As shown in Fig. 6-2A, G′ consistently exhibited higher values in SPP with the presence of L-cysteine or L-cystine, particularly in that with 0.5 % L-cysteine under 400 MPa. G′ was an essential viscoelastic component and represented the strength of gel matrix (Cando, Herranz, Borderías & Moreno, 2015). The increase in G′ indicated that SPP gels with addition of sulfur-containing amino acids behaved in a more elastic and gel-like manner. Compare with SPP without additives, the initial gelling temperature of both untreated (0.1 MPa) and HHP-treated (400 MPa) ones with the addition of L-cysteine or L-cystine significantly increased (Fig. 2A). Sulfur-containing amino acids might promote the partial aggregation of protein molecules with an increase in the number of cross-links and disulfide bonds (Cando, Moreno, Borderías & Skåra, 2016). Moreover, the gel network formation took place under HHP mainly attributed to the molecular reactions, such as denaturation, formation of cross-links or disulfide bonds produced by oxidation of SH groups, leading to a three-dimensional definitive network (De Maria, Ferrari & Maresca, 2016).

Dynamic frequency sweep was performed after the thermal processing cooling down to the 25 °C, which was aimed to determine the frequency dependence in elastic modulus of the fresh gels. As shown in Fig. 6-2B, G′ of all gels showed frequency dependence. Compare to the thermal stage, further cooling enhanced the gel network structure with a steady increase in G′, being associated to the consolidation of attractive forces, such as hydrophobic interactions, van der waals forces and hydrogen bonding (Murekatete, Hua & Chamba, et al., 2014). The maximum G′ value was observed in SPP with 0.5 % L-cysteine under 400 MPa, suggesting more continually molecular interactions within gel matrix, and a higher percentage of stored energy was recovered at shearing cycle than that of other gels (Arogundade, Mu & Añón, 2012). The observation in the current study strongly suggested that both sulfur-containing amino acids and HHP could be used to improve elastic properties of SPP gels for a better quality.

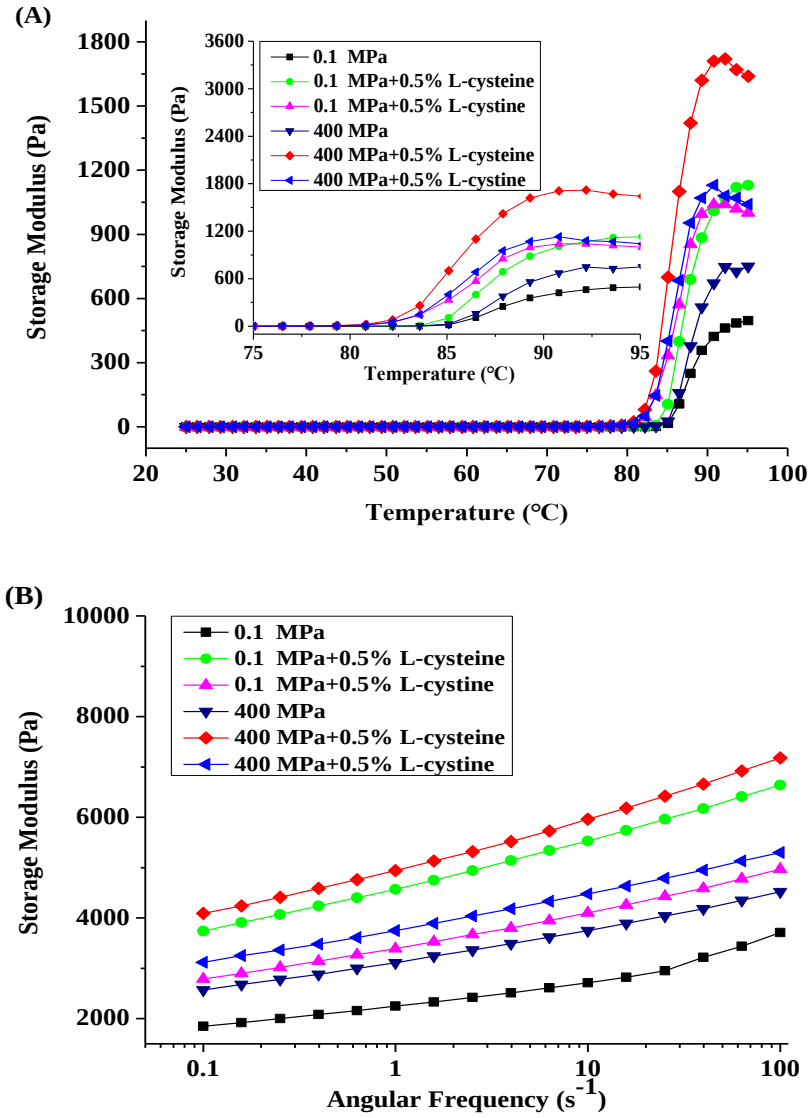

Fig. 6-2. Thermomechanical spectra (A) and corresponded dynamic frequency sweep (B) of untreated (0.1 MPa) and HHP-treated (400 MPa) SPP with the addition of 0.5 % of L-cysteine or L-cystine.

Fig. 6-3. Textural behavior in hardness, springiness and chewiness of gels from untreated (0.1 MPa) and HHP-treated (400 MPa) SPP with addition of L-cysteine or L-cystine.

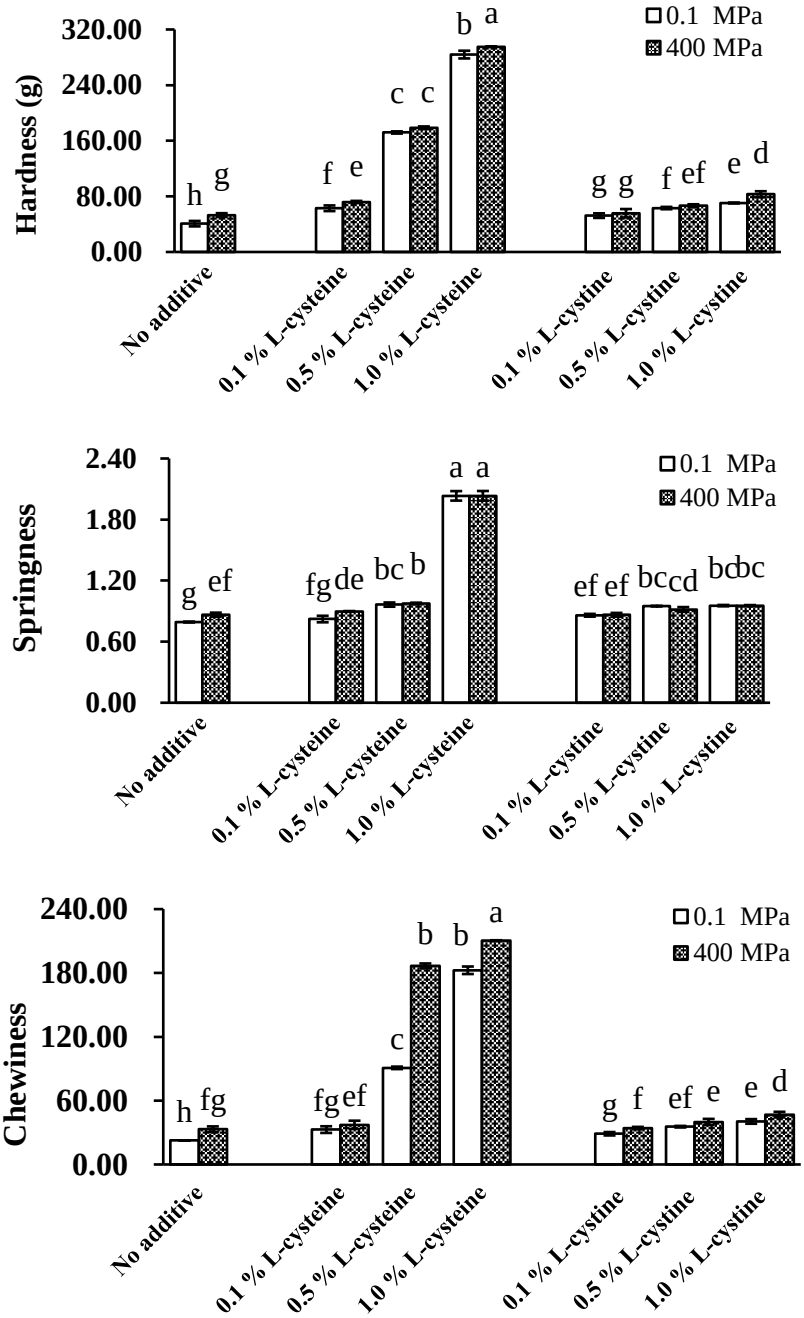

Table 6-3 Relaxation times distribution (T_{2b}, T_{21}) and proportion peak area (A_{2b}, A_{21}) of gels from untreated (0.1 MPa) and HHP-treated (400 MPa) SPP with addition of L-cysteine and L-cystine.

HHP (MPa)	Additive	Percentage (%)	T_{2b} (ms)	T_{21} (ms)	A_{2b} (%)	A_{21} (%)
0.1	No additive		0.85±0.00^{c}	80.31±3.94^{d}	0.78±0.00^{abc}	98.74±0.26^{e}
	L-cysteine	0.1	0.60±0.00^{e}	83.10±0.00^{cd}	0.86±0.03^{ab}	98.99±0.10^{de}
		0.5	0.49±0.05^{f}	83.10±0.00^{cd}	0.87±0.01^{a}	99.22±0.23^{cd}
		1.0	0.41±0.06^{g}	89.07±0.00^{b}	0.87±0.01^{a}	99.22±0.14^{cd}
	L-cystine	0.1	0.58±0.03^{e}	89.07±0.00^{b}	0.76±0.00^{bc}	99.31±0.10^{cd}
		0.5	0.56±0.00^{e}	86.09±4.22^{bc}	0.73±0.00^{cd}	99.45±0.26^{c}
		1.0	0.54±0.03^{ef}	86.09±4.22^{bc}	0.16±0.07^{gh}	99.84±0.07^{a}
400	No additive		0.56±0.00^{e}	89.07±0.00^{b}	0.50±0.14^{f}	99.50±0.14^{bc}
	L-cysteine	0.1	0.74±0.00^{d}	89.07±0.00^{b}	0.66±0.00^{de}	99.46±0.17^{c}
		0.5	0.74±0.00^{d}	89.07±0.00^{b}	0.63±0.00^{e}	99.37±0.00^{c}
		1.0	1.16±0.06^{b}	95.48±0.00^{a}	0.22±0.05^{g}	99.78±0.05^{ab}
	L-cystine	0.1	1.20±0.00^{b}	95.48±0.00^{a}	0.05±0.00^{i}	99.95±0.00^{a}
		0.5	1.29±0.00^{a}	95.48±0.00^{a}	0.08±0.00^{hi}	99.92±0.00^{a}
		1.0	1.29±0.00^{a}	95.48±0.00^{a}	0.08±0.00^{hi}	99.92±0.00^{a}

*Results are presented as mean ± standard deviation (n=3). Values followed by the different lowercase letters in the same column indicate significant differences ($p < 0.05$).

Fig. 6-4. The hypothetical illustration of covalent interactions of SPP induced by L-cysteine (A) and L-cystine (B) under HHP treatment. The correlated gel microstructure images (C) with an additive concentration of 0.5 %, and photographed by scanning electron microscope (SEM) with ×2000 magnifications.

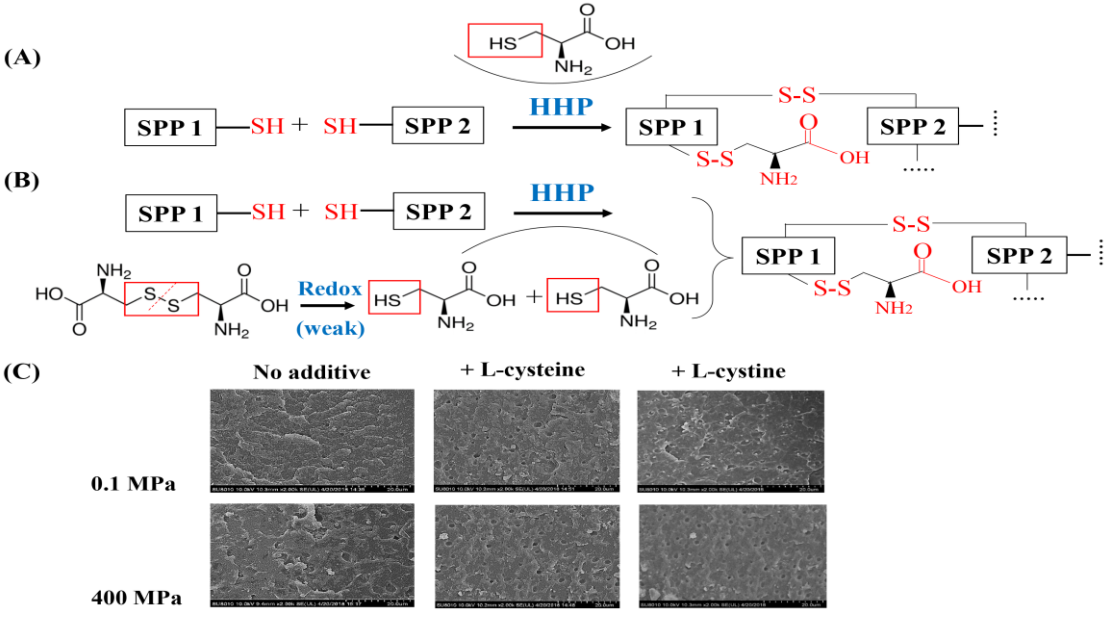

3.4.2. Textural analysis

Textural properties of the gels made from untreated (0.1 MPa) and HHP-treated SPP (400 MPa) with the addition of L-cysteine and L-cystine are presented in Fig. 6-3. The hardness, springiness and chewiness of gels from SPP with L-cysteine or L-cystine were significantly increased with the increasing of additive concentrations from 0.1 to 1.0 % ($p < 0.05$), particularly in SPP with 1.0 % L-cysteine. L-cysteine exhibited more efficiency in gel network construction compared to L-cystine, which might be due to the active sulfhydryl groups supplied by L-cysteine availably contributed to the formation of -S-S- bond through covalent crosslinks (Buchert, Ercili Cura & Ma, et al., 2010). The -SH- of L-cysteine displayed a strong chemical reactivity towards a number of compounds (formed by oxidation of L-cysteine) when compared to L-cystine, which was facilitated the electrostatic interactions and association of food protein (Cando, Moreno, Borderías & Skåra, 2016). Interestingly, an increase in textural behavior was similarly detected in gels made from HHP-treated SPP. HHP could expose endogenous sulfhydryl groups buried in the internal of protein structures, resulting in inter-molecular aggregation and following covalent disulfide bonding (Ahmed, Al-Ruwaih, Mulla & Rahman, et al., 2018). Furthermore, HHP could cause the electrostriction of charged amino acid groups, leading to water structuring around the exposed nonpolar groups, and solvation of polar groups through hydrogen bonding, thus enhanced protein gel behavior (Liang, Guo & Zhou, et al., 2016).

3.4.3. Low-field NMR

As non-destruction technique, the low-field NMR test was essentially performed to evaluate the mobility, distribution and binding state of water molecules within the food system (Han, Zhang & Zheng, et al., 2019). Water in protein matrix exists as bound, immobilized and free water components (Stangierski & Baranowska, 2015). Gels made from SPP with L-cysteine or L-cystine under HHP exhibited two relaxation time fractions in the range of 0.1-1 ms (T_{2b}) and 100-1000 ms (T_{21}), mainly correlated to bound and immobilized water fractions respectively. As showed in Table 6-3, T_{2b} was significantly decreased after the addition of L-cysteine and L-cystine. Compared to untreated SPP at 0.1 MPa, T_{2b} of SPP at 400 MPa was decreased, while it was increased by the addition of L-cysteine and L-cystine under HHP. T_{2b} normally reflected water element closely associated with proteins, and the reduction in T_{2b} suggested a weak mobility of bonded water in SPP gels with presence of sulfur-containing amino acids. The increase in T_{2b} of SPP gel with L-cysteine and L-cystine under HHP was probably correlated to the continuing molecular interactions, and protein structure unfolding and denaturation (Miklos, Cheong & Xu, et al., 2015). Regarding to T21 component, a broader relaxation time was induced by both sulfur-containing amino acids and HHP, indicating a flexible protein network with greater variation of water distribution within the gel matrix (Han, Zhang & Zheng, et al., 2019).

Considering the proportion peak area, no significant difference of A_{2b} was observed in SPP gels with sulfur-containing amino acids, only except the case that

data was decreased by adding L-cystine at high concentration of 1.0 %. While, a lower A_{2b} was detected in HHP-treated samples with or without L-cysteine or L-cystine. Furthermore, compared to untreated SPP at 0.1 MPa, A_{21} was increased in gels from SPP with L-cysteine and L-cystine with or without HHP treatment. The decrease in A_{2b} and the increase in A_{21} suggested the conversion between bonded and immobilized water fractions (Dong, Li, Song & Wang, et al., 2017). Moreover, a higher A_{21} implied that more immobilized water was trapped in the gel structure both enhanced by additive sulfur-containing amino acids and HHP treatment (Yang, Zhang & Li, et al., 2016).

3.5. Hypothetic mechanism explanation

The sulfur-containing amino acids (L-cysteine and L-cystine) induced improvement in gelation behaviors of SPP under HHP treatment is speculated in Fig. 6-4. Sulfur-containing amino acids provided available sulfhydryl groups (-SH-), significantly enhanced the access of sulfhydryl groups with SPP molecules, and made a contribution to the interface exchanges and disulfide linkages (-S-S-) (Fig. 6-4A). As a weak oxidant, L-cystine was involved in the redox reactions and could be served as the mercapto donor to maximize the cross-linkages of SPP (Fig. 6-4B). Moreover, functional groups (e.g. carboxylic and amino groups) carried by additive amino acids could enhance the protein-protein interactions and intensive electrostatic reactions (attraction or repulsion) for a better gel network construction. In addition, HHP induced exposure of inherent sulfhydryl groups similarly strengthened the cross-linking of SPP by covalent disulfide bonding. As a consequence, the scanning electron microscope (SEM) images of the gels made from HHP-treated SPP with presence of sulfur-containing amino acids exhibited a continuous gel networks with tiny water channels or smaller bore diameter (Fig. 6-4) correlated to the untreated ones (Fig. 6-4C), which indicated a highly hydrated and solid gel network. This observation was consistent with the enhancement in rheology shear process during the thermal gelation (Fig. 6-2), textural behavior (Fig. 6-3) and Low-field NMR testing (Table 6-3).

4. Conclusion

The present studies evaluated the changes in structure and gelation behavior of SPP with sulfur-containing amino acids (L-cysteine and L-cystine) and HHP treatment. L-cysteine and L-cystine altered the denaturation temperature and reduced the denaturation enthalpy of SPP. The modification of the secondary structure of SPP by L-cysteine and L-cystine was correlated to the increase in α-helical content but the decrease in β-sheet and random coil structure unit. Sulfur-containing amino acids weakened the absorbance intensity, and improved rheology properties of SPP. Textural properties of gels from untreated and HHP-treated SPP were both improved by sulfur-containing amino acids, especially by L-cysteine owe to the efficiently mercapto supply. Low-field NMR test suggested a closely association of water connects to SPP molecules in the presence of L-cysteine and L-cystine, resulting in more immobilized water

fraction trapped in the SPP gel matrix. These findings explained the importance of thiol groups for the protein gelation, and provided a novelty consideration of sulfur-containing amino acids as nutritive and functional ingredient used to improve the gelation behavior of SPP, which can also be potentially applied in other plant protein matrix for food manufacturing.

Acknowledgments

The authors gratefully acknowledge the earmarked fund for China Agriculture Research System (CARS-10-B21) and National Key R & D Program of China (2016YFE0133600).

Reference

Ahmed, J., Al-Ruwaih, N., Mulla, M., & Rahman, M. H. (2018). Effect of high pressure treatment on functional, rheological and structural properties of kidney bean protein isolate. *LWT - Food Science and Technology*, 91, 191-197.

Akin, Z., & Ozcan, T. (2017). Functional properties of fermented milk produced with plant proteins. *LWT - Food Science and Technology*, 86, 25-30.

Arogundade, L. A., Mu, T. H., & Añón, M. C. (2012). Heat-induced gelation properties of isoelectric and ultrafiltered sweet potato protein isolate and their gel microstructure. *Food Research International*, 49 (1), 216–225.

Buchert, J., Ercili Cura, D., Ma, H., Gasparetti, C., Monogioudi, E., Faccio, G., & Lantto, R. (2010). Crosslinking food proteins for improved functionality. *Annual Review of Food Science and Technology*, 1, 113-138.

Chao, D. F., Jung, S., & Aluko, R. E. (2018). Physicochemical and functional properties of high pressure-treated isolated pea protein. *Innovative Food Science & Emerging Technologies*, 45, 179-185.

Cando, D., Herranz, B., Borderías, A. J., & Moreno, H. M. (2015). Effect of high pressure on reduced sodium chloride surimi gels. *Food Hydrocolloids*, 51, 176–187.

Cando, D., Herranz, B., Borderías, A. J., & Moreno, H. M. (2016). Different additives to enhance the gelation of surimi gel with reduced sodium content. *Food Chemistry*, 196, 791-799.

Cando, D., Moreno, H. M., Borderías, A. J., & Skåra, T. (2016). Combined effect of high hydrostatic pressure and lysine or cystine addition in low-grade surimi gelation with low salt content. *Food and Bioprocess Technology*, 9 (8), 1391-1398.

Colovic, M. B., Vasic, V. M., Djuric, D. M., & Krstic, D. Z. (2018). Sulphur-containing amino acids: protective role against free radicals and heavy metals. *Current Medicinal Chemistry*, 25 (3), 324-335.

De Maria, S., Ferrari, G., & Maresca, P. (2016). Effects of high hydrostatic pressure on the conformational structure and the functional properties of Bovine Serum Albumin. *Innovative Food Science & Emerging Technologies*, 33, 67-75.

Dong, X. P., Li, Y., Song, L., & Wang, Y., et al. (2017). Changes of Water Distribution and Physicochemical Properties of Abalone (Haliotis discus) Myofibrillar Proteins during Heat-Induced Gelation. *Journal of Food Processing and Preservation*, 41 (4), e13069.

FAOSTAT. (2017). Production quantity [Internet]. Food and Agricultural Organization. http://www.fao.org/faostat/en/#data/QC. Accessed 01/06/19.

Grossi, A., Olsen, K., Bolumar, T., Rinnan, A., Øgendal, L. H., & Orlien, V. (2016). The effect of high pressure on the functional properties of pork myofibrillar proteins. *Food Chemistry*, 196, 1005-1015.

Han, Z., Zhang, J., Zheng, J., Li, X., & Shao, J. H. (2019). The study of protein conformation and hydration characteristics of meat batters at various phase transition temperatures combined with Low-field nuclear magnetic resonance and Fourier transform infrared spectroscopy. *Food Chemistry*, 280, 263-269.

Liang, Y., Guo, B., Zhou, A., et al. (2016). Effect of high pressure treatment on gel characteristics and gel formation mechanism of bighead carp (Aristichthys nobilis) surimi gels. *Journal of Food Processing and Preservation*, 40, 1–8.

Lin, D., Lu, W., Kelly, A. L., Zhang, L., Zheng, B., & Miao, S. (2017). Interactions of vegetable proteins with other polymers: Structure-function relationships and applications in the food industry. *Trends in Food Science & Technology*, 68, 130-144.

Ma, F., Chen, C., Zheng, L., Zhou, C., Cai, K., & Han, Z. (2013). Effect of high pressure processing on the gel properties of salt-soluble meat protein containing CaCl2 and κ-carrageenan. *Meat Science*, 95 (1), 22-26.

Miklos, R., Cheong, L. Z., Xu, X., Lametsch, R., & Larsen, F. H. (2015). Water and fat mobility in myofibrillar protein gels explored by low-field NMR. *Food Biophysics*, 10 (3), 316-323.

Murekatete, N., Hua, Y., Chamba, M. V. M., Djakpo, O., & Zhang, C. (2014). Gelation behavior and rheological properties of salt- or acid-induced soy proteins soft tofu-type gels. *Journal of Texture Studies*, 45 (1), 62-73.

O'sullivan, J., Murray, B., Flynn, C., & Norton, I. (2016). The effect of ultrasound treatment on the structural, physical and emulsifying properties of animal and vegetable proteins. *Food Hydrocolloids*, 53, 141-154.

Peyrano, F., Speroni, F., & Avanza, M. V. (2016). Physicochemical and functional properties of cowpea protein isolates treated with temperature or high hydrostatic pressure. *Innovative Food Science & Emerging Technologies*, 33, 38-46.

Stangierski, J., & Baranowska, H. M. (2015). The influence of heating and cooling process on the water binding in transglutaminase-modified chicken protein preparation, assessed using Low-Field NMR. *Food and Bioprocess Technology*, 8 (12), 2359-2367.

Sun, M. J., Mu, T. H., Zhang, M., & Arogundade, L. A. (2012). Nutritional assessment and effects of heat processing on digestibility of Chinese sweet potato protein. *Journal of Food Composition and Analysis*, 26 (1-2), 104-110.

Tabilo-Munizaga, G., Gordon, T. A., Villalobos-Carvajal, R., Moreno-Osorio, L., Salazar, F. N., Pérez-Won, M., & Acuña, S. (2014). Effects of high hydrostatic pressure (HHP) on the protein structure and thermal stability of Sauvignon blanc wine. *Food Chemistry*, 155, 214-220.

Tang, C. H., & Ma, C. Y. (2009). Effect of high pressure treatment on aggregation and structural properties of soy protein isolate. *LWT-Food Science and Technology*, 42 (2), 606-611.

Visschers, R. W., & De Jongh, H. H. (2005). Disulphide bond formation in food protein aggregation and gelation. *Biotechnology Advances*, 23 (1), 75-80.

Wei, J., Zhang, Z., Cai, Q., & Peng, B. (2018). Effects of high hydrostatic pressure on structural and physical properties of nisin-SPI film. *International Journal of Biological Macromolecules*, 111, 976-982.

Wanezaki, S., Tachibana, N., Nagata, M., Saito, S., Nagao, K., Yanagita, T., & Kohno, M. (2015). Soy β-conglycinin improves obesity-induced metabolic abnormalities in a rat model of nonalcoholic fatty liver disease. *Obesity Research & Clinical Practice*, 9 (2), 168-174.

Yang, H., Zhang, W., Li, T., Zheng, H., Khan, M. A., Xu, X., & Zhou, G. (2016). Effect of protein structure on water and fat distribution during meat gelling. *Food Chemistry*, 204, 239-245.

Zhang, M., & Mu, T. H. (2017). Identification and characterization of antioxidant peptides from sweet potato protein hydrolysates by Alcalase under high hydrostatic pressure. *Innovative Food Science & Emerging Technologies*, 43, 92-101.

Zhao, J., & Jiang, X. (2018). The application of sulfur-containing peptides in drug discovery. *Chinese Chemical Letters*, 29, 1079-1087.

Zhao, Z. K., Mu, T. H., Zhang, M., & Richel, A. (2018a). Chemical forces, structure, and gelation properties of sweet potato protein as affected by pH and high hydrostatic pressure. *Food and Bioprocess Technology*, 11 (9), 1719-1732.

Zhao, Z. K., Mu, T. H., Zhang, M., & Richel, A. (2018b). Effect of salts combined with high hydrostatic pressure on structure and gelation properties of sweet potato protein. *LWT - Food Science and Technology*, 93, 36-44.

Chapter VII

General discussion, conclusion and future perspective

Chapter VII General discussion, conclusion and future perspective

Abstract

This chapter provided an overview of general discussion and main conclusions of the thesis according to Chapter III, IV, V and VI, and the further consideration by using HHP treatment for novelty food manufacturing was also introduced.

Keywords

Protein; Gel-like food; Natural gelata; Gelation improver

1. General discussion

1.1. Gel formation by proteins

Protein gelation plays an essential role in preparation and acceptability of food products. The multicomponent system, such as dairy products (e.g. yogurt, cheese and butter), jelly products, tofu or other matrix in most cases is set by a protein-continuous network. As a construction element, protein can be achieved in gel formation via various mechanisms, such as thermal process, acidic training, calcium induction, enzyme catalysis, and even by usage of chemicals, like urea and glucono-δ-lactone (GDL), etc. (Arogundade, Mu & Añón, 2012; Cavallieri & Da Cunha, 2008; Kuhn, Cavallieri & Da Cunha, 2010; Grygorczyk & Corredig, 2013). Among, the heat induced gelation is still as one of the most desirable physical method in the food industry.

A protein gel can be seen as the colloidal particles cross-linking together to form a three-dimensional structure. In general, native protein becomes unfolding during thermal progress accompanied by the exposure of functional groups and binding site (Clark, Kavanagh, & Ross-Murphy, 2001). With the increasing of temperature, the protein element was tended to denaturation and aggregation, followed by the formation of pre-networks. In this case, the gel formation can be described as the denaturation of proteins followed by protein-protein interactions, which results in the exposure of nonpolar residues, and leads to clustering of aggregates (Brodkorb, Croguennec, Bouhallab & Kehoe, 2016). Notably, both of covalent (disulfide bonds or peptide linkages) and non-covalent interactions (hydrophobic interactions, electrostatic interactions and hydrogen bonds) are involved in the development and stabilization of SPP gels.

During the thermal gelation process, protein system was governed by a dynamic balance between attractive and repulsive forces, which were corresponded to the surface charges and various inter-molecular interactions (Mession, Sok, Assifaoui & Saurel, 2013). Three dimensional protein networks are therefore formed by the cross-linking of denatured proteins (Urbonaite, et al., 2016). Furthermore, thermal process was accompanied with the interruption of existing -SS- bond and active -SH- groups in proteins, namely participate in the -SH-/-SS- interchange reactions (Visschers & de Jongh, 2005). In this case, the newly formed inter-molecular disulfide bond would be made a great contribution to the formation of a highly ordered gel structure.

1.2. Factors affecting protein gelation behaviors

1.2.1. Influence of intrinsic factors on protein gelation

For globular protein element, gelation behavior is strongly depended on both intrinsic and external processing conditions, such as amino acid composition, protein concentration and protein types (Foegeding & Davis, 2011; Sun & Arntfield, 2010).

Gel is formed within a certain protein concentration. It is widely accepted that the heat-gelling ability of meat protein fractions are greater than that of plant proteins (Nicolai & Durand, 2013). Normally, gelation of plant protein occurs

within a concentration range of 5-15 %, whereas a much lower concentration of 0.5 % is sufficient to produce a heat-induced myofibrillar gels (Sun & Holley, 2011). This difference between minimal gelation concentration of meat protein fractions and plant proteins is probably due to the differences in the quantity of amino acids varied by the protein varieties, as well as average molecular weight. It is likely that the longer polypeptide chain length, rather than specific amino acids, enables protein element to have greater gelation capacities.

Moreover, gel properties exhibited a dependent manner on the protein concentrations. Typically, gel was formed above the minimum gelation concentrations, and it would become self-supporting at sufficiently high protein concentrations (Yi, et al., 2013). Consequently, the gel strength and water-holding capacity of protein increased with the increasing of protein concentrations (Kuhn, Cavallieri & Da Cunha, 2010). According to Brewer, Peterson, Carr, Mccusker, & Novakofski, (2005), the increase in gel strength could be attributed to an increase in the net matrix area occupied by the protein, which increased the potential for interlinks at junctions. As reported by Wang, Nema, & Teagarden, (2010), gels prepared at higher protein concentrations were shown to have a higher storage modulus, an indication that the networks were significantly stronger than those made at lower protein concentrations. Namely, increasing protein concentrations would increase the chances of protein–protein association, in most cases, facilitating the protein aggregation.

1.2.2. Influence of external factors on protein gelation

Compared with internal factors, environmental factors showed more practical meaning in regulating the sensory and texture of gelatinous food, particularly for applied processing technique, pH condition, enzymatic catalysis and functional additives, etc.

As a promising non-thermal technology, HHP affects non-covalent bonds (hydrogen, ionic, hydrophobic bonds) substantially, whereas the compounds with low molecular weight (responsible for nutritional and sensory characteristics) are not affected. Compared to thermal process, HHP showed similar functionality in altering -SH-/-SS- interchange reactions (Patel, Singh, Anema & Creamer, 2006). Khan, Mu, Zhang & Chen (2013) has been reported that HHP significantly induced the unfolding of SPP structure by exposure of buried sulfhydryl groups. He, et al., (2014) also suggested that the -SH- groups and -SS- bonds could be changed by the dissociation and refolding of proteins during the pressurization, as well as surface hydrophobic interactions. As a result, the soluble high molecular mass aggregates would be facilitated by the hydrophobic interactions and disulfide bonds within a sufficient pressure range (Zhao, Mu, Zhang & Richel, 2018). This phenomenon was similarly observed in walnut protein isolate by Qin et al. (2012), who reported that the -SH- group content was first increased at 300-400 MPa then decreased by a high pressure level of 400–500 MPa, being attributed to the exposure of free -SH- groups and the following formation of disulfide bond, thus leading to the improvement in gel properties.

In addition, the pH value and salt concentration have a profound effect on protein gelation behaviors by altering the balance of polar and non-polar residues (Kristinsson, & Hultin, 2003). As a functional additive, salt was not only applied

to adjust the flavor, but also was believed to affect electrostatic shielding around the proteins, particularly in divalent salt compared to that of monovalent ones (Ako, Nicolai & Durand, 2010). With the increasing of ionic strength, it is tending to reduce electrostatic repulsion forces between proteins, due to the shielding of ionizable groups by mobile ions, resulting in a weak electrostatic interaction. Generally, the globular protein can form as fine-stranded or particulate networks, which depend on whether it with or without addition of salt ions. Fine-stranded gel morphology often obtained when the electrostatic repulsion between protein molecules increases such as at a pH value far away from its isoelectric point or at low ionic strength. While, with decreasing inter-molecular repulsion by changing the pH toward the isoelectric point or by increasing the ionic strength, a coarser gel network was therefore induced, which composed of more particulate protein aggregates but along with a reduced gel strength and water holding behaviors (Hongsprabhas & Barbut, 1997; Bryant & McClements, 2000). Meanwhile, adjusting the acidic or alkaline condition may even ultimately affect the gelling characteristics by interfering with protein solubility, thermal stability and protein-protein interactions (Sağlam, et al., 2012).

The use of MTGase commonly attracts interest in the food industry, due to it enables highly elastic and irreversible gels to be obtained in different substrates, even at relatively low protein concentrations. Compare to other functional additive, MTGase catalyzed covalent cross-linking has been widely accepted, correlating to the both intra- and inter-molecular ε-(γ-glutaminyl) lysine isopeptide bonds (Yi, et al., 2006; Chanarat, Benjakul & H-Kittikun, 2012). In this case, protein functionalities, such as solubility, emulsifying capacity, foaming and gelation properties would be deeply changed by the enzymatic catalysis, as well as structural characters. According to Qiu et al. (2017), MTGase incubation led to decreasing in total free -SH- content and increase in exposed -SH-, suggesting unfolding of the peanut protein fractions. Moreover, studies carried out by Monogioudi et al. (2011) demonstrated that the MTGase catalyzed β-casein was more resistant to digestion by pepsin than that of the case with non-cross-linked ones. Due to these reasons, SPP aggregates are similarly formed by MTGase catalysis and make great contribution to the gel textural properties in present studies. Interestingly, Although the information about MTGase induced unfolding of different protein element is still limited, the function of MTGase in catalyzing aggregation and cross-linking effect has been detected in many resources, such as soy bean, peanut and myofibrillar, etc. (Jiang, & Zhao, 2010; Feng, et al., 2014; Chen & Han, 2011).

For sulfur-containing amino acids, cysteine residues exist in proteins as the free sulphydryl form or the oxidised cysteine, which displayed a strong chemical reactivity towards a number of compounds under relatively mild conditions. As the direct donor of the mercapto group, the main propose of additive cysteine/cystine is still focused on covalent cross-linking of SPP by disulfide bonds (Visschers & de Jongh, 2005). It has been reported that gel strength of whey protein increased with moderate cysteine addition (Zhu, & Labuza, 2010). Similarly, judicious addition of cysteine with low concentration of 10 mM significantly increased gel strength of whey protein concentrate, whereas it inversely decreased by a higher level of 30 mM (Schmidt, Illingworth, Deng &

Cornell, 1979). This suggested that the high concentration of sulfur-containing amino acids may also present negatively effects on protein matrix, which could be attributed to the electrostatic shielding by additives.

2. General conclusion

The present study evaluated different influence factors on structure and gelation properties of SPP combined with HHP treatment, including pH, salt, MTGase and sulfur-containing amino acids, which were correlated to the consideration of novelty processing technologies, environmental factors, functional additives and functional nutrient supplement, respectively.

SPP treated by 400 MPa at pH 9.0 were reasonable choices for preparing novelty food products with structural modification, followed by those at pH 6.0 and 3.0. HHP induced the exposure of interior hydrophobic residues and -SH-groups, modified secondary structure, and promoted the unfolding of protein chains of SPP, further enhanced the subsequent aggregation of SPP by leading the formation of higher molecular weight polymers according to the disulfide linkages with the increase of pressure level at pH 6.0 and 9.0. The rheological behavior of SPP was strongly dependent on pH values, and G′ was significantly increased after HHP treatment ($p < 0.05$). Textural properties (hardness, springiness, chewiness) and WHC of gels made from SPP treated by 250 and 400 MPa at pH 9.0 were significantly improved with a compact and uniform three-dimensional gel network.

The monovalent (NaCl) and divalent ($CaCl_2$ and $MgCl_2$) salt modified secondary structure of SPP, and altered chemical forces, such as Ho, electrostatic interactions and -SH-/-S-S- interchange reactions. Compared to the monovalent salt, divalent salt was much more efficient in reducing the electrostatic interactions of SPP, leading to the enhancement of G′, even though it decreased by the increasing of ionic strength. It suggested that divalent salt can be partially replaced the monovalent salt in order to reduce the addition of salt content in food processing. Meanwhile, the diminished WHC and textural properties of SPP gels with presence of all three types of salt were strengthened by HHP. Therefore, HHP could be potentially applied to improve gelation properties of SPP for a better quality.

HHP and MTGase (50 U/g) induced inter-molecular covalent cross-linking of SPP by the formation of disulfide bond and ε-(γ-glutaminyl) lysine isopeptide bond, respectively. The thermal denaturation temperature of SPP was increased by HHP and MTGase, especially for MTGase catalyzed SPP with HHP pretreatment. Combination treatment of HHP and further MTGase strengthened the SPP gel construction with improved textural behaviors. More bound and immobilized water fractions were trapped in the gel structure, due to the enhancement of HHP and further MTGase catalysis.

Sulfur-containing amino acids, L-cysteine and L-cystine, altered thermal denaturation temperature of SPP, and significantly reduced the denaturation enthalpy. L-cysteine and L-cystine induced modification of secondary structure of SPP with an increase in α-helical content but a decrease in β-sheet and random

coil structure unit. Both of two amino acids weakened the absorbance intensity, and improved the rheology properties of SPP, as well as textural behaviors, especially L-cysteine. Due to the mercapto supply, L-cysteine was much more efficient in improving gelation of SPP than L-cystine. As a result, the gel network showed a closely association of water connects to SPP molecules in the presence of L-cysteine and L-cystine, resulting in more immobilized water fraction trapped in the matrix.

3. Perspective

3.1. Research status of SPP

Plant protein has attracted great attention over years, based on its physical and industrial interests for healthy food. Compared to the chemical gels, new-type gelata made from natural protein element is more preferred by the consumers, both have nutrition and safety concerns.

SPP showed high solubility and nutritional values, meanwhile, the antioxidant capacity (*in vitro*), anticancer activity (*in vitro and in vivo*) and emulsifying properties of SPP also has been reported by our previous studies (Zhang, Mu & Sun, 2014; Li, Mu & Deng, 2013). HHP showed functionality in improving the emulsifying properties of SPP (Khan, Mu, Zhang & Arogundade, 2014), which provide a new consideration for us whether the HHP treatment could similarly affect gelation properties of SPP. By this case, chemical forces, structure and gelation properties of SPP affected by HHP treatment combined with four main factors were investigated in present study, including a modulation of pH conditions, addition of salt ions, enzyme microbial transglutaminase and sulfur-containing amino acids, respectively.

The findings in present study would be of great help for understanding the gelling behavior of SPP combined with different processing conditions, and might be appropriate for other plant proteins prepared from materials those contain high starch content, such as potato, yam, taro, etc. Meanwhile, the present study showed improvement of HHP in adjusting textural and gelation behaviors of SPP, which provided a new view to us for further development of HHP technique in handling of this new protein resource as functional ingredient in gel-like food, such as sausage, yogurt, beverages and ice cream, etc.

3.2. Future trends

Compared to the traditional thermal processing technology, HPP technology extends the storage life, maintains the flavors and nutritional value, and increases the value proposition of products, therefore could be afford the health-conscious consumers (Wang, Huang, Hsu, & Yang, 2016). While, the disadvantage of HHP technology also should be taken into consideration. Typically, HHP treated food products still need to store or transport under cold chains for a longer shelf life. Moreover, the operation is not applicable to powdery flour with low water content or products containing a large number of gas, due to the water as the pressure transfer medium, and products containing air bubbles will be deformed under pressure. Furthermore, the packaging material must be having a certain

compressibility (Huang, Wu, Lu, Shyu, & Wang, 2017).

In present studies, SPP gels were prepared by thermal progress after HHP pre-treatment. Actually, the applied protein concentration (10 %, w/v) is un-sufficient to form a viscoelastic gel by HHP treatment directly (even at the highest pressure level of 550 MPa). In other words, no information about the HHP-produced gel is currently available. Therefore, the gelation condition of SPP gels treated by HHP needs to be further studied. In addition, food matrix is a complicated system. The quality and acceptability of food are a comprehensive result decided by multiple components. Although the HHP treatment showed positively effect on the gelation of SPP, the interactions between different ingredients in food system under pressure treatment are still unclear, such as protein-starch, protein-additives, protein-polysaccharide, which also should be emphasized in the future.

On the other hand, health, safety and cleanliness are eternal goals in food manufacturing. Clean label food prepared by HHP pathway is gradually gaining popularity, which remain the need to meet the requirements of free chemical additives, simple ingredients and minimal processing. In this case, the MTGase and sulfur-containing amino acids may become a good choice to combine with HHP treatment for a better gel-like food quality.

Reference

Ako, K., Nicolai, T., & Durand, D. (2010). Salt-induced gelation of globular protein aggregates: structure and kinetics. *Biomacromolecules*, 11 (4), 864-871.

Arogundade, L. A., Mu, T. H., & Añón, M. C. (2012). Heat-induced gelation properties of isoelectric and ultrafiltered sweet potato protein isolate and their gel microstructure. *Food Research International*, 49 (1), 216-225.

Brewer, M. S., Peterson, W. J., Carr, T. C., Mccusker, R., & Novakofski, J. (2005). Thermal gelation properties of myofibrillar protein and gelatin combinations. *Journal of Muscle Foods*, 16 (2), 126-140.

Brodkorb, A., Croguennec, T., Bouhallab, S., & Kehoe, J. J. (2016). Heat-induced denaturation, aggregation and gelation of whey proteins. *In Advanced Dairy Chemistry* (pp. 155-178). Springer, New York, NY.

Bryant, C. M., & McClements, D. J. (2000). Influence of NaCl and $CaCl_2$ on cold‐set gelation of heat‐denatured whey protein. *Journal of Food Science*, 65 (5), 801-804.

Cavallieri, A. L. F., & Da Cunha, R. L. (2008). The effects of acidification rate, pH and ageing time on the acidic cold set gelation of whey proteins. *Food Hydrocolloids*, 22 (3), 439-448.

Chanarat, S., Benjakul, S., & H-Kittikun, A. (2012). Comparative study on protein cross-linking and gel enhancing effect of microbial transglutaminase on surimi from different fish. *Journal of the Science of Food and Agriculture*, 92 (4), 844-852.

Chen, H., & Han, M. (2011). Raman spectroscopic study of the effects of microbial transglutaminase on heat-induced gelation of pork myofibrillar proteins

and its relationship with textural characteristics. *Food Research International*, 44 (5), 1514-1520.

Clark, A. H., Kavanagh, G. M., & Ross-Murphy, S. B. (2001). Globular protein gelation—theory and experiment. *Food Hydrocolloids*, 15 (4-6), 383-400.

Feng, X. L., Liu, H. Z., Shi, A. M., Liu, L., Wang, Q., & Adhikari, B. (2014). Effects of transglutaminase catalyzed crosslinking on physicochemical characteristics of arachin and conarachin-rich peanut protein fractions. *Food Research International*, 62, 84-90.

Foegeding, E. A., & Davis, J. P. (2011). Food protein functionality: A comprehensive approach. *Food Hydrocolloids*, 25 (8), 1853-1864.

Grygorczyk, A., & Corredig, M. (2013). Acid induced gelation of soymilk, comparison between gels prepared with lactic acid bacteria and glucono-δ-lactone. *Food Chemistry*, 141(3), 1716-1721.

He, X. H., Liu, H. Z., Liu, L., Zhao, G. L., Wang, Q., & Chen, Q. L. (2014). Effects of high pressure on the physicochemical and functional properties of peanut protein isolates. *Food Hydrocolloids*, 36, 123-129.

Hongsprabhas, P., & Barbut, S. (1997). Protein and salt effects on Ca^{2+}-induced cold gelation of whey protein isolate. *Journal of Food Science*, 62 (2), 382-385.

Huang, H. W., Wu, S. J., Lu, J. K., Shyu, Y. T., & Wang, C. Y. (2017). Current status and future trends of high-pressure processing in food industry. *Food Control*, 72, 1-8.

Jiang, S. J., & Zhao, X. H. (2010). Transglutaminase-induced cross-linking and glucosamine conjugation in soybean protein isolates and its impacts on some functional properties of the products. *European Food Research and Technology*, 231 (5), 679-689.

Khan, N. M., Mu, T. H., Zhang, M., & Chen, J. W. (2013). Effects of high hydrostatic pressure on the physicochemical and emulsifying properties of sweet potato protein. *International Journal of Food Science & Technology*, 48 (6), 1260-1268.

Kristinsson, H. G., & Hultin, H. O. (2003). Effect of low and high pH treatment on the functional properties of cod muscle proteins. *Journal of Agricultural and Food Chemistry*, 51 (17), 5103-5110.

Kuhn, K. R., Cavallieri, Â. L. F., & Da Cunha, R. L. (2010). Cold-set whey protein gels induced by calcium or sodium salt addition. *International Journal of Food Science & Technology*, 45 (2), 348-357.

Mession, J. L., Sok, N., Assifaoui, A., & Saurel, R. (2013). Thermal Denaturation of Pea Globulins (Pisum sativum L.) Molecular Interactions Leading to Heat-Induced Protein Aggregation. *Journal of Agricultural and Food Chemistry*, 61 (6), 1196-1204.

Monogioudi, E., Faccio, G., Lille, M., Poutanen, K., Buchert, J., & Mattinen, M. L. (2011). Effect of enzymatic cross-linking of β-casein on proteolysis by pepsin. *Food Hydrocolloids*, 25 (1), 71-81.

Nicolai, T., & Durand, D. (2013). Controlled food protein aggregation for new functionality. *Current Opinion in Colloid & Interface Science*, 18 (4), 249-256.

Patel, H. A., Singh, H., Anema, S. G., & Creamer, L. K. (2006). Effects of heat and high hydrostatic pressure treatments on disulfide bonding interchanges among the proteins in skim milk. *Journal of Agricultural and Food Chemistry*, 54 (9), 3409-3420.

Qin, Z., Guo, X., Lin, Y., Chen, J., Liao, X., Hu, X., & Wu, J. (2013). Effects of high hydrostatic pressure on physicochemical and functional properties of walnut (*Juglans regia* L.) protein isolate. *Journal of the Science of Food and Agriculture*, 93 (5), 1105-1111.

Qiu, C., Hu, X., Li, L., Yang, X., Zhao, M., & Ren, J. (2017). Effect of transglutaminase cross-linking on the conformational and emulsifying properties of peanut arachin and conarachin fractions. *European Food Research and Technology*, 243 (6), 913-920.

Sağlam, D., Venema, P., de Vries, R., van Aelst, A., & van der Linden, E. (2012). Relation between gelation conditions and the physical properties of whey protein particles. *Langmuir*, 28 (16), 6551-6560.

Schmidt, R. H., Illingworth, B. L., & Ahmed, E. M. (1978). Heat-induced gelation of peanut protein/whey protein blends. *Journal of Food Science*, 43 (2), 613-621.

Schmidt, R. H., Illingworth, B. L., Deng, J. C., & Cornell, J. A. (1979). Multiple regression and response surface analysis of the effects of calcium chloride and cysteine on heat-induced whey protein gelation. *Journal of Agricultural and Food Chemistry*, 27 (3), 529-532.

Sun, X. D., & Arntfield, S. D. (2010). Gelation properties of salt-extracted pea protein induced by heat treatment. *Food Research International*, 43 (2), 509-515.

Sun, X. D., & Holley, R. A. (2011). Factors influencing gel formation by myofibrillar proteins in muscle foods. *Comprehensive Reviews in Food Science and Food Safety*, 10 (1), 33-51.

Urbonaite, V., van der Kaaij, S., de Jongh, H. H. J., Scholten, E., Ako, K., van der Linden, E., & Pouvreau, L. (2016). Relation between gel stiffness and water holding for coarse and fine-stranded protein gels. *Food Hydrocolloids*, 56, 334-343.

Visschers, R. W., & de Jongh, H. H. (2005). Disulphide bond formation in food protein aggregation and gelation. *Biotechnology Advances*, 23 (1), 75-80.

Wang, C. Y., Huang, H. W., Hsu, C. P., & Yang, B. B. (2016). Recent advances in food processing using high hydrostatic pressure technology. *Critical Reviews in Food Science and Nutrition*, 56 (4), 527-540.

Wang, W., Nema, S., & Teagarden, D. (2010). Protein aggregation-Pathways and influencing factors. *International Journal of Pharmaceutics*, 390 (2), 89-99.

Yi, J. B., Kim, Y. T., Bae, H. J., Whiteside, W. S., & Park, H. J. (2006). Influence of transglutaminase-induced cross-linking on properties of fish gelatin films. *Journal of Food Science*, 71 (9), E376-E383.

Yi, L., Lakemond, C. M., Sagis, L. M., Eisner-Schadler, V., van Huis, A., & van Boekel, M. A. (2013). Extraction and characterisation of protein fractions from five insect species. *Food Chemistry*, 141 (4), 3341-3348.

Zhao, Z. K., Mu, T. H., Zhang, M., & Richel, A. (2018). Chemical forces, structure, and gelation properties of sweet potato protein as affected by pH and high hydrostatic pressure. *Food and Bioprocess Technology*, 11 (9), 1719-1732.

Zhu, D., & Labuza, T. P. (2010). Effect of cysteine on lowering protein aggregation and subsequent hardening of whey protein isolate (WPI) protein bars in WPI/buffer model systems. *Journal of Agricultural and Food Chemistry*, 58 (13), 7970-7979.

Appendix-Publications

1. **Zhao, Z. K.,** Mu, T. H., Zhang, M., & Richel, A. (2018). Chemical forces, structure, and gelation properties of sweet potato protein as affected by pH and high hydrostatic pressure. *Food and Bioprocess Technology*, 11(9), 1719-1732. **(Published)**

2. **Zhao, Z. K.,** Mu, T. H., Zhang, M., & Richel, A. (2018). Effect of salts combined with high hydrostatic pressure on structure and gelation properties of sweet potato protein. *LWT*, 93, 36-44. **(Published)**

3. **Zhao, Z. K.,** Mu, T. H., Zhang, M., & Richel, A. (2019). Effects of high hydrostatic pressure and microbial transglutaminase treatment on structure and gelation properties of sweet potato protein. *LWT*. **(Under review)**

4. **Zhao, Z. K.,** Mu, T. H., Zhang, M., & Richel, A. (2019). Effects of sulfur-containing amino acids and high hydrostatic pressure on structure and gelation properties of sweet potato protein. *Food and Bioprocess Technology.* **(Under review)**